A scanning electron micrograph (SEM) showing a porous implant structure. The implant has a complex, interconnected network of channels and pores. Bone tissue, appearing as a dense, fibrous material, has grown into these pores, demonstrating the implant's potential for bone ingrowth. The overall image is in shades of brown and tan, with a semi-transparent red overlay on the right side.

Bone ingrowth potential of porous implants produced by rapid prototyping

Liesbeth Biemond

Bone ingrowth potential of porous implants produced by rapid prototyping

Liesbeth Biemond

The printing of this thesis was financially supported by:

Anna Fonds te Leiden
Eurocoating SpA, Trento, Italy
Nederlandse Orthopaedische Vereniging
Reumafonds
POM Nijmegen BV

Lay-out and design
Digit@l Xpression, the Netherlands, Bennekom

Printing
GVO drukkers & vormgevers, the Netherlands, Ede

Copyright
© 2012 Liesbeth Biemond

All rights reserved. No part of this book may be reproduced in any form without permission of the author.

Bone ingrowth potential of porous implants produced by rapid prototyping

Proefschrift

ter verkrijging van de graad van doctor
aan de Radboud Universiteit Nijmegen
op gezag van de rector magnificus prof. mr. S.C.J.J Kortmann,
volgens besluit van het college van decanen
in het openbaar te verdedigen op

dinsdag 30 oktober 2012 om 12.30 uur precies

door

Jeanne Elizabeth Biemond

geboren op 29 maart 1983
te Rotterdam

Promotoren: Prof. Dr. P. Buma
Prof. Dr. Ir. N. Verdonshot

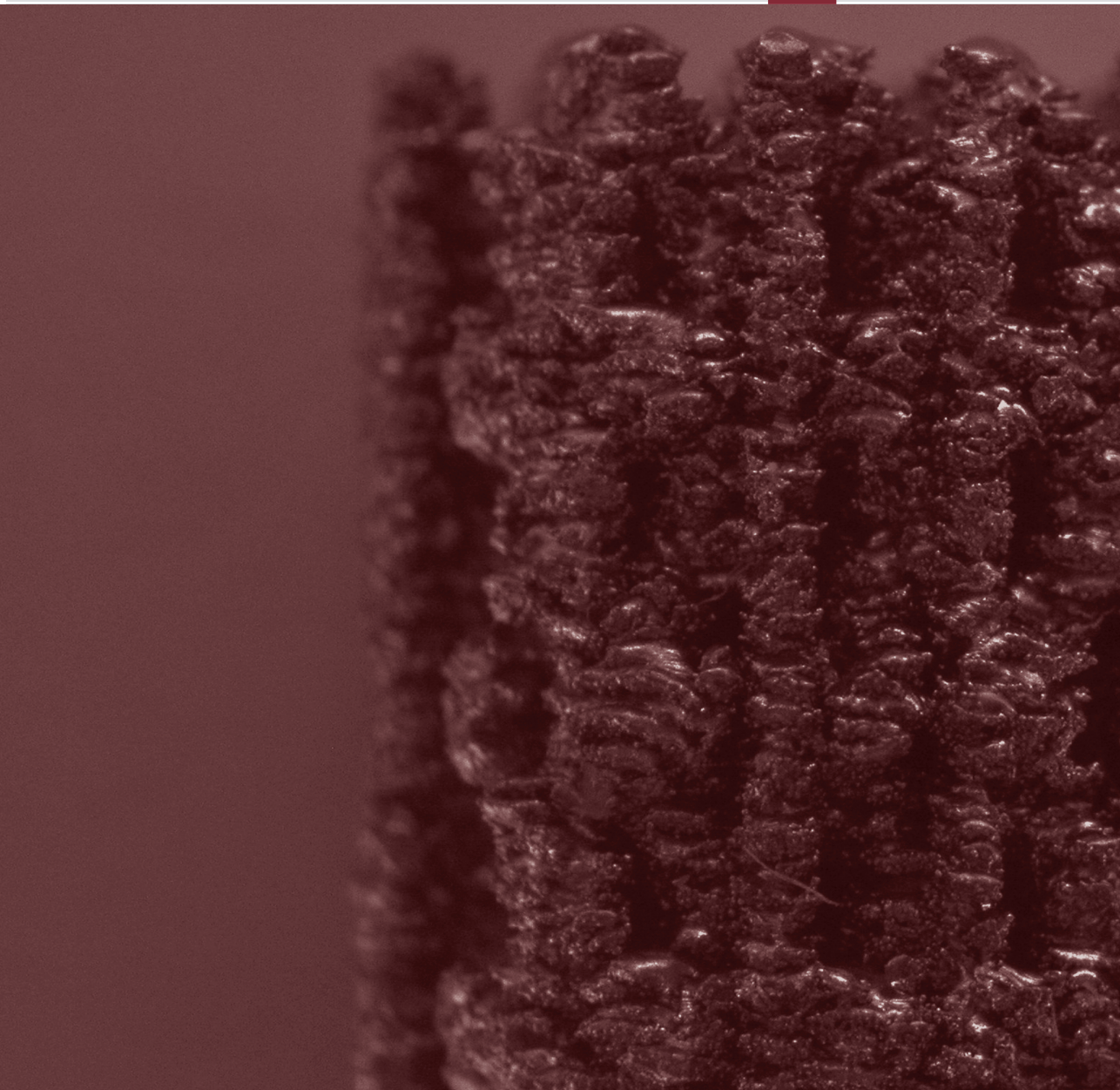
Copromotor: Dr. G. Hannink

Manuscriptcommissie: Prof. Dr. J.A. Jansen
Prof. Dr. J. Ritskes - Hoitinga
Prof. Dr. S.K. Bulstra

Contents

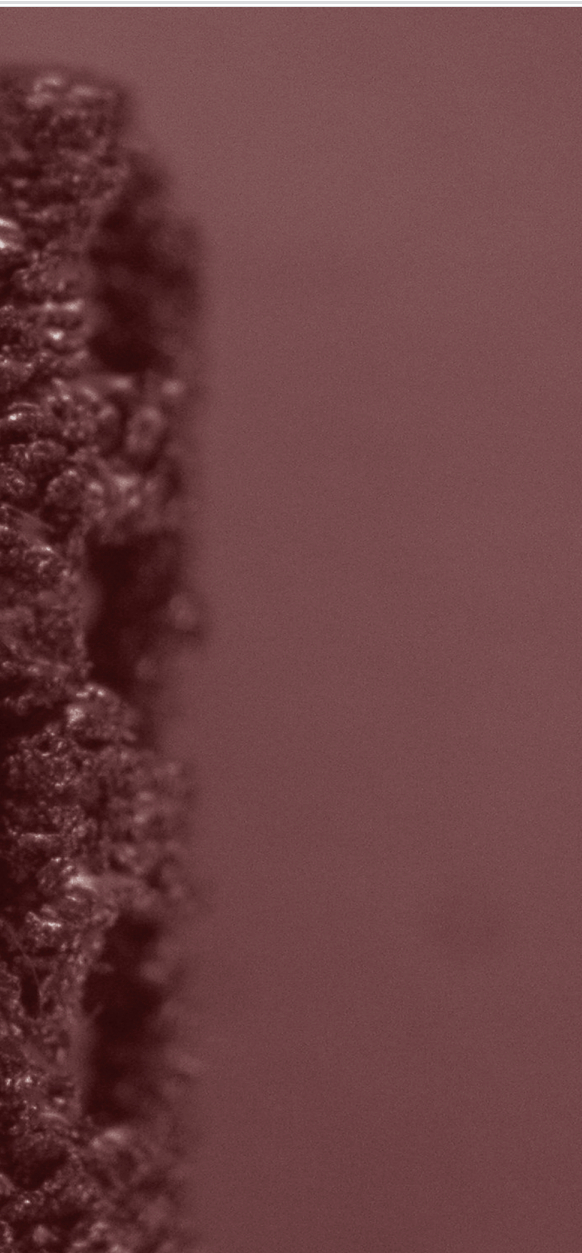
Chapter 1	Introduction	7
Chapter 2	Long-term survivorship analysis of the cementless spotorno femoral component in patients less than 50 years of age. JE Biemond, DFM Pakvis, GG van Hellemond, P Buma. <i>The Journal of Arthroplasty</i> , 2011: 26(3)386-390	21
Chapter 3	The effect of E-beam engineered surface structures on attachment, proliferation and differentiation of human mesenchymal stem cells. JE Biemond, G Hannink, N Verdonschot, P Buma. <i>Accepted for publication in Bio-medical materials and engineering</i>	31
Chapter 4	Frictional and bone ingrowth properties of engineered surface topographies produced by electron beam technology. JE Biemond, R Aquarius, N Verdonschot, P Buma. <i>Archives of orthopaedic and trauma surgery</i> , 2011: 131(5)711-718	43
Chapter 5	Assessment of bone ingrowth potential of biomimetic hydroxyapatite and brushite coated porous E-beam structures. JE Biemond, TS Eufrásio, G Hannink, N Verdonschot, P Buma. <i>Journal of Materials science: materials in medicine</i> , 2011: 22(4)917-925	59
Chapter 6	In vivo assessment of bone ingrowth potential of three-dimensional E-Beam produced implant surfaces and the effect of additional treatment by acid etching and hydroxyapatite coating. JE Biemond, G Hannink, AMG Jurrius, N Verdonschot, P Buma. <i>Journal Biomaterials Application</i> , 2012: 26(7)861-876	77
Chapter 7	Bone ingrowth potential of electron beam and selective laser melting produced trabecular-like implant surfaces with and without a biomimetic coating. JE Biemond, G Hannink, N Verdonschot, P Buma. <i>In preparation</i>	91
Chapter 8	Summary, closing remarks and future perspectives	107
Chapter 9	Samenvatting, afsluitende opmerkingen en toekomstig onderzoek	117
	List of abbreviations, Dankwoord, Curriculum vitae	127

Chapter 1



Introduction

1



Joint replacement of the hip or knee is one of the most enduring and successful orthopaedic interventions. Over 600,000 primary hip replacements and over 400,000 primary knee replacements are performed annually in Europe.[1] The clinical results are satisfying, with instant pain relief and functional improvement. It has therefore a very positive effect on health related quality of life.[2;3]

Current prosthetic systems are fixated to the bone either by cement (PMMA)(so called cemented prosthesis) or by bone ingrowth onto the implant surface (so called cementless prostheses). The survival of both cemented and cementless prostheses is approximately 90 percent after 10 years of follow-up.[2;4] This thesis focuses on cementless fixation.

The most important reason for failure of cementless prostheses within 5 years of implantation is aseptic loosening. Other reasons are instability of the implant in the bone and infection. [5] The underlying mechanism of aseptic loosening is still unknown, but it is clear that the etiology is multifactorial; wear debris, stress shielding and micromotion at the bone-implant interface play a role.[6] The frequency of failure is likely to increase due to the implantation in younger and more active patients.[6] Revision surgery after failure of an implant is a difficult procedure and creates a large burden for both the patient and society,[7] thus there is a need for improvement of cementless implants in order to avoid aseptic loosening.

Design and development of a new cementless orthopaedic implant is a complex process. In order to avoid failure of these implants, one should pay attention to the mechanical properties of the bulk material, the biocompatibility, corrosion and wear resistance and implant fixation.

Implant fixation

Although the process of aseptic loosening is not completely understood, it is clear that long term aseptic loosening is highly correlated with early post-operative migration.[8] A prolonged post-operative migration is generally considered as a failure of the ingrowth process. The bone-implant interface characteristics in the early post-operative period do play a crucial role in the success of the ingrowth process and by that in the long term success of the implant. Fixation at the bone implant interface depends on two mechanisms. Initially, press fit implantation provides primary stability and later on bone ingrowth offers secondary mechanical long-term fixation.[9;10] Successful bone ingrowth resembles the healing cascade of fractures, with the newly formed bone occupying the void spaces of the gaps at the interface and within the porous implant surface. Similar to primary fracture healing, no intermediate (fibro)cartilaginous stage occurs.[9] The bone ingrowth potential depends on the success of the primary stability at the bone implant interface. The primary stability as achieved by press-fit implantation depends on frictional forces at the bone implant interface, influenced by surgical technique, implant size, implant shape, implant material properties, surface roughness and the quality of the bone bed.[10;11] A high friction coefficient of the implant surface will enhance primary stability as it will reduce the magnitude of micromotions generated at the interface.[10;12] Micromotions at the bone-implant interface are evoked postoperatively by weight bearing of the prosthesis,

and are therefore unavoidable to some extent. Too much motion between the implant and bone leads to ingrowth of fibrous tissue rather than bone, whereas small micromotions will allow for adequate bone ingrowth and subsequent secondary fixation.[13;14]

As stated above, secondary fixation by bone ingrowth is influenced by primary stability. More specifically, interface gap size and micromotions play a key role. Besides this, bone ingrowth is also influenced by the biocompatibility and surface geometry characteristics of the implant.[9]

Secondary fixation of the implant is obtained by bone growth onto the surface and into the porous surface structure (if present). Important surface geometry characteristics which affect bone ingrowth are pore size, porosity and pore interconnectivity. It is evident that the pore size affects bone ingrowth, although there is still debate about the optimum pore size.[15] A minimum pore diameter of 100 μm is needed to allow vascularisation and subsequent bone ingrowth.[16] The maximum pore size, if there is a maximum for it, has yet to be determined. Interconnectivity between the pores is crucial for bone ingrowth, but it has been suggested in literature that the number of interconnections may be a more important factor than the size of the interconnections.[17] Implants with coatings with porosities of 50% show good survival [18] Furthermore, it has been reported that a substantial increase in fixation strength can be obtained by increasing the porosity of the implants to 75-80%.[19] There is, however, an upper limit in porosity due to the required mechanical strength of the implant surface.[15]

Bone ingrowth into a porous structure will increase the strength at the bone-implant interface. However, bone ingrowth beyond a certain depth does not enhance the strength of the bone-implant interface anymore[20], similarly as seen for the cement-bone interface.[21]

Porous implant surfaces

Three major strategies are used for the production of porous implant surfaces. Surface coatings can be prepared by sintering metal powder or fibers, plasma spray deposition of metallic or ceramic coatings and rapid prototyping. All three strategies intend to produce implant surfaces that allow bone ingrowth in order to provide a mechanical interlock of the implant and host bone.[22]

A titanium or calciumphosphate coating can be applied on implants by plasma spraying. The most widely used calciumphosphate for coating purposes is hydroxyapatite. Implants with titanium or hydroxyapatite plasma spray coating have shown good long-term survivorship. [23;24] However, some of the plasma spray coatings have been criticized for their weak bonding between coating and implant.[25;26] Furthermore, a disadvantage of the plasma spray technique is that it is impossible to apply a coating on the deep surfaces of complex 3-dimensional structures.[27]

Rapid prototyping (also called rapid manufacturing or additive manufacturing) has been introduced in the 1970s as a method to directly produce an implant and its porous implant surface in one manufacturing step. The first designs had irregular textured surfaces rather

than true porous structures with 3-dimensional interconnected openings for bone ingrowth. [22] Over the last years the rapid prototyping techniques has been improved, which made it possible to produce 3-dimensional implant surfaces.[22] Two methods of rapid prototyping which are of interest for this thesis are electron beam melting and selective laser melting techniques. Both techniques will be briefly discussed in the next paragraphs.

Electron beam melting

Electron beam melting (E-beam) is a relatively new rapid prototyping technique, with the capability to engineer a large variety of complex 3-dimensional structures. The technology may therefore be a feasible method to manufacture ingrowth surfaces for cementless implants. [28]

In the E-beam process, implants are build up out of metal powder. First, a 3D CAD model of the desired implant is designed. This CAD model is segmented into layers in order to generate layer information. Subsequently a homogeneous pre-heated powder layer is applied on the process platform. The electron beam scans the powder layer line by line and melts the powder particles at the pre-programmed locations forming a compact layer in the shape of the CAD model. Then, the platform is lowered and a new powder layer is applied after which the process is repeated.[29-31]

The layers are connected by metallurgic bonding, as in all rapid prototyping processes, resulting in one complete part. So, for prosthetic implants, the E-beam technique enables the production of a solid core and a porous surface in one manufacturing step. An additional advantage of E-beam is the fact that the implants are fabricated in a vacuum chamber, which assures impurity-free metallic implants unaffected by oxygen and other chemical elements typically present in the atmosphere. The residual stresses within the implant may also be reduced due to the vacuum processing.[28] Furthermore, fast temperature changes do not occur during the E-beam process (as these do occur in other types of rapid prototyping) further diminishing the residual stresses within the components.

During the last years only a few studies have been published on E-beam engineered surfaces in the orthopedic literature. Ponader et al.[32] demonstrated a reduced proliferation of human fetal osteoblasts on porous E-beam produced surfaces, compared to smooth and unprocessed E-beam surfaces. However, in that same study, SEM analysis demonstrated that the cells attached and spread well on all surfaces. Thomson et al.[33] demonstrated good biocompatibility of a non-porous E-beam structure in a rabbit study. In a second study of Ponader et al.[34] the in vivo performance of one porous E-beam structure was compared to the performance of a compact E-beam structure. Only scarce direct bone implant contact around the solid and porous E-beam specimens with a large variability among the specimens was found. Furthermore none or only one 3-dimensional E-beam implant surface structure was tested in vivo, showing similar results compared to conventional coatings.[33;34]

Selective laser melting

Selective laser melting (or direct metal laser sintering) is a rapid prototyping process, using a laser beam as energy source for the consolidation of metallic powder. As all rapid prototyping techniques, laser melting uses CAD data and layer-by-layer generation of the specimens. The overall accuracy is 100µm in laser melting vs. 150µm in E-beam, which implies that finer structures can be built. [35;36]

Warnke et al. showed that laser melted Titanium alloy specimens were biocompatible, with good vitality and spreading of human osteoblast on the specimens.[37] New bone formation on the surface of laser melted specimens was demonstrated when implanted in the femoral condyles of rabbits.[38]

Methods to enhance ingrowth into porous surfaces

Additional treatment of porous implant surfaces after production has the potential to increase the bone ingrowth properties of the implant. Texturing of an implant surface can occur by additive methods, like application of a CaP coating, or by removing some of the surface by methods as sandblasting [39;40] and chemical etching.[41-45]

Acid etching

Chemical etching is a method of surface roughening through acid etching.[41] The etching procedure results in a characteristic surface morphology when analyzed by SEM. The actual topography of an etched implant depends on acid mixture, etching time, temperature and structure prior to etching.[14;42] Chemical etching of an implant surface does not affect the (sharp) 3D-topography of the implant, which is an advantage over the rounded edges typically obtained by blasting processes. Furthermore, chemical etching cleans the implant surface from all particles left after the production of the implant and its surface.[46]

Although the etching procedure varies, the acid mixture consists mostly out of nitric, hydrofluoric and/or hydrochloric acid. Typically, the implant is immersed in the acid mixture either once for a longer period (up to 30 minutes) or multiple times for a short period (up to 5 minutes). After the etching procedure the implant is rinsed extensively in distilled water.[41;42;44]

Several authors found significantly enhanced bone ingrowth for etched implant compared to untreated implant surfaces.[41;42;44] Takemoto et al. even reported a large amount of bone ingrowth in an acid etched porous titanium implant, after implanting these implants in the back muscles of beagle dogs.[47]

Calcium phosphate coating

Calcium phosphate is the mineral component of bone. That is the reason that calcium phosphate is used in the form of coatings on metallic implants since the 1980s.[48] Numerous calcium phosphate compounds exist that may have a beneficial effect for orthopaedic implants. Hydroxyapatite ($\text{Ca}_{10}[\text{PO}_4]_6[\text{OH}]_2$) is the most widely applied calcium phosphate compound. Other compounds that are commonly used as coatings are tricalciumphosphate ($\text{Ca}_3[\text{PO}_4]_2$) and brushite ($\text{Ca}[\text{HPO}_4] \cdot 2[\text{H}_2\text{O}]$).[26;48-50] The crystallinity and solubility differs between these CaP coatings, which has an effect on the bonding of bone to the coating.[26]

The CaP coatings are biocompatible and considered to be bioactive in the human body. The commonly proposed mechanism of the bonding between bone and HA involves partial dissolution of the coating. Ca and P ions are released from the coating, resulting in a supersaturation of the surrounding body fluid with respect to Ca and P ions. The supersaturation provokes (re)precipitation of carbonated apatite crystals on the surface of the coating.[26;49] These crystals have been observed within hours of exposure to simulated body fluid.[51] The carbonated CaP layer that is formed in this way accommodates rapid protein adsorption and cell adhesion. This results in bone growth toward the implant. The bone-implant interface is subsequently subjected to bone remodeling and bidirectional growth resulting in biological secondary fixation.[26;49;52] This specific mechanism provides enhanced bone formation and accelerated bonding between the implant surface and the surrounding bone.[26;53;54]

Multiple total hip replacements coated with calcium phosphate are commercially available. They differ in implant shape, coating type, coating thickness and may be fully or partially coated. The long-term survival (follow up of over 10 years) of these prosthetic components is generally good, with only minor variation in between the different designs.[23;50;52;55]

A relatively new development is the application of calcium phosphate coatings on porous implant surfaces. Incorporation of hydroxyapatite into a titanium fiber mesh resulted in an enhanced push-out strength at 3 and 5 weeks, but at 8 weeks no difference between specimens with and without HA were found.[56] Bone ingrowth significantly increased for different time points by addition of an apatite coating on a porous tantalum structure[53] and porous titanium plugs[57].

The application of a calcium phosphate coating to a porous implant surface is challenging, because current direct coating techniques failed to mineralize on the deep surfaces of complex 3-dimensional structures.[27] This problem can be solved by the application of biomimetic coatings.

Biomimetic coating

An upcoming coating technique is the biomimetic coating process, which is a good alternative because of its ability to apply an homogeneous layer of the coating into porous and complex 3-dimensional geometries. The biomimetic process is based on electro-deposition, in

which the surface that has to be treated acts as cathode and the basin acts as anode. The metallic specimen is immersed in an artificially prepared supersaturated calcium/phosphate electrochemical solution usually at 37°C, forming a thin calciumphosphate layer.[53;58]

Besides the possibility to apply the coating into pores, further advantages are the possibility to incorporate biological agents, such as growth factors, in the coating due to the fact that the coating is deposited under physiological temperatures. In addition, the CaP ratio and coating thickness can be varied, and the structure of the formed crystals is more akin to bone mineral than coatings produced in conventional ways.[27;59]

Implantation of specimens with a biomimetic coating in goats, rabbits and rats showed good biocompatibility and significantly better bone ingrowth (expressed by either enhanced mechanical strength or more bone-implant contact) than uncoated controls.[53;57;60]

The coatings produced with the biomimetic technique have a higher solubility rate and a weaker coating-implant attachment than conventional coatings.[60] Part of the coating might chip off during press-fit implantation due to the weaker attachment between the coating and the implant. This loss of coating may not be so disadvantageous because the fragmented coating will remain in the surroundings of the implant.[58] The effect of the high solubility and therefore early dissolution of the coating on the bone ingrowth potential is not clear yet.

Structure of the Thesis

The general theme of this thesis is to assess how fixation of cementless components can be further optimized. The work involves analysis of primary stability by friction and secondary implant stability by bone ingrowth of new implant surface structures. An attempt was made to better understand the implant (or surface) characteristics and circumstances leading to sufficient bone ingrowth and eventually long term success. Thus, the ultimate goal of the research was to find implant surfaces that provide for an enhanced fixation potential. We focused on E-beam produced surfaces, because of the extensive possibilities in design of this technique and the fact that it enables to produce the core and surface of the implant in one manufacturing step.

The thesis starts with a long term follow-up survival study of the CLS femoral stem. (**Chapter 2**) This CLS stem is one of the most widely used cementless hips in the world. Although not performed in this thesis, the long term follow-up data of the CLS stem can act as a benchmark for new designed cementless implants.

New porous E-beam produced implant surface structures are analyzed *in vitro* and *in vivo* for their ability to provide for good fixation at the bone-implant interface. In **Chapter 3** the attachment, proliferation and differentiation of human mesenchymal stem cells (hMSCs) on new E-beam structures were evaluated as it is clear that these are crucial events in the process to achieve successful bone ingrowth. The frictional and *in vivo* bone ingrowth properties of the new 3-dimensional surface structures are analyzed in **Chapter 4**.

Chapter 5 and 6 focus on the effect of additional treatments of the 3D E-beam surface structures. A biomimetic calcium phosphate coating was applied to the porous E-beam structures. Mechanical and histological analysis of the bone ingrowth into these E-beam structures with a biomimetic coating was performed in **Chapter 5**. The effect of additional treatment on the bone ingrowth potential of the E-beam structures by addition of a plasma spray calcium phosphate coating and acid-etching of the surface was evaluated in **Chapter 6**. In **Chapter 7** electron beam melting was compared to selective laser melting, evaluating the bone ingrowth potential of the same structure produced by either technology.

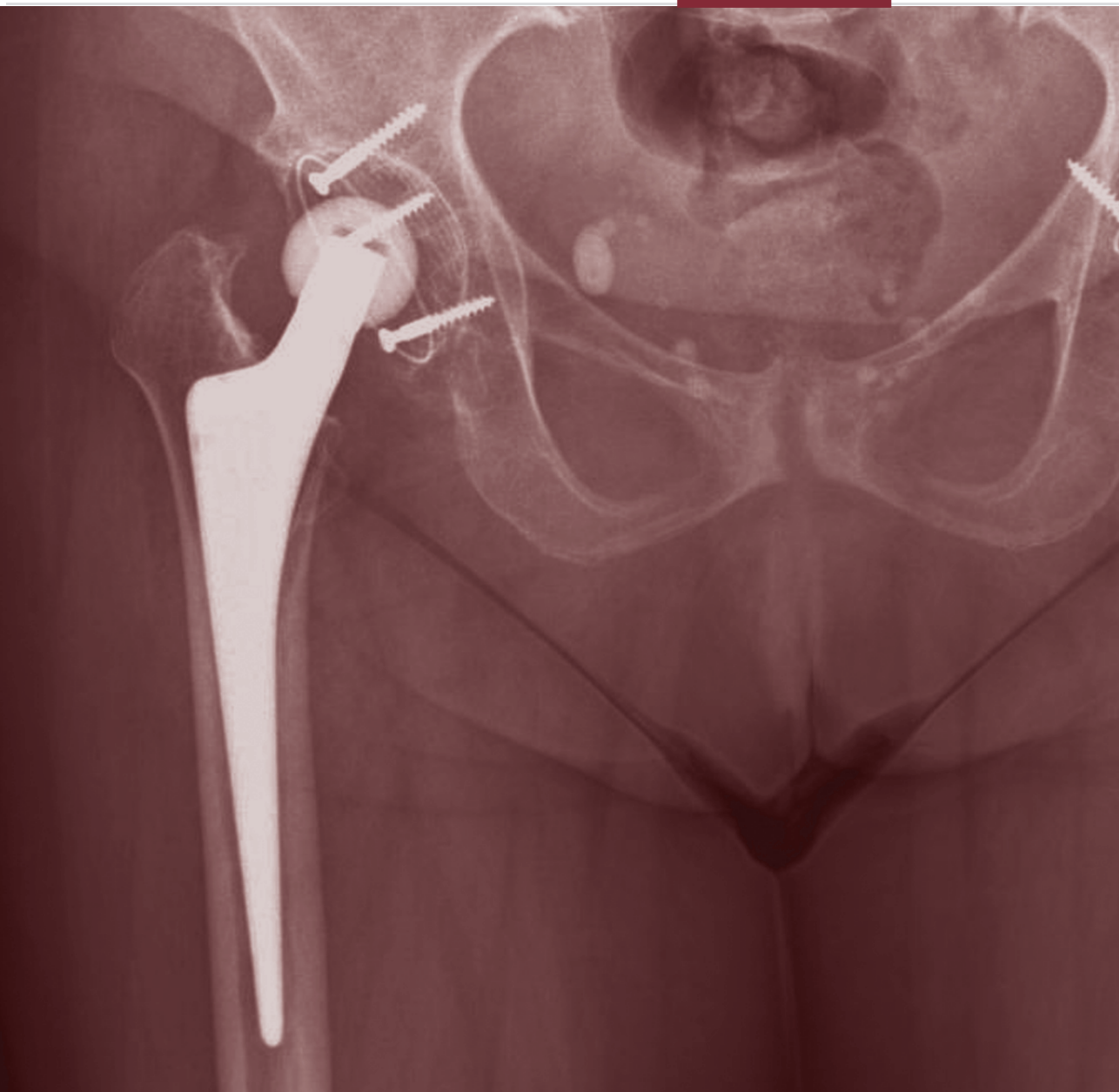
References

1. Labek G, Stöckl B, Janda W, Hübl M, Thaler M, Liebensteiner M, Williams A, Pawelka W, Frischhut St, Haselsteiner F, Schlichtherle R, Agreiter M, Abel J, Dorningen R, Sekyra K, Rosiek R, Mayr E, Hochgatterer R, Pfeiffer KP, Krismer M, Böhler N. Quality of datasets for outcome measurement, market monitoring and assessment of artificial joint implants. 2009. European Arthroplasty Register (EAR), EFORT.
2. Katz JN: Total joint replacement in osteoarthritis. *Best Pract Res Clin Rheumatol* 20(1):145, 2006
3. Rasanen P, Paavolainen P, Sintonen H, Koivisto AM, Blom M, Ryyanen OP, Roine RP: Effectiveness of hip or knee replacement surgery in terms of quality-adjusted life years and costs. *Acta Orthop* 78(1):108, 2007
4. Garellick G, Kärrholm J, Rogmark C, Herberts P. Swedish hip arthroplasty register. Annual report 2008. 2009.
5. Ulrich SD, Seyler TM, Bennett D, Delanois RE, Saleh KJ, Thongtrangan I, Kuskowski M, Cheng EY, Sharkey PF, Parvizi J, Stiehl JB, Mont MA: Total hip arthroplasties: what are the reasons for revision? *Int Orthop* 32(5):597, 2008
6. Sundfeldt M, Carlsson LV, Johansson CB, Thomsen P, Gretzer C: Aseptic loosening, not only a question of wear: a review of different theories. *Acta Orthop* 77(2):177, 2006
7. Kurtz SM, Ong KL, Schmier J, Mowat F, Saleh K, Dybvik E, Kärrholm J, Garellick G, Havelin LI, Furnes O, Malchau H, Lau E: Future clinical and economic impact of revision total hip and knee arthroplasty. *J Bone Joint Surg Am* 89 Suppl 3:144, 2007
8. Ryd L, Albrektsson BE, Carlsson L, Dansgard F, Herberts P, Lindstrand A, Regner L, Toksvig-Larsen S: Roentgen stereophotogrammetric analysis as a predictor of mechanical loosening of knee prostheses. *J Bone Joint Surg Br* 77(3):377, 1995
9. Kienapfel H, Sprey C, Wilke A, Griss P: Implant fixation by bone ingrowth. *J Arthroplasty* 14(3):355, 1999
10. Ramamurti BS, Orr TE, Bragdon CR, Lowenstein JD, Jasty M, Harris WH: Factors influencing stability at the interface between a porous surface and cancellous bone: a finite element analysis of a canine in vivo micromotion experiment. *J Biomed Mater Res* 36(2):274, 1997
11. Adler E, Stuchin SA, Kummer FJ: Stability of press-fit acetabular cups. *J Arthroplasty* 7(3):295, 1992
12. Dammak M, Shirazi-Adl A, Schwartz M, Jr., Gustavson L: Friction properties at the bone-metal interface: comparison of four different porous metal surfaces. *J Biomed Mater Res* 35(3):329, 1997
13. Soballe K, Brockstedt-Rasmussen H, Hansen ES, Bunger C: Hydroxyapatite coating modifies implant membrane formation. Controlled micromotion studied in dogs. *Acta Orthop Scand* 63(2):128, 1992
14. Szmukler-Moncler S, Salama H, Reingewirtz Y, Dubrulle JH: Timing of loading and effect of micromotion on bone-dental implant interface: review of experimental literature. *J Biomed Mater Res* 43(2):192, 1998
15. Karageorgiou V, Kaplan D: Porosity of 3D biomaterial scaffolds and osteogenesis. *Biomaterials* 26(27):5474, 2005
16. Jones JR, Ehrenfried LM, Hench LL: Optimising bioactive glass scaffolds for bone tissue engineering. *Biomaterials* 27(7):964, 2006
17. Otsuki B, Takemoto M, Fujibayashi S, Neo M, Kokubo T, Nakamura T: Pore throat size and connectivity determine bone and tissue ingrowth into porous implants: three-dimensional micro-CT based structural analyses of porous bioactive titanium implants. *Biomaterials* 27(35):5892, 2006
18. Petersilge WJ, D'Lima DD, Walker RH, Colwell CW, Jr.: Prospective study of 100 consecutive Harris-Galante porous total hip arthroplasties. 4- to 8-year follow-up study. *J Arthroplasty* 12(2):185, 1997
19. Bobyn JD, Stackpool GJ, Hacking SA, Tanzer M, Krygier JJ: Characteristics of bone ingrowth and interface mechanics of a new porous tantalum biomaterial. *J Bone Joint Surg Br* 81(5):907, 1999
20. Tarala M, Waanders D, Biemond JE, Hannink G, Janssen D, Buma P, Verdonchot N: The effect of bone ingrowth depth on the tensile and shear strength of the implant-bone e-beam produced interface. *J Mater Sci Mater Med* 22(10):2339, 2011
21. Majkowski RS, Bannister GC, Miles AW: The effect of bleeding on the cement-bone interface. An experimental study. *Clin Orthop Relat Res* (299):293, 1994
22. Pilliar RM: Cementless implant fixation--toward improved reliability. *Orthop Clin North Am* 36(1):113, 2005
23. Lombardi AV, Jr., Berend KR, Mallory TH: Hydroxyapatite-coated titanium porous plasma spray tapered stem: experience at 15 to 18 years. *Clin Orthop Relat Res* 453:81, 2006

24. Lombardi AV, Jr., Berend KR, Mallory TH, Skeels MD, Adams JB: Survivorship of 2000 tapered titanium porous plasma-sprayed femoral components. *Clin Orthop Relat Res* 467(1):146, 2009
25. Bourne RB, Rorabeck CH, Burkart BC, Kirk PG: Ingrowth surfaces. Plasma spray coating to titanium alloy hip replacements. *Clin Orthop Relat Res*(298):37, 1994
26. Sun L, Berndt CC, Gross KA, Kucuk A: Material fundamentals and clinical performance of plasma-sprayed hydroxyapatite coatings: a review. *J Biomed Mater Res* 58(5):570, 2001
27. Liu Y, Wu G, de Groot K: Biomimetic coatings for bone tissue engineering of critical-sized defects. *J R Soc Interface* 2010
28. Parthasarathy J, Starly B, Raman S, Christensen A: Mechanical evaluation of porous titanium (Ti6Al4V) structures with electron beam melting (EBM). *J Mech Behav Biomed Mater* 3(3):249, 2010
29. Chahine G, Koike M, Okabe T, Smith P, Kovacevic R: The design and production of Ti-6Al-4V ELI customized dental implants. *JOM* 60(11):50, 2008
30. Heinel P, Rottmair A, Körner C, Singer R: Cellular Titanium by Selective Electron Beam Melting. *Advanced Engineering Materials* 9(5):360, 2007
31. Heinel P, Muller L, Korner C, Singer RF, Muller FA: Cellular Ti-6Al-4V structures with interconnected macro porosity for bone implants fabricated by selective electron beam melting. *Acta Biomater* 4(5):1536, 2008
32. Ponader S, Vairaktaris E, Heinel P, Wilmowsky CV, Rottmair A, Korner C, Singer RF, Holst S, Schlegel KA, Neukam FW, Nkenke E: Effects of topographical surface modifications of electron beam melted Ti-6Al-4V titanium on human fetal osteoblasts. *J Biomed Mater Res A* 84(4):1111, 2008
33. Thomsen P, Malmstrom J, Emanuelsson L, Rene M, Snis A: Electron beam-melted, free-form-fabricated titanium alloy implants: Material surface characterization and early bone response in rabbits. *J Biomed Mater Res B Appl Biomater* 90(1):35, 2009
34. Ponader S, von WC, Widenmayer M, Lutz R, Heinel P, Korner C, Singer RF, Nkenke E, Neukam FW, Schlegel KA: In vivo performance of selective electron beam-melted Ti-6Al-4V structures. *J Biomed Mater Res A* 92(1):56, 2010
35. Facchini L, Magalini E, Robotti P, Molinari A, Hoges S, Wissenbach K: Ductility of a Ti-6Al-4V alloy produced by selective laser melting of prealloyed powders. *Rapid Prototyping Journal* 16(6):450, 2010
36. Mullen L, Stamp RC, Fox P, Jones E, Ngo C, Sutcliffe CJ: Selective laser melting: a unit cell approach for the manufacture of porous, titanium, bone in-growth constructs, suitable for orthopedic applications. II. Randomized structures. *J Biomed Mater Res B Appl Biomater* 92(1):178, 2010
37. Warnke PH, Douglas T, Wollny P, Sherry E, Steiner M, Galonska S, Becker ST, Springer IN, Wiltfang J, Sivananthan S: Rapid prototyping: porous titanium alloy scaffolds produced by selective laser melting for bone tissue engineering. *Tissue Eng Part C Methods* 15(2):115, 2009
38. Pattanayak DK, Fukuda A, Matsushita T, Takemoto M, Fujibayashi S, Sasaki K, Nishida N, Nakamura T, Kokubo T: Bioactive Ti metal analogous to human cancellous bone: Fabrication by selective laser melting and chemical treatments. *Acta Biomater* 7(3):1398, 2011
39. Feighan JE, Goldberg VM, Davy D, Parr JA, Stevenson S: The influence of surface-blasting on the incorporation of titanium-alloy implants in a rabbit intramedullary model. *J Bone Joint Surg Am* 77(9):1380, 1995
40. Goldberg VM, Stevenson S, Feighan J, Davy D: Biology of grit-blasted titanium alloy implants. *Clin Orthop Relat Res*(319):122, 1995
41. D'Lima DD, Lemperele SM, Chen PC, Holmes RE, Colwell CW, Jr.: Bone response to implant surface morphology. *J Arthroplasty* 13(8):928, 1998
42. Daugaard H, Elmengaard B, Bechtold JE, Soballe K: Bone growth enhancement in vivo on press-fit titanium alloy implants with acid etched microtexture. *J Biomed Mater Res A* 87(2):434, 2008
43. Erli HJ, Ruger M, Ragoss C, Jahnen-Dechent W, Hollander DA, Paar O, von WM: The effect of surface modification of a porous TiO₂/perlite composite on the ingrowth of bone tissue in vivo. *Biomaterials* 27(8):1270, 2006
44. Hacking SA, Harvey EJ, Tanzer M, Krygier JJ, Bobyn JD: Acid-etched microtexture for enhancement of bone growth into porous-coated implants. *J Bone Joint Surg Br* 85(8):1182, 2003
45. Stöver M, Renke-Gluszko M, Schratzenstaller T, Will J, Klink N, Behnisch B, Kastrati A, Wessely R, Hausleiter J, Schömg A, Wintermantel E: Microstructuring of stainless steel implants by electrochemical etching. *J Mater Sci* 41:5569, 2006

-
46. Giordano C, Sandrini E, Busini V, Chiesa R, Fumagalli G, Giavaresi G, Fini M, Giardino R, Cigada A: A new chemical etching process to improve endosseous implant osseointegration: in vitro evaluation on human osteoblast-like cells. *Int J Artif Organs* 29(8):772, 2006
 47. Takemoto M, Fujibayashi S, Neo M, Suzuki J, Matsushita T, Kokubo T, Nakamura T: Osteoinductive porous titanium implants: effect of sodium removal by dilute HCl treatment. *Biomaterials* 27(13):2682, 2006
 48. Best SM, Porter AE, Thian ES, Huang J: Bioceramics: past, present and for the future. *Journal of the European Ceramic Society* 28:1319, 2008
 49. Porter AE, Hobbs LW, Rosen VB, Spector M: The ultrastructure of the plasma-sprayed hydroxyapatite-bone interface predisposing to bone bonding. *Biomaterials* 23(3):725, 2002
 50. Shepperd JA, Apthorp H: A contemporary snapshot of the use of hydroxyapatite coating in orthopaedic surgery. *J Bone Joint Surg Br* 87(8):1046, 2005
 51. Weng J, Liu Q, Wolke JG, Zhang X, de GK: Formation and characteristics of the apatite layer on plasma-sprayed hydroxyapatite coatings in simulated body fluid. *Biomaterials* 18(15):1027, 1997
 52. Capello WN, D'Antonio JA, Manley MT, Feinberg JR: Hydroxyapatite coating. p. 1005. In Callaghan JJ, Rosenberg AG, Rubash HE (eds): *Adult Hip*. Lippincott Williams & Wilkins; Philadelphia, 2007
 53. Barrere F, van der Valk CM, Meijer G, Dalmeijer RA, de Groot K, Layrolle P: Osteointegration of biomimetic apatite coating applied onto dense and porous metal implants in femurs of goats. *J Biomed Mater Res B Appl Biomater* 67(1):655, 2003
 54. Davis JR: Coatings. p. 179. In Davis & Associates (ed): *Handbook of Materials for Medical Devices*. ASM International; Ohio, 2005
 55. Jaffe WL, Scott DF: Total hip arthroplasty with hydroxyapatite-coated prostheses. *J Bone Joint Surg Am* 78(12):1918, 1996
 56. Tsukeoka T, Suzuki M, Ohtsuki C, Tsuneizumi Y, Miyagi J, Sugino A, Inoue T, Michihiro R, Moriya H: Enhanced fixation of implants by bone ingrowth to titanium fiber mesh: effect of incorporation of hydroxyapatite powder. *J Biomed Mater Res B Appl Biomater* 75(1):168, 2005
 57. Redepenning J, Schlessinger T, Burnham S, Lippiello L, Miyano J: Characterization of electrolytically prepared brushite and hydroxyapatite coatings on orthopedic alloys. *J Biomed Mater Res* 30(3):287, 1996
 58. Hägi TT, Enggist L, Michel D, Ferguson SJ, Liu Y, Hunziker EB: Mechanical insertion properties of calcium-phosphate implant coatings. *Clin Oral Implants Res* 2010
 59. Habibovic P, Barrère F, van Blitterswijk CA, de Groot K, Layrolle P: Biomimetic hydroxyapatite coating on metal implants. *J Am Ceram Soc* 85(3):517, 2002
 60. Kuroda S, Virdi AS, Li P, Healy KE, Sumner DR: A low-temperature biomimetic calcium phosphate surface enhances early implant fixation in a rat model. *J Biomed Mater Res A* 70(1):66, 2004

Chapter 2



Long-term survivorship analysis of the cementless spotorno femoral component in patients less than 50 years of age

2



Abstract

The long-term survival of the cementless Spotorno (CLS) femoral component (Zimmer Inc, Warsaw, USA) was evaluated in a consecutive series of 85 patients (100 hips) less than 50 years of age. The mean follow-up was 12.3 years. Two patients (3 hips) were lost to follow-up, and 3 (4 hips) died. The survival rate of the CLS stem was 96.9% (confidence interval [CI], 93.6%-100%) after 13 years based on revision of the stem for any reason. The survival of the stem with revision for aseptic loosening as the end point was 97.9% (CI, 95.1%-100%) at 13 years. The mean Harris hip score at time of follow-up was 94. The long-term survival of the CLS stem is excellent in patients less than 50 years of age.

Introduction

Cementless fixation is used in about two-thirds of all primary total hip replacements (THR) in the United States.[1] Cementless prostheses are developed in order to reduce aseptic loosening of the prosthesis.[2] Key factors for long-term survival of cementless implants are their frictional stability and surface properties which promote secondary stability by bone ingrowth.[3]

The cementless Spotorno (CLS) femoral component was introduced in 1984 and has become one of the most widely used cementless hips in the world. **(Figure 1)** The CLS femoral component is a wedge shaped stem with proximal fins on the anterior and posterior surface designed to achieve primary proximal stability and to encourage osseointegration. The prosthesis is not designed to fill the medullary canal of the femur distally completely, thereby encouraging the transfer of load proximally in the femur.[4] Several studies showed good long term survival for the CLS femoral component.[5;6]

Younger patients place increased demands on their joint reconstruction due to a higher activity level.[7] Only few long term results of the CLS femoral component in young patients are published. [8] None of them studied the survival in patients under 50 years of age. The goal of our study is to evaluate the long term survival of the CLS femoral component in patients under 50 years of age.

Methods

Between 1992 and 1997 a consecutive series of 85 patients (100 hips) under 50 years of age received a CLS (Zimmer Inc, Warsaw, USA) femoral component in combination with a cementless

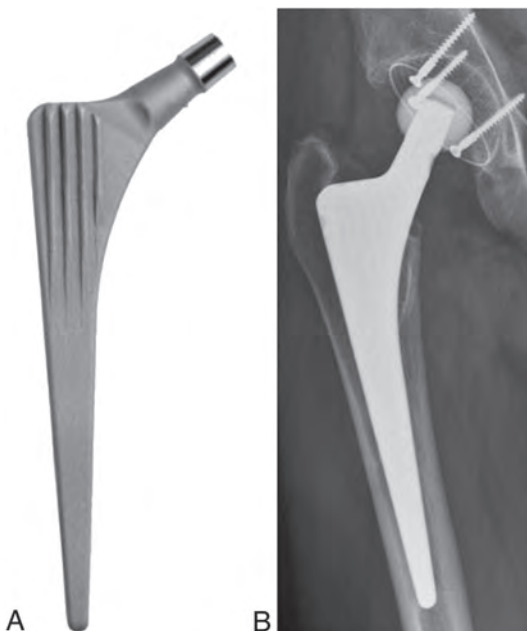


Figure 1. The CLS femoral component.
Figure 1B shows an x-ray of the CLS stem.

Table 1. Patient characteristics: primary diagnosis

Diagnosis	Number of hips
Osteoarthritis	27
Congenital dysplasia (CHD)	21
Rheumatoid arthritis	11
Avascular necrosis	10
Posttraumatic	7
Other	24

isoelastic titanium coated RM (Mathys Ltd, Betlach, Switzerland) acetabular component. The 37 men and 48 women together had mean age at the time of surgery of 44 years (range 16-50 years). The diagnoses are listed in table 1. 24 hips had undergone previous osteotomy (12 femoral, 8 acetabular and 4 both femoral and acetabular). The mean follow up was 12.3 years (range 9.8-15.5). 2 patients (3 hips) were lost to follow up and 3 patients (4 hips) died during follow-up. (Figure 2) At time of dead the joint prosthesis was in situ for all these hips.

The total hip arthroplasty was implanted press-fit using a posterolateral approach to the hip in all patients. The patients were allowed full weight bearing in the early postoperative period. Antibiotic prophylaxis was administered to all patients before surgery. Thromboprophylaxis (low molecular weight heparin) was given in the post operative period. 92% of the patients received NSAID's in order to prevent heterotopic ossification, the rest of the patients (8%) had gastric complains.

Clinical follow-up included evaluation of range of motion, gait and walking distance. The Harris hip score [9] was also calculated.

Radiological follow up was performed on recent standardized anteroposterior pelvic radiographs. Two observers scored the radiographs for alignment, subsidence, heterotopic ossification, radiolucent lines, stress shielding and pedestal formation. Varus or valgus malalignment was defined as a deviation of the longitudinal femoral axis of more than 2°.[8] Subsidence was calculated by measuring the distance between the tip of the greater trochanter and the shoulder of the prosthesis in comparison to this distance in an early post-operative radiograph. The Brooker classification was used to evaluate heterotopic ossification.[10] Radiolucent lines and cysts were allocated to Gruen zones. [11] Stress shielding was defined by the classification of Engh.[12] Classification as first degree (rounding of the medial femoral neck) was not regarded as a sign of stress shielding.[8] Pedestal formation was defined as a shelf of new endosteal bone at the tip of the stem partly or completely bridging the intramedullary canal. [8]

In case of revision, the radiographs directly before revision were analysed for radiolucent lines and stem migration. Migration was defined as > 5 mm subsidence. [13]

A Kaplan Meier survival analysis was performed to calculate the cumulative survival rate using revision of the stem for any reason and revision of the stem for aseptic loosening as the endpoint. In addition to these analyses a worst-case survival curve was plotted for revision for any reason and revision for aseptic loosening. The worst-case survival analysis is based

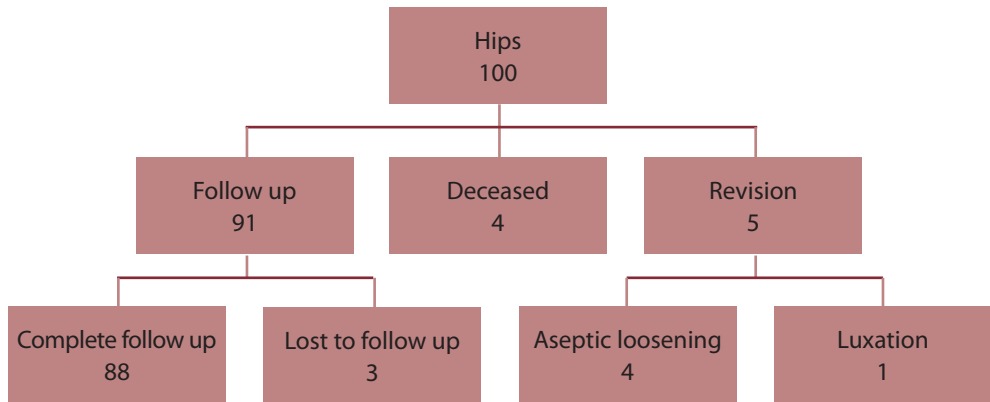


Figure 2. Distribution of the hips after implantation of a CLS femoral component

on the assumption that implants in all patients lost to follow-up have failed and have been revised. [14] The time to revision was defined as the time between the date of implantation and revision. Patients without revision were censored at the date of the radiological follow-up or at death. 95% confidence intervals of the survival rates were calculated.

Cox regression analysis was performed to examine the influence of age, gender, diagnosis, stem alignment and previous osteotomy on the survival rate of the stem.

Results

Functional outcome: At the follow-up examination, the mean HHS in the 91 hips that were available for follow-up and had not required a revision was 94 (range 35-100).

Revisions: Of the 100 femoral components 5 had been revised. 1 femoral component was revised for a luxation 2 weeks after the total hip arthroplasty and 4 stems were revised for aseptic loosening. (**Figure 2**) The mean time to revision was 8.9 years (range 0.0-14.8), detailed information on the femoral revisions is shown in **table 2**.

Radiographic findings: For the unrevised femoral component, the alignment of 78 (86%) stems was neutral. 13 femoral components had a deviation of $>2^\circ$ from the neutral axis. 12 (13%) femoral components were in varus position, whereas 1 was in valgus position. The

Table 2. Revisions of femoral component in chronological order

Case	Gender	Diagnosis	Age	Time to revision	Reason	Osteolysis	Migration
1	M	OA	47.1	0.0	Luxation	-	-
2	M	PT	40.5	4.9	AL	Zone 1 + 2	-
3	V	AVN	33.9	8.9	AL	Zone 1	-
4	M	OA	48.7	14.3	AL	Zone 1	-
5	M	AVN	43.3	14.8	AL	Zone 1	-

OA= osteoarthritis PT= posttraumatic, AVN= avascular necrosis AL = aseptic loosening

Migration = subsidence > 5 mm

mean subsidence was 1.9 mm (range 0-15mm). Subsidence of >5mm was seen in 2 femoral components (2%) , none of which needed revision. Grade 4 heterotopic ossification was seen in 1 hip (1%), grade 3 in 12 hips (13%), grade 2 in 11 hips (12%) and grade 1 in 16 hips (18%). Radiolucent lines or cysts were mainly seen in Gruen zone 1 and 7 (**Figure 3**). Stress shielding was classified as 2nd degree (loss of medial cortical density in Gruen zone 1) for 22 hips (24%), and as 3rd degree (more extensive resorption of cortical bone) for 2 hips (2%). No hips showed cortical resorption extended below Gruen zone 6 and 7 into the diaphysis, 4th degree stress shielding. Pedestal formation at the tip of the prosthesis was noted in 26% of the hips. The radiographic findings on revised components are listed in **table 2**. Analysis of the radiographs directly before revision showed no migration of the femoral components, however radiolucent lines or cysts occurred in 4 hips.

Complications and re-surgery: During surgery a fissure of the femur occurred in 3 patients. 1 patients suffered from a transient sciatic nerve palsy. No wound infections or deep infections occurred. 6 patients had a dislocation, one of them underwent revision 2 week after surgery and 5 hips were treated conservatively and stabilised.

12 patients underwent re-surgery that was not related to the femoral component. One patient had a femoral head exchange due to a restricted range of motion and severe heterotopic ossification was resected in one patient. Ten patients had a revision of the acetabular component after a mean of 12.1 years due to wear (6 patients), aseptic loosening (2 patients) and trauma (2 patients).

Survival analysis: The survival rate of the CLS femoral component was 96.9% (CI 93.6% to 100%) after 10 and 13 years based on revision of the femoral component for any reason. The worst case scenario showed a survival of 94.0% (CI 89.3% to 98.7%) after 10 and 13 years. The survival of the femoral component with revision for aseptic loosening as the endpoint, was 97.9% (CI 95.1% to 100%) at 10 and 13 years. For aseptic loosening as the endpoint, the survival rate of the worst case scenario was 95.0% (CI 90.6% to 99.3%) at 10 and 13 years. (**Figure 4**)

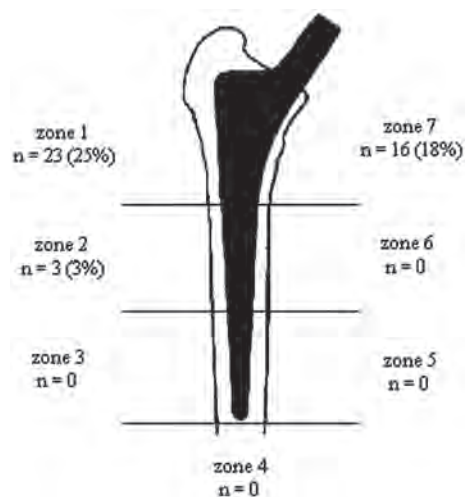


Figure 3. Distribution of radiolucent lines or cysts allocated to Gruen zones

Regression analysis: Cox regression analysis showed no influence of age, gender, diagnosis, stem alignment and previous osteotomy on the survival rate of the stem.

Discussion

In this study, a 13 year survival of 96.9% was found for the CLS femoral component. This is a good result according to the NICE criteria, that defined prostheses with a revision rate of 10% or less at 10 years best prosthesis.[15] One should take in account that these survival was established in a group of young patients, that place increased demands on the joint replacement.[7] Patients lost to follow-up are likely to have a worse outcome[14] , therefore a worst case survival analysis was performed. Even in this worst case scenario the criteria for best prostheses are met. An excellent survival of the CLS femoral component is showed with revision for aseptic loosening as the endpoint at 10 and 13 years. Clinical outcome based on the Harris Hip score was excellent.[16]

The strength of this study is the long follow-up and the small number of patients lost to follow-up. The inclusion of patients was restricted to patients that received a CLS stem in combination with a RM acetabular component. This is a potential selection bias. However, the diversity in diagnosis is high, suggesting most groups of patients were included.

Radiographic analysis showed migration in two stems that were not revised. These patients were asymptomatic and had a Harris Hip score of 81 and 91 respectively. No revision was scheduled for these patients at latest follow-up. Therefore, these hips were not counted as failures. Radiolucent lines or cysts were found in 35% of the hips and 26% showed pedestal formation. Although both are identified as a sign of instability[17], they appeared not to affect clinical outcome, but should be monitored carefully.

Ten patients had a isolated revision of the acetabular component, the femoral component was left in place. The decision to revise a well-fixed femoral component in hips requiring isolated acetabular revision is challenging. Revision can result in destruction of bone stock and increased operation time.[18] On the contrary, retaining of the femoral component can compromise the isolated acetabular revision. Isolated acetabular revision is by example associated with a higher rate of dislocation.[19] Retaining of the femoral component showed continues good clinical results of the femoral component at 8 years after the isolated cup revision.[18]

Long-term follow up studies of CLS survival show overall survival rates of 92% at 12 years and 89% at 17 years in patients of all ages. Aldinger, Thomsen et al.[8] investigated the survival in young patients as well. The survival in patients <55 years was 97% at 12 years. This is comparable to the current study (97% at 13 years). However, the group of patients in the current study is more challenging, because of differences in age and previous surgery.

The survival rate of implants in young patients declines with increasing age per year.[20] The population of Aldinger, Thomson et al.[8] (<55 years) has therefore a reduced risk of revision compared to the population in the current study. The reduced survival in young patients is mainly due to a higher activity level, which place increased demands on the implants.[7;21]

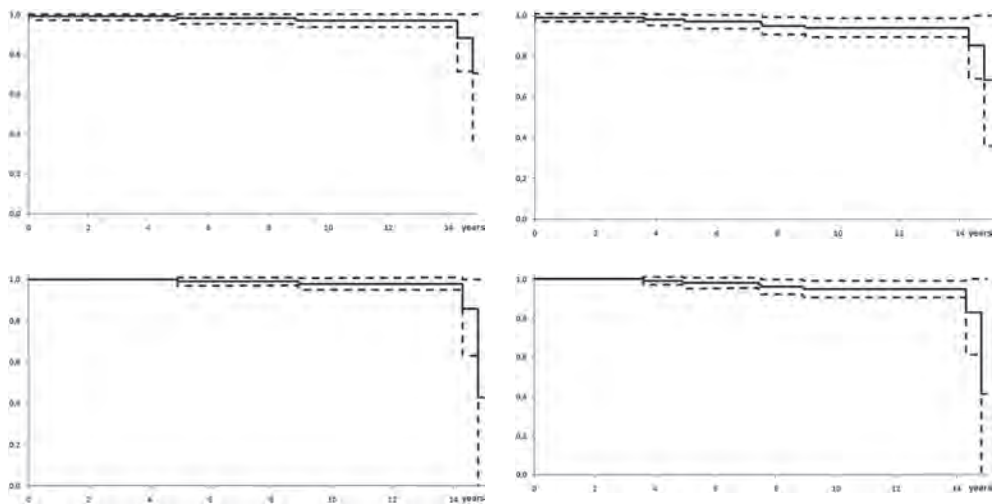


Figure 4. Survival analysis of the CLS femoral component for patients less than 50 years old. Panel (A) shows the survival with revision for any reason as the end point, the worst-case survival is shown in panel (B). The survival and worst-case survival with aseptic loosening as the end point is shown in panels (C) and (D), respectively. The broken lines indicate the 95% confidence interval.

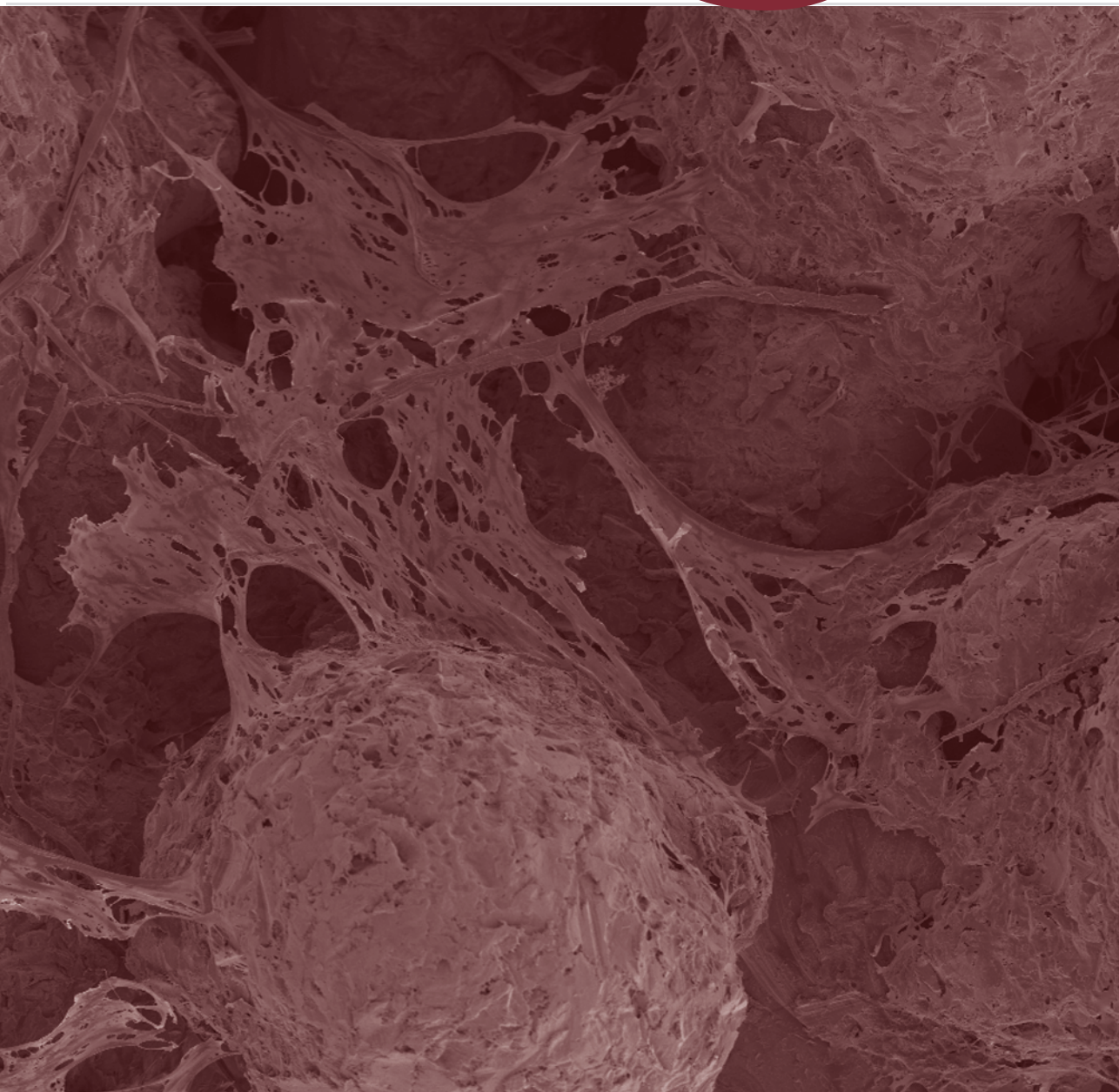
The amount of hips that had previous osteotomy was high compared to the study of Aldinger, Thomson et al.[8] Total hip arthroplasty after previous femoral osteotomy can be technically demanding due to distortion of the proximal femur.[22] Boos, Krushell et al.[22] showed a trend towards decreased implant survival in hips with previous osteotomy. Although this trend was not replicated in this study (due to small numbers), it is likely that previous femoral osteotomy influence survival of the femoral component.

In conclusion, the long-term survival rate found for the CLS femoral component is excellent, particularly considering the young age and diversity in diagnosis of the population.

References

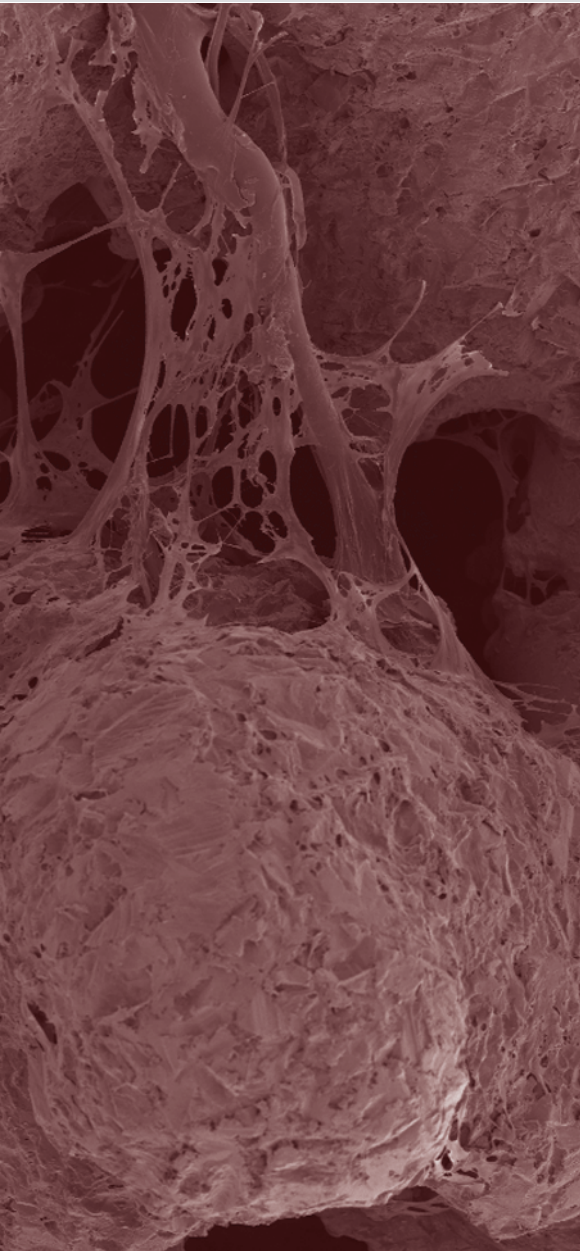
1. Mendenhall S. Hip and knee implant review. 1-16. 2004. Orthopedic network 14 (3).
2. Duffy GP, Berry DJ, Rowland C, Cabanela ME: Primary uncemented total hip arthroplasty in patients <40 years old: 10- to 14-year results using first-generation proximally porous-coated implants. *J Arthroplasty* 16(8 Suppl 1):140, 2001
3. Ihle M, Mai S, Pfluger D, Siebert W: The results of the titanium-coated RM acetabular component at 20 years: a long-term follow-up of an uncemented primary total hip replacement. *J Bone Joint Surg Br* 90(10):1284, 2008
4. Spotorno L, Romagnoli S, Ivaldo N, Grappiolo G, Bibbiani E, Blaha DJ, Guen TA: The CLS system. Theoretical concept and results. *Acta Orthop Belg* 59 Suppl 1:144, 1993
5. Aldinger PR, Breusch SJ, Lukoschek M, Mau H, Ewerbeck V, Thomsen M: A ten- to 15-year follow-up of the cementless spotorno stem. *J Bone Joint Surg Br* 85(2):209, 2003
6. Jung A, Parsch D, Ewerbeck V, Aldinger PR. Langzeitergebnisse (15 - 20 Jahre) des zementfreien CLS Schaftes. Deutscher Kongress für Orthopädie und Unfallchirurgie. 2006.
7. McAuley JP, Szuszczewicz ES, Young A, Engh CA, Sr.: Total hip arthroplasty in patients 50 years and younger. *Clin Orthop Relat Res*(418):119, 2004
8. Aldinger PR, Thomsen M, Mau H, Ewerbeck V, Breusch SJ: Cementless Spotorno tapered titanium stems: excellent 10-15-year survival in 141 young patients. *Acta Orthop Scand* 74(3):253, 2003
9. Harris WH: Traumatic arthritis of the hip after dislocation and acetabular fractures: treatment by mold arthroplasty. An end-result study using a new method of result evaluation. *J Bone Joint Surg Am* 51(4):737, 1969
10. Brooker AF, Bowerman JW, Robinson RA, Riley LH, Jr.: Ectopic ossification following total hip replacement. Incidence and a method of classification. *J Bone Joint Surg Am* 55(8):1629, 1973
11. Gruen TA, McNeice GM, Amstutz HC: „Modes of failure“ of cemented stem-type femoral components: a radiographic analysis of loosening. *Clin Orthop Relat Res*(141):17, 1979
12. Engh CA, Bobyn JD, Glassman AH: Porous-coated hip replacement. The factors governing bone ingrowth, stress shielding, and clinical results. *J Bone Joint Surg Br* 69(1):45, 1987
13. Takatori Y, Nagai I, Moro T, Kuruta Y, Karita T, Mabuchi A, Ninomiya S: Ten-year follow-up of a proximal circumferential porous-coated femoral prosthesis: radiographic evaluation and stability. *J Orthop Sci* 7(1):68, 2002
14. Murray DW, Britton AR, Bulstrode CJ: Loss to follow-up matters. *J Bone Joint Surg Br* 79(2):254, 1997
15. NHS National Institute for Clinical Excellence (NICE). Guidance on the selection of prostheses for primary total hip replacement. 2000.
16. Marchetti P, Binazzi R, Vaccari V, Girolami M, Morici F, Impallomeni C, Commessatti M, Silvello L: Long-term results with cementless Fitek (or Fitmore) cups. *J Arthroplasty* 20(6):730, 2005
17. Engh CA, Massin P, Suthers KE: Roentgenographic assessment of the biologic fixation of porous-surfaced femoral components. *Clin Orthop Relat Res*(257):107, 1990
18. Moskal JT, Shen FH, Brown TE: The fate of stable femoral components retained during isolated acetabular revision: a six-to-twelve-year follow-up study. *J Bone Joint Surg Am* 84-A(2):250, 2002
19. Jones CP, Lachiewicz PF: Factors influencing the longer-term survival of uncemented acetabular components used in total hip revisions. *J Bone Joint Surg Am* 86-A(2):342, 2004
20. Karrholm J, Garellick G, Herberts P. Annual Report 2006. Swedish National Hip Arthroplasty Register. 2007.
21. Schreurs BW, Busch VJ, Veth RP: [Choice of hip prosthesis in patients younger than 50 years]. *Ned Tijdschr Geneesk* 151(35):1918, 2007
22. Boos N, Krushell R, Ganz R, Muller ME: Total hip arthroplasty after previous proximal femoral osteotomy. *J Bone Joint Surg Br* 79(2):247, 1997

Chapter 3



The effect of E-beam engineered surface structures on attachment, proliferation and differentiation of human mesenchymal stem cells

3



Abstract

Electron beam melting (E-beam) is a new technology to produce 3-dimensional surface topographies for cementless orthopedic implants. The effect of two newly designed highly porous E-beam engineered surface structures (cubic and star) on attachment, proliferation and differentiation of human mesenchymal stem cells (hMSCs) was investigated and compared to a solid sandblasted control. SEM analysis showed that the E-beam structures allowed cells to attach and spread. Proliferation on the new surface structures was comparable to the solid control. Furthermore, differentiation on the 3D structures was comparable to the control specimen. When culturing 300.000 cells for 10 days, the cubic structure showed a significantly higher differentiation rate compared to the sandblasted specimen. We conclude that the results for attachment, proliferation and differentiation of mesenchymal stem cells on the newly engineered 3-dimensional E-beam surface topographies are promising. In vivo experiments are necessary to assess the bone ingrowth potential of the new surface structures.

Introduction

Cementless implants are used in about two-thirds of all primary total hip replacements (THR) in the United States.[1] The long term success of cementless implants is dependent on post-operative bone ingrowth, whereby the initial press fit fixation transfers to a secondary mechanical fixation.[2;3] In order to achieve successful bone ingrowth, a series of events on cellular level should occur, consisting of protein adsorption onto the implant surface, cellular ingrowth and adhesion, proliferation and differentiation of stem cells or pre-osteoblasts, matrix production by osteoblasts and calcification.[4]

Surface characteristics, like roughness, pore size and porosity play a key role in these processes leading to bone ingrowth.[5] A rough surface promotes attachment of fibrin, which acts as a matrix enabling the migration of stem cells to the surface of the implant.[6] The surface characteristics in itself might be even more important for the stimulation of differentiation of stem cells or pre-osteoblasts into bone. Takahashi et al.[5] demonstrated that mesenchymal stem cells attach, proliferate and differentiate well on scaffolds with high porosities. Large pores (500 μm) are favorable for cell proliferation due to better supply of oxygen and nutrients that enhance survival and maintenance of biological activities. On the contrary, small pores (200 μm) show faster differentiation.[7] Pore sizes of at least 200 μm are needed for bone differentiation. Smaller pores will induce fibrous tissue ingrowth.[8]

During the last decade considerable efforts have been made to modify the surface characteristics of orthopedic implants in order to improve the initial bonding between the implant and its biological environment.[9] Electron beam melting (E-beam) is a new and promising technique to produce surface structures for implants and allows manufacturing of complex 3-dimensional geometries. Based on rapid prototyping technology, implants are build up from metal powder in a layer-by-layer fashion. Each layer is melted by electron beam exposure to reproduce the geometry defined by a 3D CAD model. E-beam technology enables the production of unique specimens with both solid and porous surface zones in one manufacturing step.[10] Using this technique a variety of surfaces with different characteristics can be engineered for optimal cell attachment, proliferation and differentiation.

After implantation into bone, an implant initially interacts mainly with undifferentiated mesenchymal stem cells, which will subsequently differentiate into osteoblasts.[4] Therefore, the ability to enhance cell differentiation of stem cells is a critical requisite for new surface structures to achieve bone ingrowth. So far only the reaction of pre-osteoblasts were studies on E-beam produced surfaces.[9] Although a reduced proliferation rate of human fetal osteoblasts on porous, compared to smooth and unprocessed E-beam surfaces was found, in that same study, SEM analysis demonstrated that the cells attached and spread well on all surfaces. Pore size, porosity and interconnectivity of the pores of these surfaces were limited. This suggests that the surface characteristics do indeed play an important role in cell viability and proliferation and that E-beam produced materials in itself allows cellular proliferation.

The fact that only pre-osteoblastic cells were used to test the suitability of E-beam engineered surfaces [9;11] limits the value of these studies since these cells are already differentiated into the osteoblast lineage. Hence, it remains unknown whether these surfaces would facilitate non-differentiated stem cells to differentiate into osteoblasts that would enhance secondary fixation of cementless implants. Therefore, the goal of this study was to investigate the effect of two newly designed highly porous E-beam engineered surface structures on attachment, proliferation and differentiation of human mesenchymal stem cells (hMSCs) and to compare this to the effect of conventionally made surfaces.

Materials and Methods

Materials

The specimens (Ø12 mm, height 5 mm) were made out of Ti6Al4V powder and produced with E-beam technology. The powder particles used in the E-beam technique ranged from 45-100 µm and were melted by the electron beam into the desired shapes based on CAD data. After the generation of each layer, the process platform was lowered by one layer thickness (0.1 mm), a new powder layer was applied and the process was repeated.[12;13] The overall accuracy of the E-beam technology in terms of computer model reconstruction is in the order of 300 µm. The specimens were sandblasted with corundum (particle size 100-200 µm) and biologically cleaned afterwards. Furthermore the specimens were steam sterilized.

Two different topographic surfaces were produced, each with a unique structure (a cubic and a star structure; see figure 1). As a control, a plain sample as formed by the E-beam process, that was sandblasted afterwards, was tested (**Figure 1**)

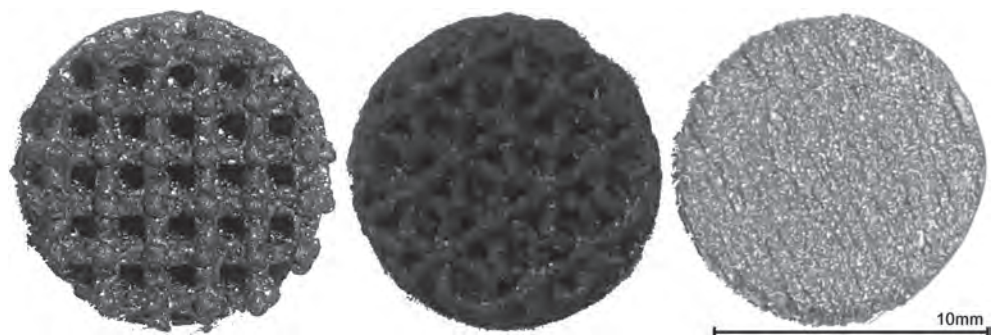


Figure 1. Surface structures. From left to right: cubic structure, star structure and the sandblasted surface.

Bar = 10mm

Surface characterization

To characterize the topographic surface structures, the specimens were embedded in methylmethacrylate (MMA) and slices of ca. 40 µm were cut using a sawing microtome (SP 1600, Leitz, Wetzlar, Germany). Subsequently the slices were analyzed by light microscopy for pore size, porosity and layer thickness.

Morphology of surface microtexture

Scanning electron microscopy (SEM, SEM6310, Jeol, Tokyo, Japan) was performed to examine the surface microtexture.

Roughness

Cell behavior is mainly influenced by microtexture of the surface rather than the 3D macrostructure. Therefore intrinsic surface roughness values, representing the microtexture of the specimens, were determined for the specimens using a Universal Surface Tester (UST) (Innowep, Wurzburg, Germany).

Cell culture

Human mesenchymal stem cells (hMSCs, Lonza, Walkersville, USA) were cultured up to passage 10 on mesenchymal stem cell growth medium (MSCGM BulletKit PT-3001, Lonza, Walkersville, USA) in a 5% CO₂ incubator at 37°C. After primary culture, cells were detached using trypsin/EDTA (Invitrogen Corporation, Carlsbad, USA). For each surface, three different cell densities (300.000, 600.000 and 1.200.000) were seeded in triplo.

The specimens were placed in 24-well plates. The cells were suspended in 1 ml medium and were put on top of the specimen. The cells were allowed to attach for 1 day. After cell attachment, cells were cultured on osteogenic differentiation medium with dexamethasone (hMSC osteogenic BulletKit PT-3002, Lonza, Walkersville, USA) and BMP-2 (10 µl/ml, rhBMP-2, R&D Systems Europe Ltd., Abingdon, United Kingdom) for 7, 10 and 14 days. Medium was changed every 3 days. All experiments were performed in triplo.

SEM analysis

One specimen of each surface structure with each amount of cells was cultured 7, 10 and 14 days for analysis with Scanning Electron Microscopy (SEM). After 7 days of culture, the specimen was washed with phosphate buffer solution (PBS). Cells were fixed with 2% glutaraldehyde in a phosphate buffer (0.1M) and washed again with PBS. Subsequently, they were dehydrated through increasing concentrations of ethanol. The specimens were processed by 2 hour critical point drying, then sputter-coated with gold and examined by a SEM (SEM6310, Jeol, Tokyo, Japan) operating in high vacuum mode.

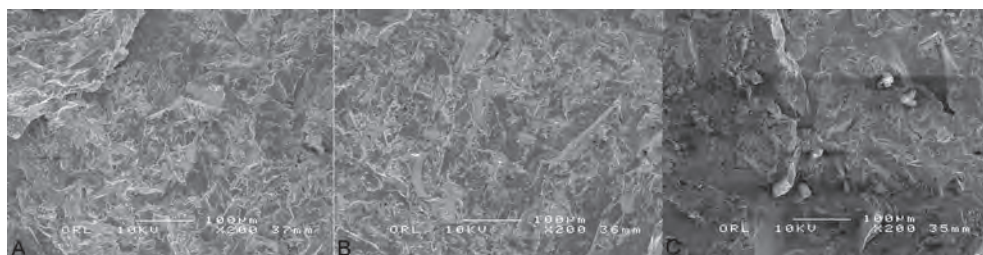


Figure 2. SEM analysis of surfaces. Surface morphology of the cubic structure (picture A), star structure (picture B) and the sandblasted surface (picture C).

Picogreen assay

Medium was removed from the specimens at the end of the culture time. The specimens were washed twice with PBS and 1 ml milliQ water was added to the well. The culture plate was frozen at -80°C , thawed and resuspended three times to remove the DNA from the cells in the specimen. A picogreen assay kit (Quant-iT PicoGreen dsDNA Assay Kit, Invitrogen Corporation, Carlsbad, USA) was used to measure DNA content.

Alkaline Phosphatase assay

An alkaline phosphatase assay was used to measure alkaline phosphatase activity. Standards and samples were added at $80\text{ }\mu\text{l/well}$. Working alkaline buffer solution (A9226, Sigma-Aldrich, St. Louis, USA) was added at $20\text{ }\mu\text{l/well}$ and the substrate solution (P5994, Sigma-Aldrich, St. Louis, USA) was added at $100\text{ }\mu\text{l/well}$. The plate was incubated for 30 minutes at 37°C . After the incubation period, the reaction was stopped by adding $100\text{ }\mu\text{l}$ of 0.3 M NaOH . An ELISA reader was used to determine the enzyme concentration. The ALP activities were normalized to protein contents of the cell lysate as measured by DNA.

Statistical analysis

Statistical analysis of the results of the picogreen and alkaline phosphatase assay was performed using one way ANOVA with a Tukey post hoc test. Significance level was set at $p < 0.05$.

Results

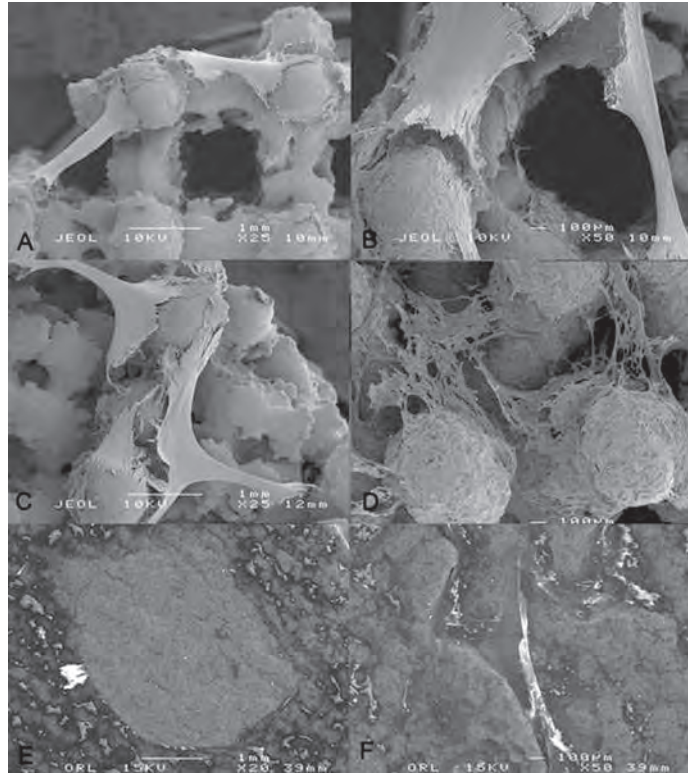
Surface characterization

The cubic structure had a pore size of 1.2 mm and a porosity of 77% and the star structure had a pore size of 1.1 mm and a porosity of 32% . The layer thickness of the cubic structure was 1.9 mm and the layer thickness of the star structure was 1.7 mm .

The SEM images of the E-beam specimens are shown in **figure 2**.

The results of the intrinsic surface roughness measurements, representing the microtexture, using UST showed a surface roughness value (R_a) of $5.18\text{ }\mu\text{m}$ for the cubic structure, $5.62\text{ }\mu\text{m}$ for the star structure and $3.67\text{ }\mu\text{m}$ for the sandblasted surface.

Figure 3. SEM analysis of cell culture. SEM analysis of cell culture on the cubic structure (picture A and B), star structure (picture C and D) and sandblasted surface (picture E and F). Cells bridge the porous of the cubic and star specimen (picture A,B and C). A network of cells was formed reaching deep inside the specimens (picture D). A plain layer of cells was formed on the sandblasted structure (picture E and F)



SEM analysis

The cells attached to the superficial and deep layers of all new surface structures. The cells spread well on the new surfaces, the top of the specimens was covered with an equally distributed layer of cells. In all specimens cells bridged the pores, particularly superficial. The amount of cells deep inside the specimen was less compared to the number of cells on the top. A network of cells was formed reaching deep inside the specimens. This network was most developed in the star structure. A plain layer of cells was formed on the sandblasted structure. (Figure 3)

Proliferation

No significant difference in DNA content was found between the specimens at 7, 10 and 14 days of culture. As expected, the amount of DNA was higher when more cells were seeded. (Figure 4)

Differentiation

After 10 days of culture with 300.000 cells, the cubic specimens showed significant higher alkaline phosphatase activity than the sandblasted specimens ($p=0.04$). No further differences between the specimens were found.

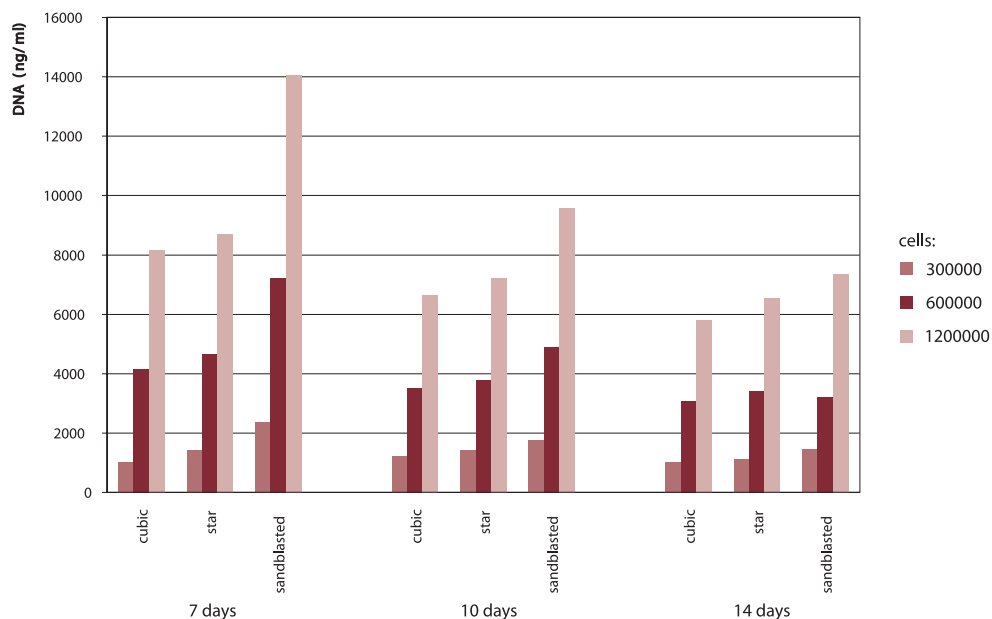


Figure 4. Cell proliferation. Graph showing the DNA content of the tested surfaces representing the cell proliferation.

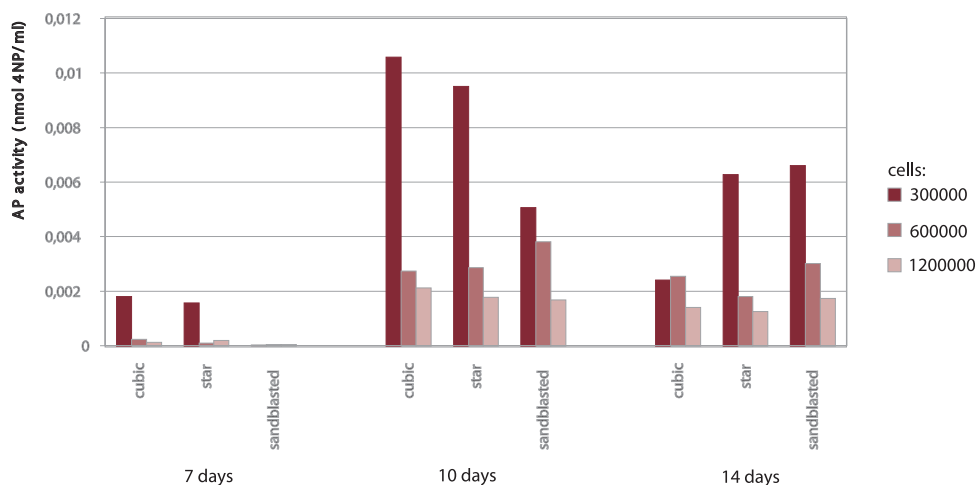


Figure 5. Cell differentiation. Graph showing the Alkaline Phosphatase activity of the tested surfaces representing the cell differentiation.

The ALP peak for the cubic and star structure occurred 10 days after seeding of the cells, whereas the peak of the sandblasted structure was not reached at 10 days. ALP activity after seeding of 300.000 cells was significantly higher than seeding of 600.000 or 1.200.000 cells ($p < 0.001$). (**Figure 5**)

Discussion

Electron beam melting is a relatively new rapid prototyping technique to produce surface structures for implants and allows manufacturing of complex 3-dimensional geometries. Using this technique, many possible surface characteristics can be engineered in order to develop the optimal surface structure for cellular attachment, proliferation and differentiation for cementless prostheses. However, the overall accuracy of the E-beam technology is limited to 300 μm . This study examined the effect of two highly porous E-beam engineered surface structures on attachment, proliferation and differentiation of human mesenchymal stem cells (hMSCs) and to compare this to the effect of a solid control surface.

Scanning electron microscopy showed that mesenchymal stem cells were able to attach and spread on both new surface structures. Previously it was demonstrated that the enlarged surface area in porous implants assists stable attachment of fibrin.[14] This stable fibrin matrix will permit stem cells and pre-osteoblastic cells to migrate to the surface of the implant where they can initiate bone formation.[14] Several groups [14-16] showed a more extensive coverage of the fibrin matrix with increasing surface area. The porous area of the new surface structures might also favor the attachment of fibrin and subsequently cell migration, although this could not be demonstrated in this in vitro study.

In vitro the formation of a continuous cell layer in cell seeding studies is more challenging in 3-dimensional geometric structures compared to smooth surfaces. The surface area of 3-dimensional surfaces is larger than flat surfaces and the attachment of cells may be compromised by for example micro-roughness induced by sandblasting treatments.[11] However if the formation of a 3-dimensional network of cells can be accomplished on complex 3-dimensional surfaces, these 'disorganized' cell layers could be the basis for optimal tissue differentiation within the pores of the surface structures. Schmidt et al.[6] even suggested that surfaces that provide the ability to form a 3-D network could push mesenchymal stem cells to differentiate into osteoblasts rather than to fibroblasts.[6] Our SEM analysis showed that a plain layer of cells was formed on the non-porous control, whereas on the new surface structures a 3-D cellular network was formed. It is likely that this cellular network enhances bone ingrowth, although this has not been adequately proven.[17]

No significant differences in cell proliferation were found between the surface structures and the control specimen. The proliferation on the 3D E-beam structures appeared to perform similarly as the solid control. This is remarkable, because the cubic and the star structure are highly porous and have a large surface area. Due to this large surface area and consequently a lack of cell-cell interactions, one can expect impaired cell proliferation.[18] Hence, the porous

E-beam structures seemed capable to overcome the disadvantage of a large surface area. In a later stage of the bone ingrowth process, a large surface area has been shown to enhance bone ingrowth and therefore provide improved bone anchorage in vivo.[19] Obviously, a great deal of cell behaviour is influenced by the microtexture of the surfaces rather than the 3D macrostructure.[11;20]

With respect to differentiation, cells on both new E-beam surface structures showed comparable differentiation potential to the control surface. However, the ALP activity of the cubic structure was significantly higher compared to the sandblasted specimen when seeding 300.000 cells at 10 day of culturing. As for proliferation, the surface characteristics play an important role in this increased differentiation. The 3-dimensional macrostructure of the cubic and star structures enable the cells to form a 3D network. As explained above, this 3D network could guide mesenchymal stem cells to differentiate into osteoblasts.[6] Furthermore, increased roughness (as seen for the microtexture of the cubic and star structures) is known to enhance cell differentiation.[4]

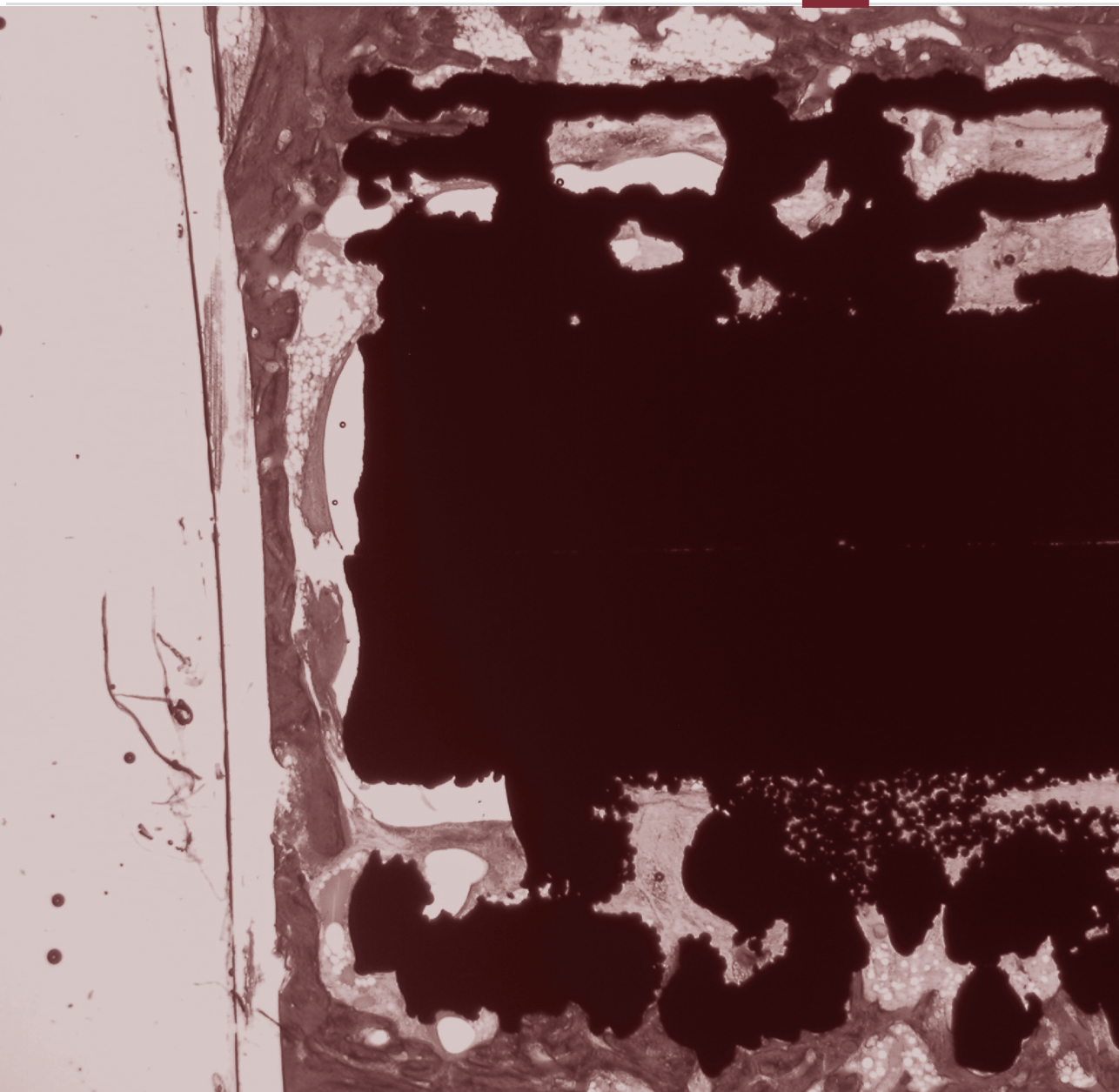
In conclusion, the newly developed surface structures as engineered in this study allow cells to attach and spread. Proliferation on the new surface structures is comparable to a solid control. The porous E-beam structures are capable to overcome the disadvantage of a large surface area in the proliferation phase. Differentiation of the 3D structures is comparable to the control specimen. When culturing 300.000 cells for 10 days, the cubic structure showed a significantly higher differentiation rate compared to the sandblasted specimen. Surface characteristics of the E-beam produced surfaces on micro and 3-dimensional macro level do influence both proliferation and differentiation rate, corresponding with the literature.[4;6;11;20]

The results for attachment, proliferation and differentiation of mesenchymal stem cells on the newly engineered 3-dimensional E-beam surface topographies are promising. In vivo experiments are necessary to assess the bone ingrowth potential of the new surface structures.

References

1. Mendenhall S. Hip and knee implant review. 1-16. 2004. Orthopedic network 14 (3).
2. Froimson MI, Garino J, Machenau A, Vidalain JP: Minimum 10-year results of a tapered, titanium, hydroxyapatite-coated hip stem: an independent review. *J Arthroplasty* 22(1):1, 2007
3. Story BJ, Wagner WR, Gaisser DM, Cook SD, Rust-Dawicki AM: In vivo performance of a modified CSTi dental implant coating. *Int J Oral Maxillofac Implants* 13(6):749, 1998
4. Kieswetter K, Schwartz Z, Dean DD, Boyan BD: The role of implant surface characteristics in the healing of bone. *Crit Rev Oral Biol Med* 7(4):329, 1996
5. Takahashi Y, Tabata Y: Effect of the fiber diameter and porosity of non-woven PET fabrics on the osteogenic differentiation of mesenchymal stem cells. *J Biomater Sci Polym Ed* 15(1):41, 2004
6. Schmidt C, Kaspar D, Sarkar MR, Claes LE, Ignatius AA: A scanning electron microscopy study of human osteoblast morphology on five orthopedic metals. *J Biomed Mater Res* 63(3):252, 2002
7. Mygind T, Stiehler M, Baatrup A, Li H, Zou X, Flyvbjerg A, Kassem M, Bunger C: Mesenchymal stem cell ingrowth and differentiation on coralline hydroxyapatite scaffolds. *Biomaterials* 28(6):1036, 2007
8. Klawitter JJ, Hulbert SF: Application of porous ceramics for the attachment of load bearing internal orthopedic applications. *J Biomed Mater Res Supp* 5(6):161, 1971
9. Ponader S, Vairaktaris E, Heintz P, Wilmowsky CV, Rottmair A, Korner C, Singer RF, Holst S, Schlegel KA, Neukam FW, Nkenke E: Effects of topographical surface modifications of electron beam melted Ti-6Al-4V titanium on human fetal osteoblasts. *J Biomed Mater Res A* 84(4):1111, 2008
10. Larsson M, Lindhe U, Harrysson O: Rapid manufacturing with electron beam melting (EBM) - A manufacturing revolution? p. 433. In Bourell D (ed): *Proceedings Solid freeform fabrication symposium*. Austin, 2003
11. Anselme K, Biggerelle M, Noel B, Dufresne E, Judas D, Iost A, Hardouin P: Qualitative and quantitative study of human osteoblast adhesion on materials with various surface roughnesses. *J Biomed Mater Res* 49(2):155, 2000
12. Heintz P, Rottmair A, Körner C, Singer R: Cellular Titanium by Selective Electron Beam Melting. *Advanced Engineering Materials* 9(5):360, 2007
13. Heintz P, Müller L, Korner C, Singer RF, Müller FA: Cellular Ti-6Al-4V structures with interconnected macro porosity for bone implants fabricated by selective electron beam melting. *Acta Biomater* 4(5):1536, 2008
14. Simmons CA, Valiquette N, Pilliar RM: Osseointegration of sintered porous-surfaced and plasma spray-coated implants: An animal model study of early postimplantation healing response and mechanical stability. *J Biomed Mater Res* 47(2):127, 1999
15. Di ID, Traini T, Degidi M, Caputi S, Neugebauer J, Piattelli A: Quantitative evaluation of the fibrin clot extension on different implant surfaces: an in vitro study. *J Biomed Mater Res B Appl Biomater* 74(1):636, 2005
16. Schwarz F, Herten M, Sager M, Wieland M, Dard M, Becker J: Histological and immunohistochemical analysis of initial and early osseous integration at chemically modified and conventional SLA titanium implants: preliminary results of a pilot study in dogs. *Clin Oral Implants Res* 18(4):481, 2007
17. Cooper LF: A role for surface topography in creating and maintaining bone at titanium endosseous implants. *J Prosthet Dent* 84(5):522, 2000
18. Kacena MA, Shivdasani RA, Wilson K, Xi Y, Troiano N, Nazarian A, Gundberg CM, Boussein ML, Lorenzo JA, Horowitz MC: Megakaryocyte-osteoblast interaction revealed in mice deficient in transcription factors GATA-1 and NF-E2. *J Bone Miner Res* 19(4):652, 2004
19. Bobyn JD, Stackpool GJ, Hacking SA, Tanzer M, Krygier JJ: Characteristics of bone ingrowth and interface mechanics of a new porous tantalum biomaterial. *J Bone Joint Surg Br* 81(5):907, 1999
20. Meyle J, Gultig K, Wolburg H, von Recum AF: Fibroblast anchorage to microtextured surfaces. *J Biomed Mater Res* 27(12):1553, 1993

Chapter 4



Frictional and bone ingrowth properties of engineered surface topographies produced by electron beam technology

4



Abstract

Electron beam melting (E-beam) is a new technology to produce 3-dimensional surface topographies for cementless orthopedic implants. The friction coefficients of two newly developed E-beam produced surface topographies were in vitro compared with sandblasted E-beam and titanium plasma sprayed controls. Bone ingrowth (direct bone–implant contact) was determined by implanting the samples in the femoral condyles of 6 goats for a period of 6 weeks.

Friction coefficients of the new structures were comparable to the titanium plasma sprayed control. The direct bone–implant contact was 23.9 and 24.5% for the new surface structures. Bone–implant contact of the sandblasted and titanium plasma sprayed control was 18.2 and 25.5%, respectively. The frictional and bone ingrowth properties of the E-beam produced surface structures are similar to the plasma-sprayed control. However, since the maximal bone ingrowth had not been reached for the E-beam structures during the relatively short-term period, longer-term follow up studies are needed to assess whether the E-beam structures lead to a better long-term performance than surfaces currently in use, such as titanium plasma spray coating.

Introduction

Cementless fixation is used in about two-thirds of all primary total hip replacements (THR) in the United States.[1] Although the overall results of THR are good, 5 to 10 percent of the cementless implants still fail within 10 years of implantation. [2;3] Instability, aseptic loosening and infection are the most important reasons for implant failure within 5 years of implantation, whereas aseptic loosening is by far the main reason for failure after 5 years.[4] The etiology of aseptic loosening is multifactorial; wear debris, stress shielding and micromotion at the bone-implant interface play a role.[5] The frequency of failure is likely to increase due to the implantation in younger and more active patients.[6] Revision surgery after failure of an implant creates a large burdens for both the patient and society[7]; thus there is a need for improvement of cementless implants in order to avoid aseptic loosening. Although the process of aseptic loosening is not completely understood,[2] roentgen stereo-photogrammetric analysis studies have shown that long-term loosening rates after a mean follow-up period of 8 years were highly correlated with early post-operative migration.[8] This strongly suggests that inadequate direct postoperative bone-implant interface characteristics play a crucial role in the fate of the implant behavior and its survival. A high friction coefficient between the implant and the bone will enhance initial stability with low micromotions at the interface.[9] Sufficient frictional stability will enable bone ingrowth into the surface of the implant, resulting in a long lasting mechanical interlock of the implant and optimal secondary mechanical stability.

In this light, a new implant should be designed not only with respect to mechanical properties (mechanical strength and elastic modulus of the bulk material) and surface chemistry, but frictional and bone ingrowth properties should be taken in account as well in order to avoid implant failure.[10] This can be achieved by selecting the optimal combination of surface roughness, pore size and porosity of the ingrowth layer.[11] With respect to initial stability, it has been demonstrated that an increased roughness creates more interface friction in addition to an increase in bone ingrowth (measured by bone implant contact).[12;13] With respect to secondary stability, coatings with porosities of 50 % show good survival;[14] furthermore a substantial increase in fixation strength can be obtained by increasing the porosity of implants to 75-80%.[15] It is necessary to have interconnectivity between the pores in order to permit bone ingrowth.[16] There is, however, an upper limit in the porosity due to the restrictions associated with mechanical strength properties.[17] In general, a high porosity is related to an increased pore size. With respect to pore size, a diameter of at least 100 μm is needed to allow bone ingrowth and eventually vascularisation.[18] Although the optimal pore size has yet to be determined, it is evident that this parameter too affects bone ingrowth.[17]

The aforementioned surface characteristics of cementless implants can be modified by various techniques, such as plasma spraying or sintering of metal powder and fibers. A particularly promising and relatively new technology to produce new surface geometries is Electron Beam Melting (E-beam).[19-22] Based on rapid prototyping technology, implants are built up from metal powder in a 'layer-by-layer' fashion. Each layer is melted by electron beam exposure to

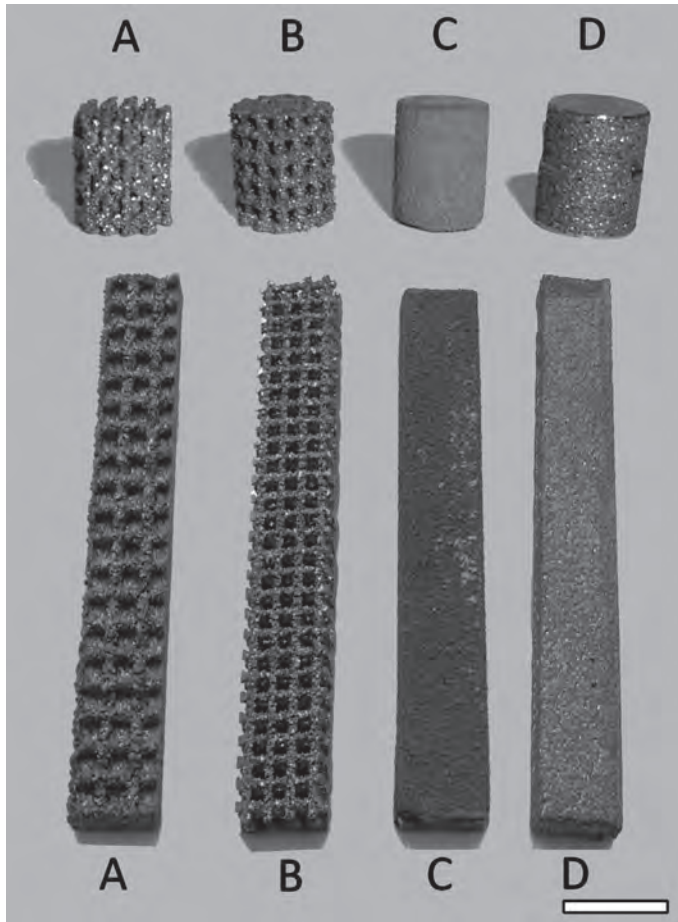


Figure 1. Specimens. On top the specimens for the in vivo experiment, below the specimens for the friction test. A = wave structure, B = cubic structure, C = plasma spray coating and D = sandblasted surface. (bar = 10 mm)

reproduce the geometry defined by a 3D CAD model. The E-beam technology enables the production of specimens with both solid and porous zones, which makes it possible to produce a solid implant with a porous surface structure in one manufacturing step.[21]

For this study two new E-beam engineered surface topographies were produced. It was hypothesized these two structures referred to as the 'wave' and 'cubic' topographies would provide for both high frictional properties and adequate bone ingrowth characteristics.

This resulted in the following research questions: 1) Do the new surface structures provide enough friction at the bone-implant interface in order to achieve initial stability? 2) Do the new surface structures allow good bone ingrowth compared to conventionally made implant surfaces?

Materials and methods

Implants

The implants were made out of Ti6Al4V powder and produced with E-beam technology (Eurocoating SpA, Trento, Italy). In total 28 flat specimen were produced for the friction experiment and 24 cylindric specimens for the in-vivo experiment. The powder size used in the E-beam process ranged from 45 to 100 μm . The E-beam specimens were created using a 3D CAD model which was segmented into layers of 0.1 mm in order to generate layer information. Subsequently, a homogeneous powder layer was applied on the process platform in a vacuum chamber at constant high temperature ($\pm 700^\circ\text{C}$). The electron beam scanned the powder layer line by line and melted the loose powder particles at programmed locations forming a compact layer in the desired shape. The process platform was then lowered by one layer thickness (0.1 mm) and a new powder layer (of 0.1 mm thickness) was applied after which the process is repeated.[19;20] Upon completion, all specimens were sandblasted with corundum and cleaned in a specific washer for medical devices. Subsequently the specimens are dried, packed and steam sterilized in an autoclave. The overall accuracy of the E-beam technology in terms of computer model reconstruction, and thereby the tolerance of the E-beam specimens, is ± 0.15 mm. The adhesive strength (test described in ASTM F1147) of the specimens was $>50\text{MPa}$ and the taber abrasion test (as described in ASTM F1978) showed a weight loss after 100 cycles of $44.00 \pm 8.42\text{mg}$ for the wave and 27.78 ± 4.51 mg for the cubic structure. Four different specimens were made with the E-beam technique. Two experimental, porous specimens, each with a unique surface topography (either “wave” or “cubic”, Figure 1). And two solid, control specimens; one with a commercially available conventional titanium plasma spray coating (TiPore, thickness $350\mu\text{m}$) [23] and one that was only sandblasted in order to remove particulate debris). (**Figure 1**) To characterize the topographic surface structures, the specimens were embedded in methylmethacrylate (MMA) and analyzed by light microscopy (Axioplan 2, Zeiss, Oberkochen, Deutschland). Surface roughness values of the specimens were determined using a Universal Surface Tester (UST) (Innowep, Wurzburg, Germany).

Friction experiment

Friction at the bone-implant interface of the 2 new surface structures and the 2 control surfaces was evaluated using 7 specimens from each group. The surface structure was applied on one side of the flat specimen ($7 \times 55 \times 4\text{mm}$), whereas the other side was polished.

A complete femur was obtained from a fresh frozen human cadaver provided by the Anatomy department of the Radboud University Nijmegen Medical Center according to Dutch law. Box shaped bone samples ($12 \times 20 \times 4$ mm) were machined from the cortical bone of this femur. A DEXA scan (QDR 4500, Hologic Inc., Bedford, MA, USA) was performed to define the bone mineral density of each bone sample (average BMD = 0.371 g/cm^2 , SD = 0.047 g/cm^2). Subsequently each specimen was assigned to a specific bone sample, randomizing for BMD. The bone sample was securely placed in a jig and the specimen was positioned against the

bone sample, clamping it with a low-friction roller bearing. Subsequently this setup was placed in a 37°C water basin and stabilized by a counterweight providing a normal force (F_n , 40N). (**Figure 2**).

A material testing system (MTS 458.2 MicroConsole™, Minneapolis, MN, USA) was used to rub the titanium specimens alongside the bone specimen with a fixed displacement rate (0.33 mm/sec) over a distance of 30 mm. The required force was measured and divided by the normal force in order to define the friction coefficient.

In-vivo experiment

Surgery was performed on six (sample size calculation: power = 0.8, $\alpha = 0.05$) female, skeletal mature goats (*Capra Hircus Sana*), weighing 47-72 kg (mean 55 kg). Each goat received four different cylindrical implants (\varnothing 8 mm, length 10 mm), two with the new topographic structures and two controls. Three different implantation areas on each of the hind legs were used: the lateral femoral condyle, the medial femoral condyle and the region dorsal of the femoral trochlea. The used model was combined out of two existing models[24;25] in order to maximize the amount of specimens in each goat. The new and control surface structures were

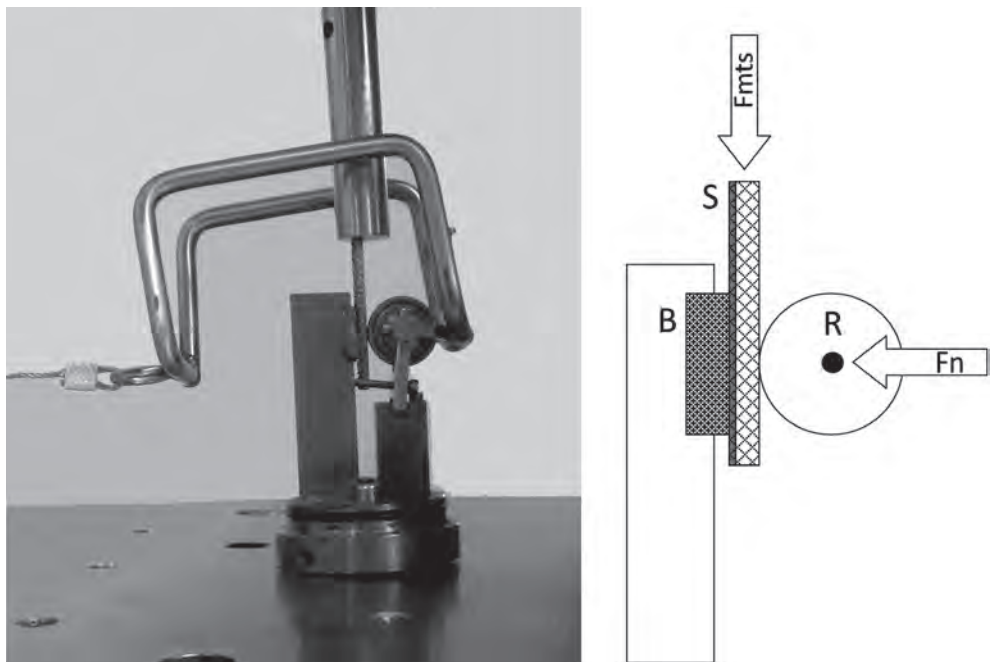


Figure 2. Friction test apparatus. A picture and schematic drawing of the friction apparatus. A roller bearing (R) was used to position the specimen (S) on the bone sample (B). A normal force (F_n) was used to stabilize the specimen on the bone. The specimen was pushed alongside the bone sample by the MTS (F_{mts}).

equally divided among the implantation areas, by which two out of six implantation areas in each goat were not used.

The goats were anaesthetized with propofol (4 mg/kg, B.Brown, Melsungen, Germany), intubated and anesthesia was maintained using isoflurane. The goats were placed in a supine position and the implantation procedure was performed under strict sterile conditions. The knee was approached medially, visualizing the origin of the medial collateral ligament. Just proximal to the origin a hole was drilled into the medial condyle. Sharp cannulated drills with an increasing diameter (Ø 6.0 and 8.0 mm) were used. Saline was used during the drilling to prevent heat induced necrosis. The hole was inspected to guarantee the specimen would be completely surrounded by trabecular bone. The implant was inserted into the hole and the fascia and skin were closed separately with resorbable sutures. This procedure was repeated on the lateral condyle and a third area located proximal to the hole in the lateral condyle, perpendicular on the cortex. In this way the specimen was implanted dorsal of the femoral trochlea. The goats received postoperative ampicillin (7.5 mg/kg Intervet, Boxmeer, The Netherlands) during 4 days and were housed at a farm. Fluorochromes were administered by subcutaneous injection at 2 (Tetracyclin), 4 (Xylenol Orange) and 6 weeks (Calcein green) after surgery during two days in order to make it possible to assess bone ingrowth at these time points. Goats were sacrificed 6 weeks and 2 days post-operative by an overdose of sodium pentobarbital (Euthesate, Ceva Santa Animale, Libourne, France). This study was approved by the animal ethics committee of the Radboud University Nijmegen and the NIH principles of laboratory animal care were followed.

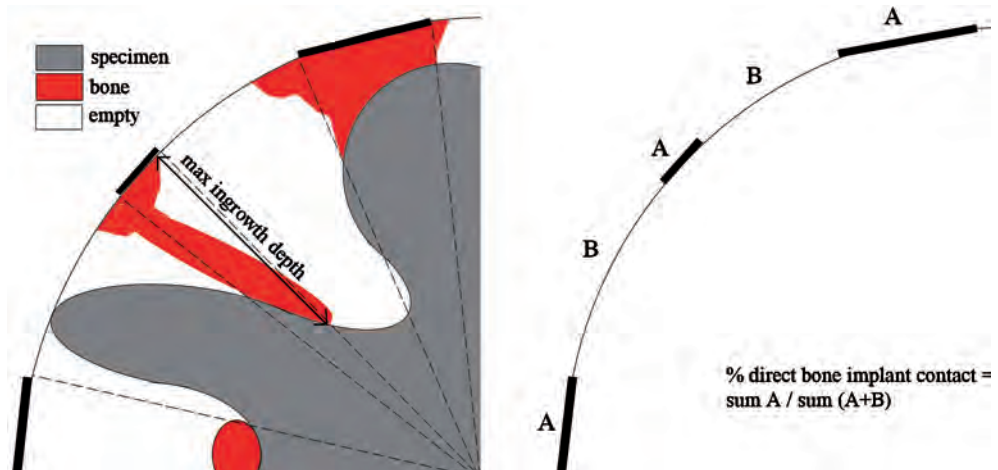


Figure 3. Measurement method for bone ingrowth depth and direct bone-implant contact. The arrow represents the maximum bone ingrowth depth of this quadrant. Direct bone-implant contact was projected onto a circle representing the circumference of the implant in order to determine the percentage of direct bone-implant contact.

Histological analysis

After sacrificing the animals, the distal femurs were retrieved. Each specimen and the surrounding bone tissue was fixed in phosphate-buffered 4% formaldehyde solution for 4 days and embedded in MMA. Slices of ca. 40 μ m, perpendicular to the length of the specimen, were cut using a sawing microtome (SP 1600, Leitz, Wetzlar, Germany). Quantitative analysis of bone ingrowth was performed using fluorescence microscopy on unstained slices and light microscopy on Hematoxylin/Eosin (HE) stained slices.

Each slice was analyzed using AnalySIS (AnalySIS 3.2 Soft Imaging System, Münster, Germany). For the bone ingrowth depth measurement, the sectioned specimen was divided into 4 quadrants and bone ingrowth depth after 4 and 6 weeks was measured in each quadrant. The ingrowth depth used for analysis was defined as the average of the maximum ingrowth depth for bone (distance from the outline of the specimen to the deepest fluorochrome label, **figure 3**) in each of these quadrants. The surface areas of bone and pores inside the specimen were measured. Subsequently the percentage of bone (bone area %) in the porous area of the specimen was calculated by bone area / porous area. It was not possible to measure ingrowth depth and bone area % for the sandblasted and the plasma sprayed coated specimens, due to the solid structure of these control specimens.

Direct contact between bone and the specimen inside the pores was projected on the circumference of the implant. The percentage of direct bone-implant contact was defined as the sum of these projections divided by the circumference of the specimen. (**Figure 3**)

Statistical analyses

An unpaired T test was used to compare the friction coefficients of the new surface structures with the controls. SPSS (16.0, SPSS Inc., Chicago, USA) was used to perform a multivariate regression analysis of friction, with surface structure and BMD as predictor variables.

Statistical analysis of the *in vivo* experiment was performed using a Mann-Whitney U test for both ingrowth depth and bone area percentage. An univariate analysis of variance of the ranked results was performed for direct bone-implant contact using the following fixed factors: surface structure, implantation area and goat. Statistical significance was set at $p < 0.05$.

Results

Implant characterization

Analysis of the embedded specimens by light microscopy showed that the wave and cubic structures had average pore sizes of 0.9 mm and 1.2 mm and porosities of 49% and 77%, respectively. The nominal thickness of the porous layer was 1.35 mm and 1.95 mm for the wave and cubic structure, respectively.

The results of the roughness measurements showed an average surface roughness (R_a) of 6.34 for the wave structure, 5.22 for the cubic structure, 6.09 for the titanium plasma sprayed surface and 3.52 for the sandblasted surface.

Friction experiment

The average friction coefficient was 0.68 (SD = 0.04) for the wave structure and 0.63 (SD = 0.03) for the cubic structure. The average friction coefficient of the controls was 0.64 (SD = 0.04) and 0.49 (SD = 0.06) for the titanium plasma sprayed and the sandblasted specimen, respectively. The friction coefficient of the sandblasted specimen was significantly ($p < 0.001$) lower than the new surface structures and the titanium plasma sprayed control. (**Table 1**)

The multivariate regression analysis showed that the variation in BMD had no significant influence on the frictional properties of the surface structures.

In vivo experiment

Clinical evaluation

No intraoperative complications occurred during surgery. All goats were fully weight bearing within 1 week after surgery. Swelling of the knee was seen in three goats, without causing general illness of the goats. This indicates that there was no infection, which was confirmed by post-mortem tissue cultures beside the implantation locations.

Histology

The HE stained slices showed bone ingrowth into the pores of the new surface structures. (**Figure 4**) The results for ingrowth depth at 4 and 6 weeks (as measured using the Xylenol orange and Calceine green fluorochrome labeling, respectively), bone area percentage and direct bone-implant contact (both measured on HE stained sliced) are listed in **Table 1**.

The bone ingrowth depth of the cubic structure was greater compared to the wave structure at 4 and 6 weeks after surgery (1.18 vs 0.78 and 1.47 vs 0.98 mm respectively, $p = 0.009$). Contrastingly, the wave structure showed better results for bone area percentage than the cubic ($p = 0.009$). (**Table 1**)

The bone-implant contact of the new topographic surface structures was comparable to the titanium plasma sprayed control. No significant differences in bone-implant contact were observed throughout the four tested surfaces ($p = 0.400$), due to a large variation for the wave structure and the control surfaces. (**Table 1**)

Statistical analysis showed that differences between the goats did not affect the bone-implant contact ($p = 0.195$). However the location of the implantation had an effect on the bone-implant

Table 1. Friction coefficients (n=7) and bone ingrowth characteristics (n=6)

Specimen	Friction coefficient	Ingrowth depth (mm)		Bone area (%)	Bone implant contact (%)
		4 weeks	6 weeks		
Wave	0.68 (0.04) *	0.78 (0.19)*	0.98 (0.29)*	18.1 (3.6)*	23.9 (11.6)
Cubic	0.63 (0.03) *	1.18 (0.10)*	1.47 (0.20)*	13.9 (4.7)*	24.5 (5.6)
Ti-coated	0.64 (0.04) *	NA	NA	NA	25.5 (13.3)
Sandblasted	0.49 (0.06) *	NA	NA	NA	18.2 (16.0)

Results and SD. * $p < 0.05$

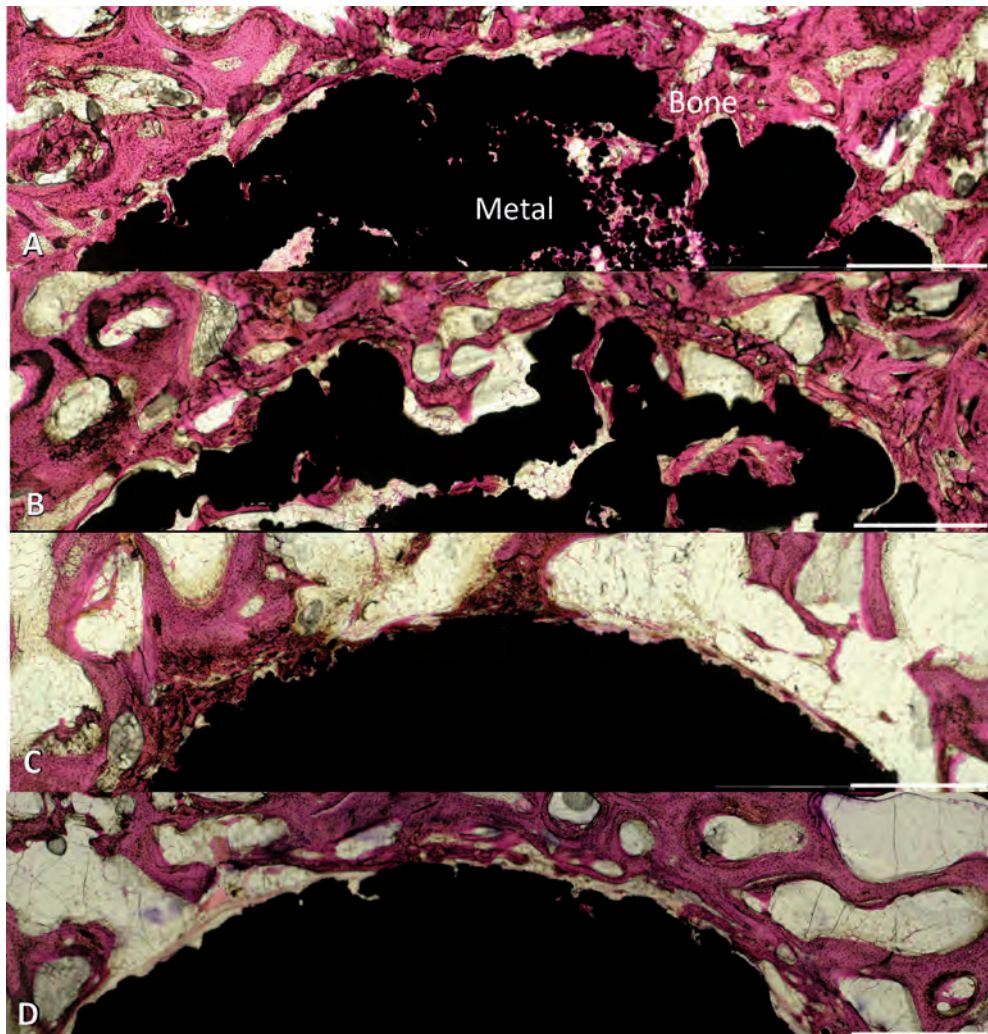


Figure 4. Qualitative analysis of bone ingrowth. HE stained slices of the wave (a) and cubic structure (b) with extensive bone ingrowth into the pores. Bone ingrowth on the titanium plasma sprayed (c) and sandblasted (d) control. (bar = 1mm)

contact; it appeared that the direct bone implant contact was less in specimens implanted dorsally of the femoral trochlea relative to the two condyle areas. ($p = 0.027$)

Discussion

Electron beam melting is a relatively new technique capable of producing complex 3-dimensional geometries.[21] With this technique many possible surface characteristics can be engineered thus aiding in the development of an optimal surface structure for bone

Table 2. Frictional properties of coatings for orthopedic implants

Author	Coating	Friction coefficient	
		Cortical bone	Trabecular bone
Heiner[28]	Sintered spherical titanium beads	0.63(0.10)	1.18 (0.39)
Fitzpatrick[27]	Porous tantalum	0.74 (0.07)	0.88 (0.09)
Zhang[29]	Porous tantalum	0.74 (0.07)	0.88 (0.09)
Dammak[9]	Vitallium beaded porous surface		0.68 (0.09)
Shirazi[31]	Titanium bead		0.58 (0.12)
	Titanium fiber mesh		0.60 (0.11)
Rancourt[30]	Sintered titanium beads		0.53 (0.07)
	Titanium fiber mesh		0.47 (0.03)
Current study	Wave	0.68 (0.04)	
	Cubic	0.63 (0.03)	
	Ti plasma sprayed coating	0.64 (0.04)	
	Sandblasted	0.49 (0.06)	

Results and SD.

ingrowth for cementless prostheses. In this study two controls were selected; a titanium plasma sprayed and a sandblasted specimen. The titanium plasma spray coating was selected as this coating is already widely used on femoral stems. Coated stems produce good medium- to long-term survival rates[23] and they perform better than uncoated cementless stems.[26] The plain sandblasted control was chosen to determine the effect of the E-beam technology itself. Some limitations of the present study should be acknowledged. First of all, the frictional properties in contact with cortical bone were determined, whereas a prosthetic surface is also in contact with trabecular bone. The friction coefficient of a metal surface on cortical bone is generally lower than the same specimen on trabecular bone.[27-29] Therefore, the reported friction values are probably in the lower range of frictional values that occur around a hip prosthesis. Secondly, no chemical surface analysis was performed. Thirdly, the results for bone ingrowth showed a large variability, partly due to the rather large tolerance of the E-beam technology and differences in implantation location. Although not statistically significant it is likely that in between goat differences, overall biological variability and unavoidable differences in surgical precision (i.e. the quality of the press fit implantation) will affect this.

In this study the frictional properties of the surfaces were determined as these values have a direct effect on the stability potential of the metal surface relative to the bone surface. Obviously, the friction is influenced by the roughness of the metal structure and we considered quantifying the roughness of the investigated surfaces. However, it appeared to be impossible to define the roughness of the new surface structures accurately, because of the three dimensional character of the new surface structures.

The friction coefficients of the new E-beam specimens were significantly higher compared to the sandblasted specimens and are in the same range of the titanium plasma sprayed control. Since implants with a titanium plasma sprayed surface have a high survival rate (indicating sufficient initial stability)[23], it can be deduced that the two new surface structures can also provide sufficient initial stability (albeit that this will also largely depend on prosthetic shape).

Several other studies have reported the frictional properties of coatings for orthopedic implants. (**Table 2**) [9;27-31] Although the values of the friction coefficient may depend to some extent on the testing method which vary amongst the different studies, comparison to our results indicate that the new surface structures result in relatively high friction coefficients.

In this study three different methods were used to quantify bone ingrowth; all have advantages and disadvantages with regard to the interpretation of the results. For example bone ingrowth depth is restricted by pore depth and measuring direct bone-implant contact is the only method which enables comparison of porous and solid specimens.

The amount of direct bone-implant contact of the E-beam produced surface structures appeared to be comparable to the titanium plasma sprayed control. Hence, the new surface structures have the potential to be successful surface structures for orthopedic implants.

The cubic structure showed greater bone ingrowth depth compared to the wave structure. On the contrary, the wave structure showed better results for bone area percentage. This difference in outcome can be explained by differences in the structure of the coating. The cubic specimen has a high porosity and large pores deep inside the core material, which were too deep for the bone to reach in the limited post-operative time (six weeks) of the study. Consequently bone area percentage of the cubic specimen was less than the wave specimen.

Furthermore, the importance of pore size and porosity influencing bone ingrowth is supported by the differences in bone ingrowth between the 3-dimensional surface structures and the rough E-beam control. Although made of the same material and manufactured using the same methods, the bone ingrowth of the new surface structures (large pores, high porosity) was greater compared to the sandblasted (plain) E-beam control.

Although it is clear that pore size affects bone ingrowth, the optimal pore size has yet to be determined. Bobyn et al.[32] considered 100 to 400 μm as the optimum pore size range for bone ingrowth, but revealed no significant differences in bone ingrowth between pore sizes in this range and larger pores at twelve weeks after implantation. Similar results were found by Fisher et al.[33] Bobyn et al. showed that the extent of ingrowth of implants with pores of 710 μm was significantly greater compared to those with pores of 550 μm at four and sixteen weeks after implantation.[15] This indicates that 400 μm is not the maximum pore size to enhance bone ingrowth.

One set back of a larger pore size and a higher porosity is the length of time it takes for full integration of bone into the implant. Hing et al.[34] showed that the volume of bone ingrowth and the bone-implant contact of specimens with high porosities (80%) increases gradually from five, thirteen and twenty-six weeks after implantation. Bobyn et al.[15] demonstrated the same effect for pore sizes of 430 and 650 μm . These observations concur with the results of our study showing that the ultimate bone ingrowth is not accomplished for the new E-beam structures in the six weeks study period. Based on the current results bone ingrowth is likely to continue after the six weeks study period and will further anchor the implant to the bone. However, one can expect that ingrowth beyond a certain depth does not enhance the strength of the bone-implant interface, similar as seen for the cement-bone interface.[35]

One of the few studies on E-beam engineered surfaces in the orthopedic literature is reported by Ponader et al. [22] They demonstrated a reduced proliferation of human fetal osteoblasts on porous E-beam produced surfaces, compared to smooth and unprocessed E-beam surfaces. However, in that same study, SEM analysis demonstrated that the cells attached and spread well on all surfaces.[22] This indicates that the E-beam produced material itself does not hamper cell viability and proliferation, but that this may be influenced by the micro and macro geometrical characteristics. In contrast to the study of Ponader et al.[22] the E-beam produced surface structures used in this study were superior compared to a sandblasted E-beam produced specimen.

Several explanations can clarify this difference; differences in finishing surface treatment, testing methods and surface characteristics. With respect to the finishing treatment, an additional step was added in the surface structures tested in this study. Before biological cleaning and sterilization a sandblasting step was performed in order to remove all residual powder particles. Regarding the method of testing, it is questionable whether the examination of pre-osteoblastic cell proliferation of Ponader et al.[22] provides valid data for bone ingrowth of prosthetic components. In this process stroma cells probably play a more prominent role. [36] Concerning surface characteristics, two out of the three surface structures tested by Ponader et al.[22] had smaller pores than the structures used in this study. The pore size of the third surface structure was comparable. Additionally, the porosity of these structures was lower as well. The superiority of our structures suggests that a large pore size and high porosity enhance bone ingrowth and support the importance of surface characteristics influencing bone ingrowth.

In conclusion, the newly developed surface structures engineered in this study provide sufficient friction at the bone-implant interface thus achieving initial stability. The ultimate bone ingrowth was not accomplished in this study, due to the high porosity and large average pore size of the new E-beam surface structures. However, the bone ingrowth into the new surface structures appears to be comparable to more conventionally made surfaces of clinically successful implants at six weeks after surgery.

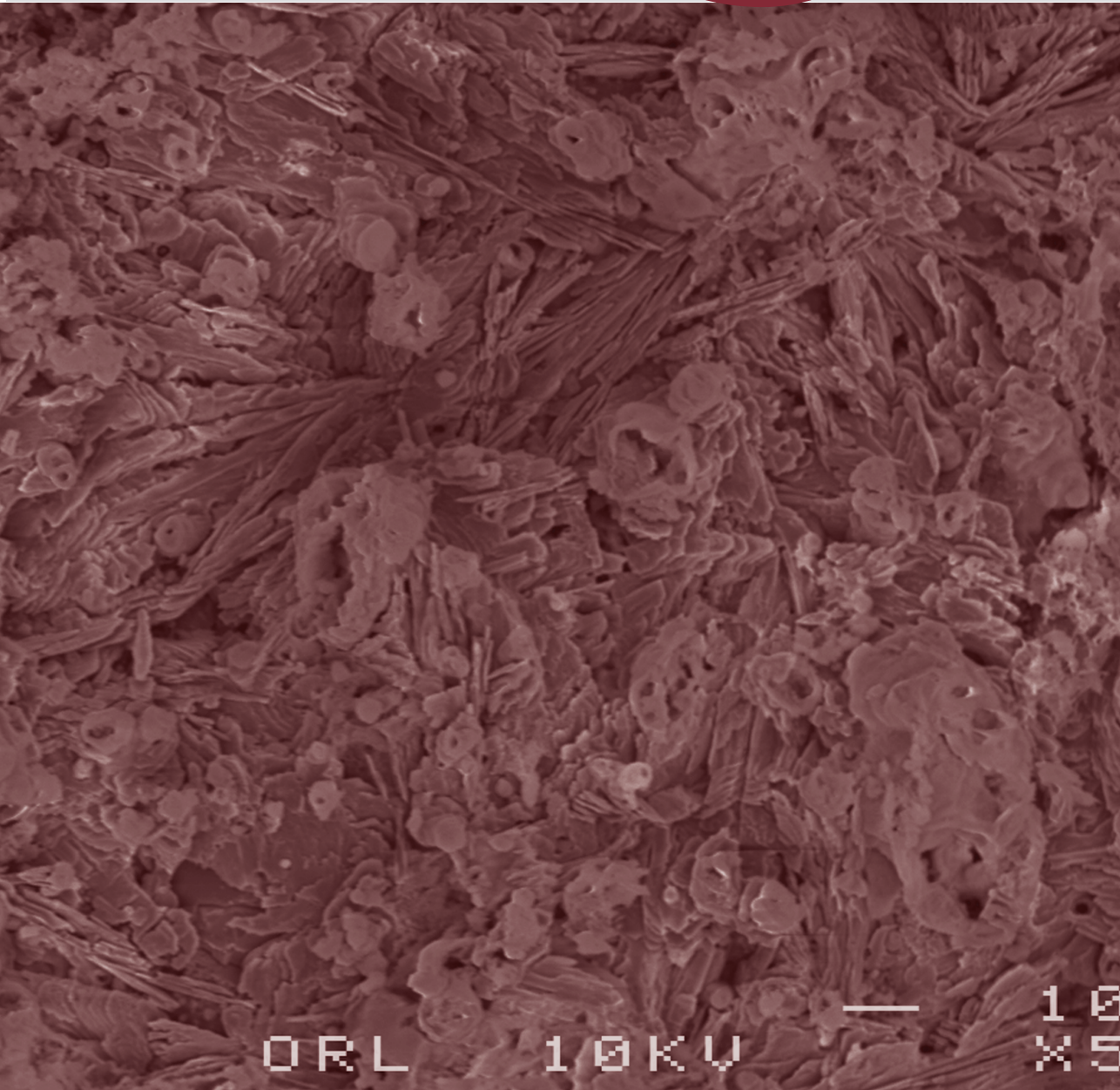
The results of these study are promising as bone ingrowth is likely to continue after the six weeks allotted for this study. Testing of bone ingrowth for an extended period is necessary to support our hypothesis that the new surface structures can provide improved fixation properties compared to conventionally made surfaces.

References

1. Mendenhall S. Hip and knee implant review. 1-16. 2004. Orthopedic network 14 (3).
2. Eskelinen A, Remes V, Helenius I, Pulkkinen P, Nevalainen J, Paavolainen P: Uncemented total hip arthroplasty for primary osteoarthritis in young patients: a mid-to long-term follow-up study from the Finnish Arthroplasty Register. *Acta Orthop* 77(1):57, 2006
3. Karrholm J, Garellick G, Herberts P. Annual Report 2006. Swedish National Hip Arthroplasty Register. 2007.
4. Ulrich SD, Seyler TM, Bennett D, Delanois RE, Saleh KJ, Thongtrangan I, Kuskowski M, Cheng EY, Sharkey PF, Parvizi J, Stiehl JB, Mont MA: Total hip arthroplasties: what are the reasons for revision? *Int Orthop* 32(5):597, 2008
5. Sundfeldt M, Carlsson LV, Johansson CB, Thomsen P, Gretzer C: Aseptic loosening, not only a question of wear: a review of different theories. *Acta Orthop* 77(2):177, 2006
6. McAuley JP, Szuszczewicz ES, Young A, Engh CA, Sr.: Total hip arthroplasty in patients 50 years and younger. *Clin Orthop Relat Res*(418):119, 2004
7. Kurtz SM, Ong KL, Schmier J, Mowat F, Saleh K, Dybvik E, Karrholm J, Garellick G, Havelin LI, Furnes O, Malchau H, Lau E: Future clinical and economic impact of revision total hip and knee arthroplasty. *J Bone Joint Surg Am* 89 Suppl 3:144, 2007
8. Ryd L, Albrektsson BE, Carlsson L, Dansgard F, Herberts P, Lindstrand A, Regner L, Toksvig-Larsen S: Roentgen stereophotogrammetric analysis as a predictor of mechanical loosening of knee prostheses. *J Bone Joint Surg Br* 77(3):377, 1995
9. Dammak M, Shirazi-Adl A, Schwartz M, Jr., Gustavson L: Friction properties at the bone-metal interface: comparison of four different porous metal surfaces. *J Biomed Mater Res* 35(3):329, 1997
10. Geetha M, Singh AK, Asokamani R, Gogia AK: Ti based biomaterials, the ultimate choice for orthopaedic implants - A review. *Progress in Materials Science* 54:397, 2009
11. Kienapfel H, Sprey C, Wilke A, Griss P: Implant fixation by bone ingrowth. *J Arthroplasty* 14(3):355, 1999
12. Buser D, Schenk RK, Steinemann S, Fiorellini JP, Fox CH, Stich H: Influence of surface characteristics on bone integration of titanium implants. A histomorphometric study in miniature pigs. *J Biomed Mater Res* 25(7):889, 1991
13. Shalabi MM, Gortemaker A, Van't Hof MA, Jansen JA, Creugers NH: Implant surface roughness and bone healing: a systematic review. *J Dent Res* 85(6):496, 2006
14. Petersilge WJ, D'Lima DD, Walker RH, Colwell CW, Jr.: Prospective study of 100 consecutive Harris-Galante porous total hip arthroplasties. 4- to 8-year follow-up study. *J Arthroplasty* 12(2):185, 1997
15. Bobyn JD, Stackpool GJ, Hacking SA, Tanzer M, Krygier JJ: Characteristics of bone ingrowth and interface mechanics of a new porous tantalum biomaterial. *J Bone Joint Surg Br* 81(5):907, 1999
16. Otsuki B, Takemoto M, Fujibayashi S, Neo M, Kokubo T, Nakamura T: Pore throat size and connectivity determine bone and tissue ingrowth into porous implants: three-dimensional micro-CT based structural analyses of porous bioactive titanium implants. *Biomaterials* 27(35):5892, 2006
17. Karageorgiou V, Kaplan D: Porosity of 3D biomaterial scaffolds and osteogenesis. *Biomaterials* 26(27):5474, 2005
18. Jones JR, Ehrenfried LM, Hench LL: Optimising bioactive glass scaffolds for bone tissue engineering. *Biomaterials* 27(7):964, 2006
19. Heini P, Rottmair A, Körner C, Singer R: Cellular Titanium by Selective Electron Beam Melting. *Advanced Engineering Materials* 9(5):360, 2007
20. Heini P, Müller L, Körner C, Singer RF, Müller FA: Cellular Ti-6Al-4V structures with interconnected macro porosity for bone implants fabricated by selective electron beam melting. *Acta Biomater* 4(5):1536, 2008
21. Lindhe U, Harrysson O. Rapid manufacturing with electron beam melting (EBM) - A manufacturing revolution? Arcam lecture at SME, direct metal forum in Dearborn, Michigan. 2003.
22. Ponader S, Vairaktaris E, Heini P, Wilmosky CV, Rottmair A, Körner C, Singer RF, Holst S, Schlegel KA, Neukam FW, Nkenke E: Effects of topographical surface modifications of electron beam melted Ti-6Al-4V titanium on human fetal osteoblasts. *J Biomed Mater Res A* 84(4):1111, 2008

23. De Palma F, Erriquez A, Rossi R, Spinelli M: Duofit total hip arthroplasty: a medium- to long-term clinical and radiographic evaluation. *Journal of Orthopaedics and Traumatology*(8):117, 2007
24. Fellah BH, Gauthier O, Weiss P, Chappard D, Layrolle P: Osteogenicity of biphasic calcium phosphate ceramics and bone autograft in a goat model. *Biomaterials* 29(9):1177, 2008
25. Manders PJ, Wolke JG, Jansen JA: Bone response adjacent to calcium phosphate electrostatic spray deposition coated implants: an experimental study in goats. *Clin Oral Implants Res* 17(5):548, 2006
26. Bordini B, Stea S, De CM, Strazzari S, Sasdelli A, Toni A: Factors affecting aseptic loosening of 4750 total hip arthroplasties: multivariate survival analysis. *BMC Musculoskelet Disord* 8:69, 2007
27. Fitzpatrick D, Ahn P, Brown T, Poggie R: Friction coefficients of porous tantalum and cancellous & cortical bone. Twenty-first annual meeting of the American Society of Biomechanics. 1997.
28. Heiner AD, Brown TD: Frictional coefficients of a new bone ingrowth structure. 53rd annual meeting of the Orthopaedic Research society. 2007.
29. Zhang: Interfacial frictional behavior: cancellous bone, cortical bone, and a novel porous tantalum biomaterial. *Journal of musculoskeletal research* 3(4):245, 1999
30. Rancourt D, Shirazi-Adl A, Drouin G, Paiement G: Friction properties of the interface between porous-surfaced metals and tibial cancellous bone. *J Biomed Mater Res* 24(11):1503, 1990
31. Shirazi-Adl A, Dammak M, Paiement G: Experimental determination of friction characteristics at the trabecular bone/porous-coated metal interface in cementless implants. *J Biomed Mater Res* 27(2):167, 1993
32. Bobyn JD, Pilliar RM, Cameron HU, Weatherly GC: The optimum pore size for the fixation of porous-surfaced metal implants by the ingrowth of bone. *Clin Orthop Relat Res*(150):263, 1980
33. Fisher JP, Vehof JW, Dean D, van der Waerden JP, Holland TA, Mikos AG, Jansen JA: Soft and hard tissue response to photocrosslinked poly(propylene fumarate) scaffolds in a rabbit model. *J Biomed Mater Res* 59(3):547, 2002
34. Hing KA, Best SM, Tanner KE, Bonfield W, Revell PA: Mediation of bone ingrowth in porous hydroxyapatite bone graft substitutes. *J Biomed Mater Res A* 68(1):187, 2004
35. Majkowski RS, Bannister GC, Miles AW: The effect of bleeding on the cement-bone interface. An experimental study. *Clin Orthop Relat Res*(299):293, 1994
36. Wall I, Donos N, Carlqvist K, Jones F, Brett P: Modified titanium surfaces promote accelerated osteogenic differentiation of mesenchymal stromal cells in vitro. *Bone* 2009

Chapter 5



ORL

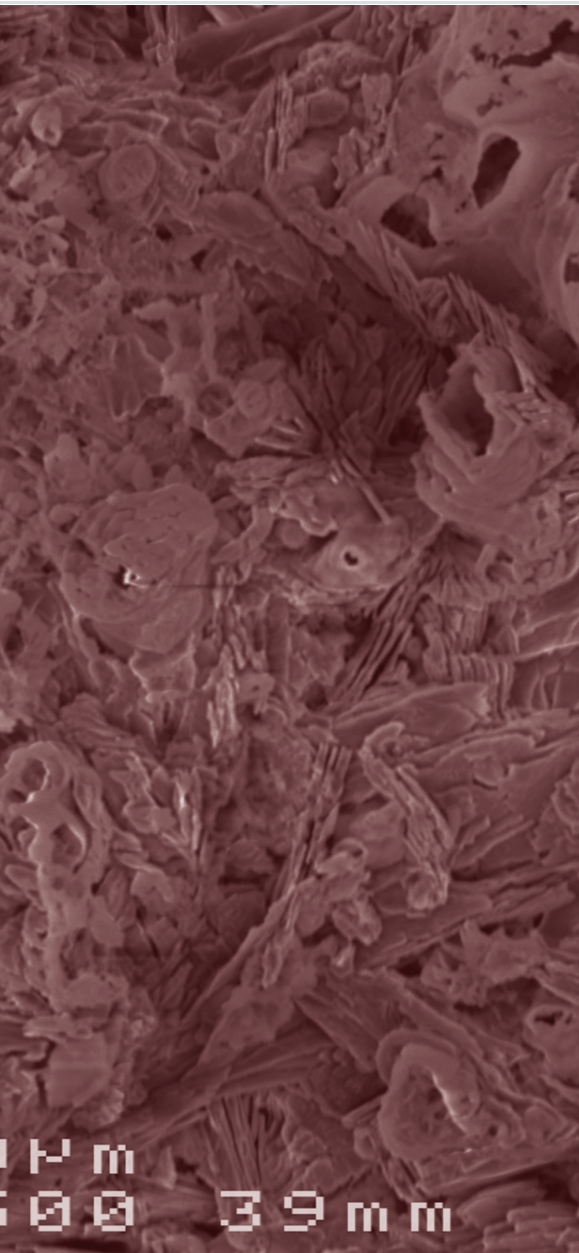
10KV

—

10
X5

Assessment of bone ingrowth potential of biomimetic hydroxyapatite and brushite coated porous E-beam structures

5



Abstract

The bone ingrowth potential of biomimetic hydroxyapatite and brushite coatings applied on porous E-beam structure was examined in goats and compared to a similar uncoated porous structure and a conventional titanium plasma spray coating. Specimens were implanted in the iliac crest of goats for a period of 3 (4 goats) or 15 weeks (8 goats). Mechanical implant fixation generated by bone ingrowth was analyzed by a push out test. Histomorphometry was performed to assess the bone ingrowth depth and bone implant contact. The uncoated and hydroxyapatite-coated cubic structure had significantly higher mechanical strength at the interface compared to the Ti plasma spray coating at 15 weeks of implantation. Bone ingrowth depth was significantly larger for the hydroxyapatite- and brushite-coated structures compared to the uncoated structure. In conclusion, the porous E-beam surface structure showed higher bone ingrowth potential compared to a conventional implant surface after 15 weeks of implantation. Addition of a calcium phosphate coating to the E-beam structure enhanced bone ingrowth significantly. Furthermore, the calcium phosphate coating appears to work as an accelerator for bone ingrowth.

Introduction

Total hip arthroplasty is one of the most successful medical procedures. However, 5 to 10 percent of the cementless implants still fail within 10 years of implantation. [1, 2] The frequency of failure is likely to increase due to the implantation in younger and more active patients. [3] The long term success of cementless orthopaedic implants depends on biological fixation by new bone formation. [4, 5, 6] Surface topography (e.g. pore size, porosity) and coating influence the process of bone ingrowth and by that the fixation in the critical postoperative period. It is evident that the size of the pores affects bone ingrowth, although there is still debate about the optimum pore size.[7, 8, 9] A minimum pore diameter of 100 μm is needed to allow vascularisation and bone ingrowth. [10] The maximum pore size has yet to be determined. It has been shown that enhanced fixation strength can be obtained by increasing the porosity of an implant up to 75-80%. [11] However, full bone ingrowth takes more time in implants with increased porosity, whereas fast bone formation permits more rapid loading of the implant. [12]

Electron beam melting is a rapid prototyping technology that can be used to produce implants with computer designed surface characteristics. The implant is build up out of metal powder to reproduce a geometry defined by a 3-dimensional CAD model. The technique enables for production of the solid core and the porous surface in one manufacturing step, with the capability to engineer a large variety of complex 3-dimensional structures as implant surface. [13, 14, 15] Ponader et al. showed that osteoblastic cells attach, proliferate and differentiate well on new developed E-beam produced surface structures.[16] Previous work of our group showed that the bone ingrowth potential of these porous E-beam surface topographies was comparable to a clinical used, conventionally made surface. However, as can be expected for a highly porous surface, complete bone ingrowth was not reached in a post operative period of 6 weeks.[17]

Calciumphosphate (CaP) coatings have been successfully applied on orthopedic and dental implants.[18, 19, 20, 21] Stimulation of new bone formation around CaP coated implants is based on dissolution of the coating soon after implantation followed by formation of a bone-inductive carbonated calcium phosphate layer.[20] The biological advantages of these coatings include the enhancement of bone formation and accelerated bonding between the implant surface and the surrounding bone.[22, 23, 20] Calcium phosphate coatings can be applied on porous implant surfaces in order to enhance the bone ingrowth potential.[22, 21] Furthermore, the acceleration of bone ingrowth that can be achieved by these coatings could be beneficial regarding to shortening the post-operative partial weight-bearing and rehabilitation periods. [18]

Although the calciumphosphate coatings are applied successfully on implant surfaces, current direct coating techniques failed to mineralize on the deep surfaces of complex 3-dimensional structures.[24] Biomimetic coating deposition is a relatively new coating technique with the possibility to produce a homogeneous coating on these complex 3-dimensional structures. The

coating is deposited under physiological temperatures, which makes it possible to incorporate functional biological agents, such as growth factors, in the coating. In addition, the CaP ratio and coating thickness can be varied, and the structure of the formed crystals is more akin to bone mineral than those produced in conventional ways.[18, 24]

For this study a porous E-beam structure was combined with two biomimetic CaP coatings. It was hypothesized that these CaP coated E-beam structures would provide for accelerated and enhanced bone ingrowth. Therefore the goal of this study was to characterize the materials in detail and to assess the mechanical strength of the bone-implant interface and the bone ingrowth potential of a porous E-beam implant surface structure coated with a hydroxyapatite and brushite calciumphosphate coating and to compare this to an uncoated E-beam structure and a conventionally made implant surface.

Materials and Methods

Specimens

The implants were made out of Ti6Al4V powder and produced with E-beam technology (Eurocoating, Trento, Italy). The powder particles used ranged from 45-100 μm and were melted by the electron beam into the desired shapes based on CAD data. In short, a homogeneous powder layer was applied on the process platform in a vacuum chamber at high temperature ($\pm 700^\circ\text{C}$) and scanned by the electron beam. The powder particles were melted at the programmed locations. The process platform was lowered by one layer thickness (0.1mm)

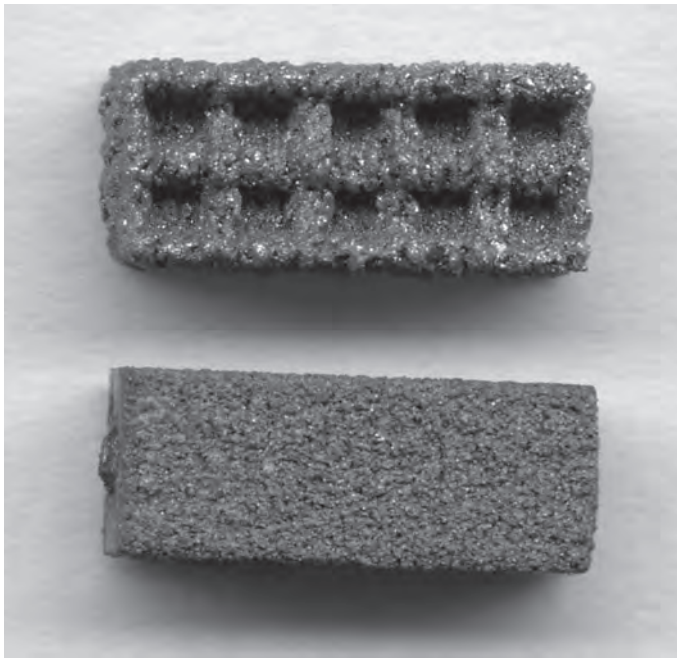


Figure 1. Surfaces. Cubic structure (top) and TiPS (bottom).

after the melting of each layer and the process was repeated.[25, 13] Upon completion, all specimens were sandblasted and cleaned according to protocols for medical implants. The overall accuracy of the E-beam technology in terms of computer model reconstruction is ± 0.15 mm.

A 3-dimensional structure with quadrangular pores (cubic) was used as surface topography for all E-beam specimens. The cubic structure has a pore size of 1.2 mm and a porosity of 77%. The structure was applied on two opposite sides of the specimens, the other two sides were closed. The adhesive strength (test described in ASTM F1147) of the E-beam specimens was >50 MPa and the taber abrasion test (as described in ASTM F1978) showed a weight loss after 100 cycles of 27.78 ± 4.51 mg. One group of cubic specimens was left uncoated (cubic), two were coated afterwards with CaP coatings. As a control, a commercially available titanium plasma spray coating (TiPS) was tested [26]. (**Figure 1**)

Coatings

A biomimetic coating was applied on two groups of cubic E-beam specimens. In the biomimetic coating process, a bioactive coating was produced using an electrodeposition system. A calciumphosphate layer was formed on the metallic specimen after immersion in an artificially prepared supersaturated calcium/phosphate electrochemical solution (Eurocoating, Trento, Italy).[19] The brushite coating obtained with this method, has a high solubility. With a two-step procedure, this high soluble coating can be modified to a hydroxyapatite coating.[27] One group of cubic E-beam specimens was coated with a biomimetic brushite coating (cubicBR). The other group was coated with biomimetic hydroxyapatite (cubicHA).

Material characterization

Scanning electron microscopy (SEM)

The surface morphology and coating thickness were examined by scanning electron microscopy (SEM, SEM6310, Jeol, Tokyo, Japan). The SEM was coupled with an Energy Dispersive X-ray Spectroscopy (EDS, JSM-5500, Jeol, Tokyo, Japan) which was used to determine the elemental composition of the biomimetic coatings.

Roughness

Surface roughness values of the specimens were determined using a Universal Surface Tester (UST) (Innowep, Wurzburg, Germany).

In vitro coating dissolution

The dissolution behavior of the hydroxyapatite and brushite coating was evaluated in vitro. For each group 10 samples (cylindrical, 25 mm height, \varnothing 10mm) were tested in pH 5.5 ($n=5$) and in pH 7.3 ($n=5$). The specimens were positioned in polyethylene bottles filled with 250 ml buffer solution [28] with a pH of 5.5 and 7.3, using continuous stirring (200 ± 10 rpm) for 21 days.

The bottles were kept at $37.0 \pm 0.1^{\circ}\text{C}$ under nitrogen atmosphere. The pH, Ca and P content were determined daily by drawing 0.5 ml aliquot of each solution. 0.5 ml buffer solution was then added to the bottles to compensate the sampling. The supernatant aliquots were then diluted to be analyzed by inductively coupled plasma atomic emission spectrometry (ICP-AES 76004527, Spectro analytical instruments, Kleve, Germany).

Animal experiment

Surgery was performed on twelve female, skeletal mature goats (*Capra Hircus Sana*), weighing 43-62 kg (mean 55 kg). The specimens (4x4x10 mm) were implanted in the trabecular bone of the iliac crest.[29] Each goat received 8 specimens in total (one set of 4 specimens for the push out test and one set for histology). The location of the implants was alternated systematically between goats with a random start.

The goats were anaesthetized with propofol (4 mg/kg B.Brown, Melsungen, Germany), intubated and anesthesia was maintained using isoflurane. The goats were placed in a prone position and the implantation procedure was performed under strict sterile conditions. A transverse skin incision was made over the iliac crest. The incision was continued subcutaneously to the periosteum. The periosteum was opened, after which the iliac crest was fully exposed. Four implant areas were created in the iliac crest using a sharp drill (\varnothing 4.0mm). Saline was used during the drilling to prevent heat induced necrosis. A quadrangular osteotome (4x4mm) was used to shape the drilled hole to the size of the specimen. The implantation area was inspected to guarantee the specimen was completely surrounded by trabecular bone. The specimens were inserted press-fit into the holes and the periosteum and skin were closed separately with resorbable sutures. This procedure was repeated on the contralateral side.

The goats received postoperative ampicillin (7.5 mg/kg Intervet, Boxmeer, The Netherlands) during 4 days and were housed at a farm. The goats were killed by an overdose of sodium pentobarbital (Euthesate, Ceva Santa Animale, Libourne, France). Four goats were sacrificed 3 weeks after surgery, eight goats 15 weeks after surgery. After sacrificing the animals, the iliac crests were retrieved. The goats that were sacrificed 15 weeks after surgery received fluorochromes at 5 (Calcein green, 25 mg/kg) , 10 (Xylenol Orange, 30 mg/kg) and 15 weeks (Tetracyclin, 25 mg/kg). After sacrificing contact x-rays (Faxitron 43805N, Hewlett Packard, Palo Alto, California, USA) were taken of the iliac crests to evaluate the position of the implants. The two medial implants of each iliac crest were used for mechanical testing and the two on the lateral side were used for histological analysis. All procedures have been approved by the animal ethics committee of the Radboud University Nijmegen.

Mechanical testing

The specimens and the surrounding bone were stored in the freezer until the test was performed. Based on the X-ray images the surrounding bone was sawed into a cube with the implant surrounded by bone, the top and bottom of the specimen free of tissues and the implant exactly perpendicular to the surfaces of top and bottom. Subsequently this cube was

placed in a jig, which supported only the surrounding bone and not the implanted specimen. The clearance between specimen and support by the jig was 0.7 mm.[30] The load (MTS, load cell 1kN) was placed on top of the specimen and pushed the specimen out the surrounding bone with a fixed speed (1 mm/min) and continuous load versus displacement data were recorded. The maximum force was identified in order to define the mechanical strength of the bone-implant interface.

Histological analysis

The specimens for histology were fixated in phosphate-buffered 4% formaldehyde solution for 4 days and embedded in polymethylacrylate (PMMA). 10 sections of 30 μ m thickness, perpendicular to the length of the specimen, were prepared using a sawing microtome (SP 1600, Leitz, Wetzlar, Germany).

Quantitative analysis of bone ingrowth was performed using fluorescence microscopy on unstained slices and light microscopy on Hematoxylin/Eosin (HE) stained slices. Each slice was analyzed blinded in random order using specialized software (AnalySIS 3.2 Soft Imaging System, Münster, Germany). For each specimen all ten sections were analyzed, subsequently the data were pooled.

Bone ingrowth depth was measured at 5, 10 and 15 weeks using fluorescence microscopy (group sacrificed at 15 weeks). A line was drawn from the outline of the specimen to the deepest fluorochrome label (perpendicular to the outline of the specimen). The ingrowth depth was defined as the average of this measurement on each side of the specimen. Due to the solid structure of the plasma spray coating, it was impossible to measure bone ingrowth depth for this control. The direct bone-implant contact (BIC) was determined by direct bone surface contact divided by the total surface perimeter of the implant.

SEM analysis of coating dissolution

The implanted hydroxyapatite and brushite coated specimens and their surrounding bone (after implantation), were analyzed by SEM for coating dissolution after sawing sections and polishing the surface of the specimens.

Statistical analysis

Both mechanical (push-out test) and histological (bone ingrowth depth and bone-implant contact) datasets were evaluated non-parametrically, as a normal distribution could not be assumed. Since each goat received all implants types (cubic, cubicHA, cubicBR, and TiPs), the experiment has a paired design with four groups. All datasets were evaluated with Friedman's repeated measures analysis of variance by ranks followed by Wilcoxon's signed-rank test. For all datasets, differences between medians were considered statistically significant for p-values <0.05. Statistical analysis was performed using SPSS 16.0 software (SPSS Inc., Chicago, IL, US).

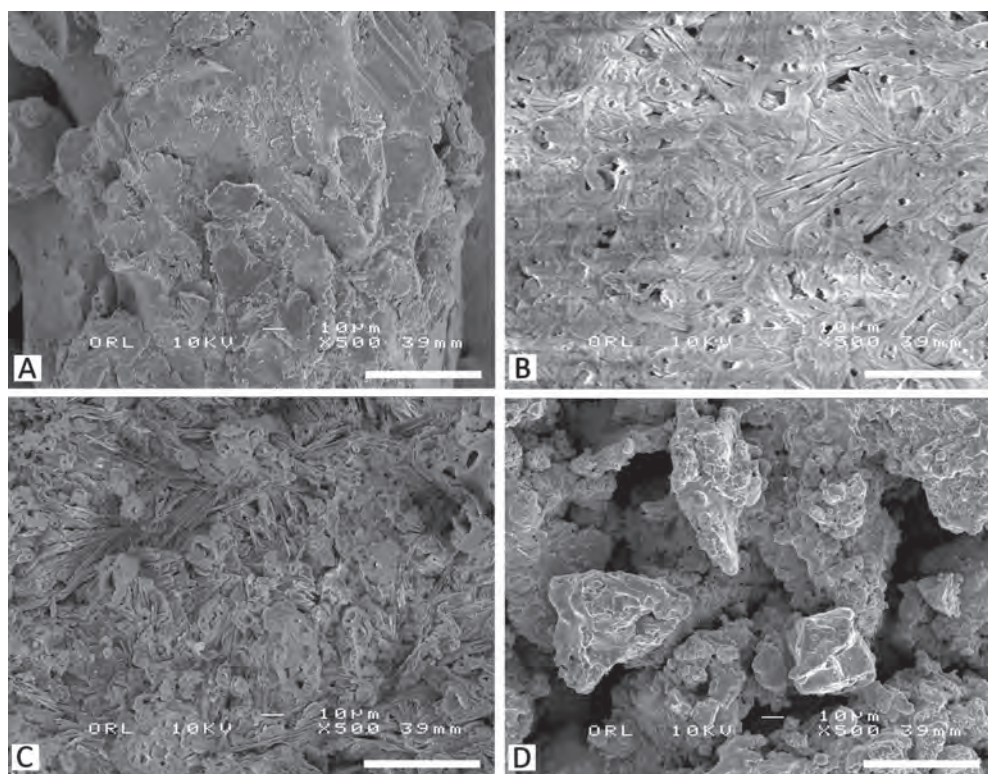


Figure 2. Surface characterization. SEM images of the cubic (a), cubicHA (b), cubicBR (c) and TIPS (d) implant surfaces. Bar = 50 μm

Results

Surface characterization

The surface morphology before implantation showed the characteristic appearances of non-coated and HA and brushite coated cubic specimens. (**Figure 2**) The coating thickness of both coatings analyzed by SEM was $15 \pm 5 \mu\text{m}$. EDS analysis confirmed the presence of hydroxyapatite and brushite on the cubicHA and cubicBR surfaces, respectively. (**Figure 3**) The roughness measurements showed an average surface roughness (R_a) of $5.77 \mu\text{m}$ for the cubic structure, $4.43 \mu\text{m}$ for the cubicHA, $5.29 \mu\text{m}$ for the cubicBR and $6.64 \mu\text{m}$ for the titanium plasma sprayed surface.

The in vitro coating dissolution analysis showed that the dissolution behavior presented periods of dissolution and recrystallization during the in vitro test with predominance of dissolution. The biomimetic coatings presented dissolution immediately after their immersion in pH 5.5. Both hydroxyapatite and brushite showed almost full dissolution of the deposited layer within the first days of immersion in pH 5.5. In pH 7.3 the dissolution process did not start immediately. (**Figure 4**) The brushite coating was completely dissolved after exposure to pH

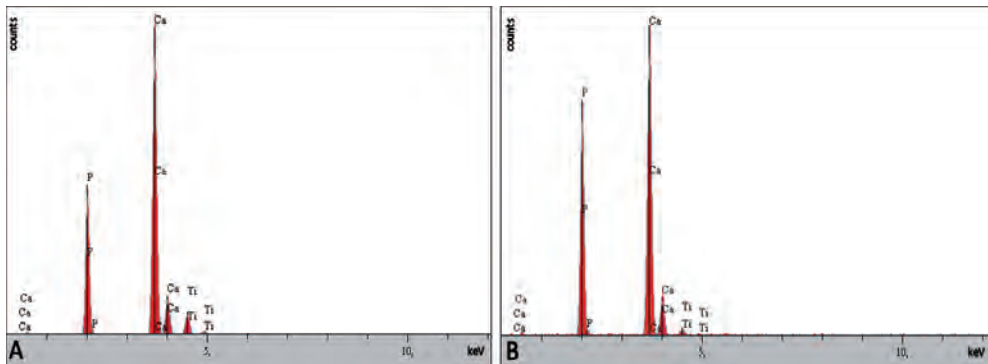


Figure 3. EDS analysis. EDS analysis confirming the presence of hydroxyapatite and brushite on the cubicHA (a) and cubicBR (b) surfaces

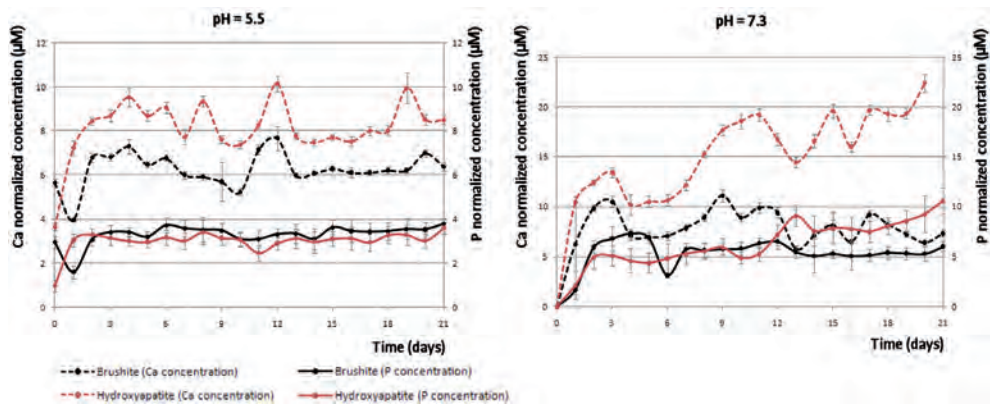


Figure 4. Ca and P concentration after immersion. Ca and P concentration after immersion of the specimens in pH 5.5 and pH 7.3. Periods of dissolution and recrystallization occur during the in vitro test with predominance of dissolution.

7.3 at the end of the test, but HA coated specimens exposed to pH 7.3 showed that the coating is not completely dissolved after 21 days. (**Figure 5**)

Mechanical testing

At 3 weeks after implantation no differences in mechanical strength of the bone implant interface were found. At 15 weeks the cubic ($p = 0.043$) and cubicHA structure ($p = 0.043$) had significantly higher mechanical strength at the interface compared to the Ti plasma spray coated specimens. (**Figure 6a**)

Histology (Figure 7)

The bone ingrowth depth at 5 and 15 weeks after implantation was significantly larger for cubicHA ($p=0.028$ and $p=0.018$ respectively) and cubicBR ($p=0.028$ and $p=0.018$ respectively)

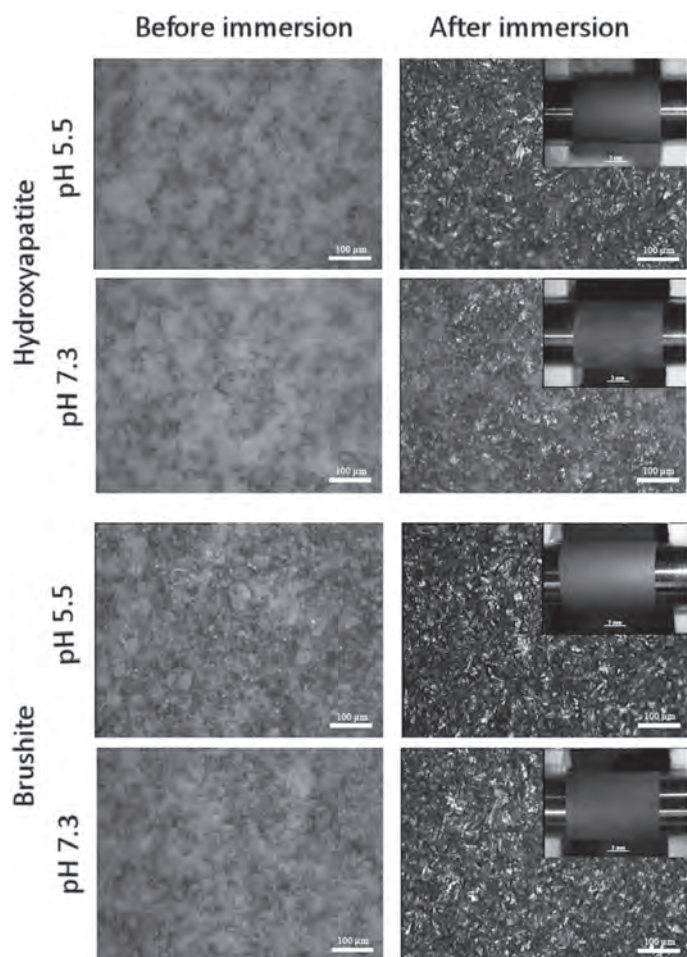


Figure 5. Images of in vitro coating dissolution. Pictures of the specimens before and after immersion for the in vitro dissolution test. Both hydroxyapatite and brushite were completely dissolved after exposure to pH 5.5. After exposure to pH 7.3, the brushite coating was completely dissolved, but the HA coating was not completely dissolved at the end of the test. (The remaining CaP coating on the substrate has a light-opaque colour, bar = 100 µm)

compared to the cubic. At 15 weeks ingrowth depth of cubicBR was significantly higher than cubicHA ($p=0.043$). (**Figure 6b**)

With respect to direct bone implant contact no significant differences between the four groups of implants were found. (**Figure 6c**)

Coating dissolution

SEM analysis of the embedded hydroxyapatite and brushite coated specimens and their surrounding bone showed that the HA coating was still visible in some areas 3 weeks after implantation. In other areas no HA coating could be detected. At 15 weeks very little spots with HA coating were seen as most of the coating was dissolved. With respect to the brushite coated specimens, no coating could be found at 3 and 15 weeks.

Figure 6. Results. Results of mechanical (a) and histological analysis of bone ingrowth. Histological analysis consisted of bone ingrowth depth (b) and percentage direct bone implant contact (c) $\dagger p=0.043$ $\ast p<0.05$

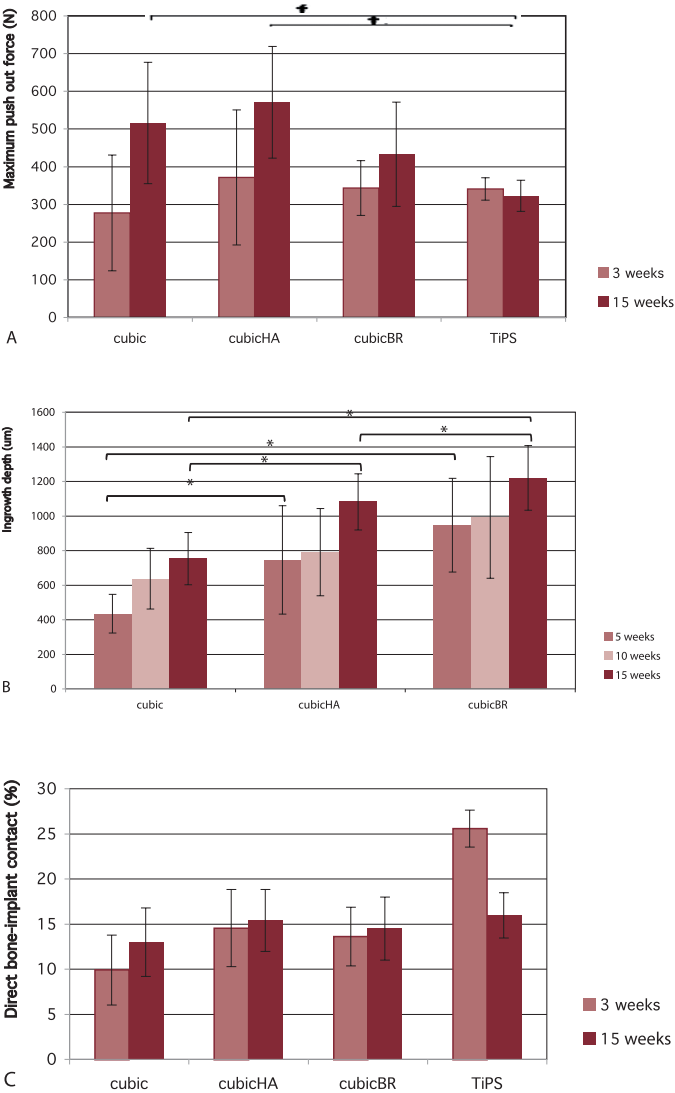




Figure 7. Histology. Histological images of cubic (a), cubicHA (b), cubicBR (c) and TiPS (d). bar = 2mm

Discussion

Two different CaP coatings were added to E-beam structures to enhance the bone ingrowth potential in an attempt to overcome the disadvantage of the prolonged time in which full bone ingrowth can be reached in highly porous structures. Although no differences between the coated and uncoated cubic structure were found for direct bone-implant contact and mechanical push out strength, addition of hydroxyapatite or brushite to the E-beam structure resulted in significantly greater bone ingrowth depth. Thus, addition of biomimetic CaP coatings appears to enhance bone ingrowth. With respect to the acceleration of bone ingrowth, significantly greater ingrowth depth at 5 weeks suggests the acceleration of bone ingrowth by addition of a calcium phosphate coating to the porous E-beam structure.

The absence of load in this model is a limitation of this study. Especially with regard to early bone ingrowth (and its acceleration) load bearing is an important factor [31, 6]. Furthermore only one 3-dimensional E-beam structure was tested.

Several groups tested porous structures in combination with CaP coatings and reported similar findings as the present study. Bone ingrowth of a porous tantalum structure with a biomimetic coating was significantly higher for coated specimens than for uncoated specimens at different time points.[22] Tsukeoka et al. [21] investigated the effect of the incorporation of hydroxyapatite into a titanium fiber mesh and found an increased push-out strength at 3 and 5 weeks, whereas after 8 weeks, no differences between specimens with and without hydroxyapatite were found. Porous titanium plugs implanted in a rabbit femur showed a significant increase in bone ingrowth for HA coated implants compared to uncoated implants after 6 weeks.[19] Furthermore, the study of Tsukeoka et al [21] supports our findings with regard to the speed of bone ingrowth, that suggests that calcium phosphate coatings work as an accelerator of bone ingrowth.

Dissolution analysis *in vitro* and *in vivo* show that the brushite coating was completely dissolved after 3 weeks, whereas only a minority of the hydroxyapatite coating was present at that time. However, *in vivo* the effect of the addition of both CaP coatings was still visible after 15 weeks. This prolonged effect could be explained by initial osteoblast activation induced by coating degradation and release of calcium and phosphate ions, that also might act as a reservoir for new synthesis of HA.[32, 33]

The attachment between the biomimetic coating and the implant might be weaker than the attachment between the bone and the coating. This can be seen in other calcium phosphate coatings as well. However, because of the intended use of this coating on porous, 3-dimensional structures, where the long term fixation will be maintained by the interlock between bone and implant, this weaker attachment of the coating to the implant appears to be not a problem.[34] Part of the coating might chip off during press-fit implantation due to the weaker attachment between the coating and the implant. This loss of coating may not be so disadvantageous because the fragmented coating will remain in the surroundings of the implant.[35]

Three different methods to assess bone ingrowth potential were used in the present study; a push-out test for mechanical evaluation of the bone-implant interface and two methods for histological analysis (bone ingrowth depth and percentage direct bone implant contact). Both histological methods have a different focus and it is difficult to say which one best defines bone ingrowth. Therefore, these two methods become more valuable when compared with the results of the push-out test that represents the actual mechanical strength at the bone-implant interface. In our study there was less agreement between the BIC measurements and the push out test. One could suggest therefore that BIC is not a good method to assess the effect of bone ingrowth on mechanical strength. This suggestion has been reported in literature as well.[36] Correlation between bone ingrowth depth and mechanical strength of the bone-implant interface is likely to be influenced by the fact that ingrowth beyond a certain depth does not enhance the strength of the bone-implant interface, similar as seen for the cement-bone interface.[37]

In conclusion, the porous E-beam surface structure showed higher bone ingrowth potential compared to a conventional titanium plasma spray coating after 15 weeks of implantation.

Based on histology findings, addition of a biomimetic calcium phosphate coating to the E-beam structure enhances bone ingrowth significantly. The biomimetic calcium phosphate coating appears to work as an accelerator of bone ingrowth.

References

1. Eskelinen A, Remes V, Helenius I, Pulkkinen P, Nevalainen J, Paavolainen P. Uncemented total hip arthroplasty for primary osteoarthritis in young patients: a mid-to long-term follow-up study from the Finnish Arthroplasty Register. *Acta Orthop*.2006;77:57-70.
2. Karrholm J, Garellick G, Herberts P. Annual Report 2006. Swedish National Hip Arthroplasty Register. 2007;
3. McAuley JP, Szuszczewicz ES, Young A, Engh CA, Sr. Total hip arthroplasty in patients 50 years and younger. *Clin Orthop Relat Res*.2004;119:25.
4. Bragdon CR, Doherty AM, Rubash HE, Jasty M, Li XJ, Seeherman H, Harris WH. The efficacy of BMP-2 to induce bone ingrowth in a total hip replacement model. *Clin Orthop Relat Res*.2003;50-61.
5. Geesink RG, de Groot K, Klein CP. Bonding of bone to apatite-coated implants. *J Bone Joint Surg Br*.1988;70:17-22.
6. Kienapfel H, Sprey C, Wilke A, Griss P. Implant fixation by bone ingrowth. *J Arthroplasty*.1999;14:355-68.
7. Bobyn JD, Pilliar RM, Cameron HU, Weatherly GC. The optimum pore size for the fixation of porous-surfaced metal implants by the ingrowth of bone. *Clin Orthop Relat Res*.1980;263-70.
8. Gauthier O, Bouler JM, Aguado E, Pilet P, Daculsi G. Macroporous biphasic calcium phosphate ceramics: influence of macropore diameter and macroporosity percentage on bone ingrowth. *Biomaterials*.1998;19:133-9.
9. Karageorgiou V, Kaplan D. Porosity of 3D biomaterial scaffolds and osteogenesis. *Biomaterials*. 2005;26:5474-91.
10. Jones JR, Ehrenfried LM, Hench LL. Optimising bioactive glass scaffolds for bone tissue engineering. *Biomaterials*.2006;27:964-73.
11. Bobyn JD, Stackpool GJ, Hacking SA, Tanzer M, Krygier JJ. Characteristics of bone ingrowth and interface mechanics of a new porous tantalum biomaterial. *J Bone Joint Surg Br*.1999;81:907-14.
12. Wennerberg A, Albrektsson T. Structural influence from calcium phosphate coatings and its possible effect on enhanced bone integration. *Acta Odontol Scand*.2009;1-8.
13. Heintz P, Muller L, Korner C, Singer RF, Muller FA. Cellular Ti-6Al-4V structures with interconnected macro porosity for bone implants fabricated by selective electron beam melting. *Acta Biomater*.2008;4:1536-44.
14. Parthasarathy J, Starly B, Raman S, Christensen A. Mechanical evaluation of porous titanium (Ti6Al4V) structures with electron beam melting (EBM). *J Mech Behav Biomed Mater*.2010;3:249-59.
15. Thomsen P, Malmstrom J, Emanuelsson L, Rene M, Snis A. Electron beam-melted, free-form-fabricated titanium alloy implants: Material surface characterization and early bone response in rabbits. *J Biomed Mater Res B Appl Biomater*.2009;90:35-44.
16. Ponader S, Vairaktaris E, Heintz P, Wilmosky CV, Rottmair A, Korner C, Singer RF, Holst S, Schlegel KA, Neukam FW, Nkenke E. Effects of topographical surface modifications of electron beam melted Ti-6Al-4V titanium on human fetal osteoblasts. *J Biomed Mater Res A*.2008;84:1111-9.
17. Biemond JE, Aquarius R, Verdonschot N, Buma P. Frictional and bone ingrowth properties of engineered surface topographies produced by Electron Beam technology. *Archives of Orthopaedic and Trauma Surgery*.2010;
18. Habibovic P, Barrère F, van Blitterswijk CA, de Groot K, Layrolle P. Biomimetic hydroxyapatite coating on metal implants. *J Am Ceram Soc*.2002;85:517-22.
19. Redepenning J, Schlessinger T, Burnham S, Lippiello L, Miyano J. Characterization of electrolytically prepared brushite and hydroxyapatite coatings on orthopedic alloys. *J Biomed Mater Res*.1996;30:287-94.
20. Sun L, Berndt CC, Gross KA, Kucuk A. Material fundamentals and clinical performance of plasma-sprayed hydroxyapatite coatings: a review. *J Biomed Mater Res*.2001;58:570-92.
21. Tsukeoka T, Suzuki M, Ohtsuki C, Tsuneizumi Y, Miyagi J, Sugino A, Inoue T, Michihiro R, Moriya H. Enhanced fixation of implants by bone ingrowth to titanium fiber mesh: effect of incorporation of hydroxyapatite powder. *J Biomed Mater Res B Appl Biomater*.2005;75:168-76.
22. Barrere F, van der Valk CM, Meijer G, Dalmeijer RA, de Groot K, Layrolle P. Osteointegration of biomimetic apatite coating applied onto dense and porous metal implants in femurs of goats. *J Biomed Mater Res B Appl Biomater*.2003;67:655-65.

-
23. Davis JR: Coatings. p. 179. In Davis & Associates (ed): Handbook of Materials for Medical Devices. ASM International; Ohio, 2005
 24. Liu Y, Wu G, de Groot K. Biomimetic coatings for bone tissue engineering of critical-sized defects. *J R Soc Interface*.2010;
 25. Heini P, Rottmair A, Körner C, Singer R. Cellular Titanium by Selective Electron Beam Melting. *Advanced Engineering Materials*.2007;9:360-4.
 26. De Palma F, Erriquez A, Rossi R, Spinelli M. Duofit total hip arthroplasty: a medium- to long-term clinical and radiographic evaluation. *Journal of Orthopaedics and Traumatology*.2007;117-22.
 27. Kumar M, Dasarathy H, Riley C. Electrodeposition of brushite coatings and their transformation to hydroxyapatite in aqueous solutions. *J Biomed Mater Res*.1999;45:302-10.
 28. McDowell H, Gregory TM, Brown WE. Solubility of $\text{Ca}_5(\text{PO}_4)_3\text{OH}$ in system $\text{Ca}(\text{OH})_2\text{-H}_3\text{PO}_4\text{-H}_2\text{O}$ at 5, 10 25 and 37 °C. *J Res Natl Bur Stand (Phys Chem)*.1977;81A:273-81.
 29. Schouten C, Meijer GJ, van den Beucken JJ, Leeuwenburgh SC, de Jonge LT, Wolke JG, Spauwen PH, Jansen JA. In vivo bone response and mechanical evaluation of electrosprayed CaP nanoparticle coatings using the iliac crest of goats as an implantation model. *Acta Biomater*.2010;6:2227-38.
 30. Dhert WJ, Verheyen CC, Braak LH, de Wijn JR, Klein CP, de Groot K, Rozing PM. A finite element analysis of the push-out test: influence of test conditions. *J Biomed Mater Res*.1992;26:119-30.
 31. Chang YS, Oka M, Kobayashi M, Gu HO, Li ZL, Nakamura T, Ikada Y. Significance of interstitial bone ingrowth under load-bearing conditions: a comparison between solid and porous implant materials. *Biomaterials*.1996;17:1141-8.
 32. Becker P, Neumann HG, Nebe B, Luthen F, Rychly J. Cellular investigations on electrochemically deposited calcium phosphate composites. *J Mater Sci Mater Med*.2004;15:437-40.
 33. Reigstad O, Franke-Stenport V, Johansson CB, Wennerberg A, Rokkum M, Reigstad A. Improved bone ingrowth and fixation with a thin calcium phosphate coating intended for complete resorption. *J Biomed Mater Res B Appl Biomater*.2007;83:9-15.
 34. Kuroda S, Virdi AS, Li P, Healy KE, Sumner DR. A low-temperature biomimetic calcium phosphate surface enhances early implant fixation in a rat model. *J Biomed Mater Res A*.2004;70:66-73.
 35. Hägi TT, Enggist L, Michel D, Ferguson SJ, Liu Y, Hunziker EB. Mechanical insertion properties of calcium-phosphate implant coatings. *Clin Oral Implants Res*.2010;
 36. Moriyama Y, Ayukawa Y, Ogino Y, Atsuta I, Todo M, Takao Y, Koyano K. Local application of fluvastatin improves peri-implant bone quantity and mechanical properties: a rodent study. *Acta Biomater*.2010;6:1610-8.
 37. Majkowski RS, Bannister GC, Miles AW. The effect of bleeding on the cement-bone interface. An experimental study. *Clin Orthop Relat Res*.1994;293-7.

Chapter 6



In vivo assessment of bone ingrowth potential of three-dimensional E-Beam produced implant surfaces and the effect of additional treatment by acid etching and hydroxyapatite coating



Abstract

The bone ingrowth potential of three-dimensional E-beam-produced implant surfaces was examined by histology and compared to a porous plasma-sprayed control. The effects of acid etching and a hydroxyapatite (HA) coating were also evaluated by histology. Specimens were implanted in the distal femur of 10 goats. Histological analysis of bone ingrowth was performed 6 weeks after implantation. The E-beam-produced surfaces showed significantly better bone ingrowth compared to the plasma-sprayed control. Additional treatment of the E-beam surface structures with a HA coating, further improved bone ingrowth potential of these structures significantly. Acid etching of the E-beam structures did not influence bone ingrowth significantly. In conclusion, the HA-coated, E-beam-produced structures are promising potential implant surfaces.

Introduction

Although total hip arthroplasty is a very successful orthopaedic procedure, 5 to 10 percent of the cementless implants still fail within 10 years of implantation, mainly due to aseptic loosening.[1;2] The frequency of failure is likely to increase due to the implantation in younger and more active patients.[3]

The long term success of cementless prostheses depends on fixation by bone ingrowth in the early postoperative period.[4] Bone ingrowth is influenced by the implant surface characteristics, such as pore size and porosity. Although the optimal pore size has yet to be determined, it is evident that this parameter too affects bone ingrowth.[5] It has been shown that a substantial increase in fixation strength can be obtained by increasing the porosity of implants to 75-80%.[6] Furthermore, interconnectivity between the pores is crucial in order to permit bone ingrowth.[7] Bone ingrowth into a porous structure might increase the strength at the bone-implant interface. However, one can expect that ingrowth beyond a certain depth does not enhance the strength of the bone-implant interface, similar as seen for the cement-bone interface.[8]

Electron beam melting is a rapid-prototyping technique that can be utilized to produce a solid implant and a porous surface structure in one manufacturing step. The implant is build up out of metal powder to reproduce a geometry defined by a 3-dimensional CAD model.[9;10] Therefore, it is possible to design implant surfaces with many different surface characteristics. By adapting the surface characteristics bone ingrowth could be further enhanced, resulting in better bone ingrowth than conventional implant surfaces.

Several (post-production) implant surface modifications are investigated in an attempt to improve bone ingrowth, including application of a calciumphosphat coating (e.g. hydroxyapatite) and texturing by chemical etching.[11] Hydroxyapatite (HA) has been applied on porous implant surfaces in order to enhance the bone ingrowth potential.[12;13] The process of bone formation onto HA coated implants might be mediated by dissolution of the coating soon after implantation followed by formation of a carbonated calcium phosphate layer and bone growth towards the implant.[14]

Acid-etching of the surface has been shown to enhance the bone ingrowth potential of porous implant surfaces.[15] The topography of an etched implant relies on acid mixture, etching time, temperature and topography prior to etching.[11] However, the treatment results in relatively low roughness values.[16;17]

The goal of this study was to evaluate the bone ingrowth potential of 3 new E-beam produced structures and compare this to a highly porous titanium plasma spray coating. Furthermore the influence of addition of hydroxyapatite and acid-etching was tested.

Materials and Methods

Specimens

The specimens (8 x 4 x 10 mm³, Eurocoating Spa, Trento, Italy) were produced by electron beam melting. In this rapid prototyping process, the implants were build up out of Ti6Al4V powder. The powder size used in the E-beam process ranged from 45 to 100 µm. The E-beam specimens were created using a 3D CAD model which was segmented into layers of 0.1 mm in order to generate layer information. Subsequently, a homogeneous powder layer was applied on the process platform in a vacuum chamber at constant high temperature (±700°C). The electron beam scanned the powder layer line by line and melted the loose powder particles at programmed locations forming a compact layer in the desired shape. The process platform was then lowered by one layer thickness (0.1mm) and a new powder layer (of 0.1 mm thickness) was applied after which the process is repeated [9;10]. Upon completion, all specimens were sandblasted with corundum and cleaned in a specific washer for medical devices.

Three different 3-dimensional E-beam surface structures were developed; the gyroid structure, the star small structure and the cubic enlarged structure. The design of the gyroid structure is based on the mathematical gyroid surface (infinitely connected periodic surface containing no straight lines). The star structure consisted of 3-D cross-shapes and the cubic enlarged structure had large quadrangular pores. (Figure 1) As a control a highly porous titanium plasma spray coating (Ti sponge) and a plain, rough E-beam surface with hydroxyapatite coating (Osprovit®, Eurocoating Spa, Trento, Italy) were tested. (Figure 2)

To evaluate the effect of further treatment of the E-beam structures, an acid-etching procedure (with a mixture of nitric and fluoridic acid solution) was performed on the gyroid and star small structure. For the star small structure only the etched form was tested, for the gyroid structure an untreated surface was tested as well. Furthermore the cubic enlarged structure was tested with and without a hydroxyapatite coating (applied by plasma spray technique, coating thickness 70 ± 10 µm). All surfaces and their treatments are listed in Table 1.

Two different surfaces were combined on 1 specimen except for the titanium plasma sprayed sponge coating, resulting in 4 different specimens.

Table 1. The 3D surface structure, production process and additional treatment of the tested surfaces.

Surface	Structure	E-beam produced	Additional treatment
Gyroid	Gyroid	yes	none
Cubic enlarged	Cubic enlarged	yes	none
Gyroid etched	Gyroid	yes	etching
Star etched	Star	yes	etching
Cubic enlarged HA	Cubic enlarged	yes	HA
Rough HA	none	yes	HA
Ti sponge	plasma spray coating	no	none



Figure 1. CAD-files. The CAD-files of the elements forming the gyroid, cubic enlarged and star E-beam structures (from left to right).

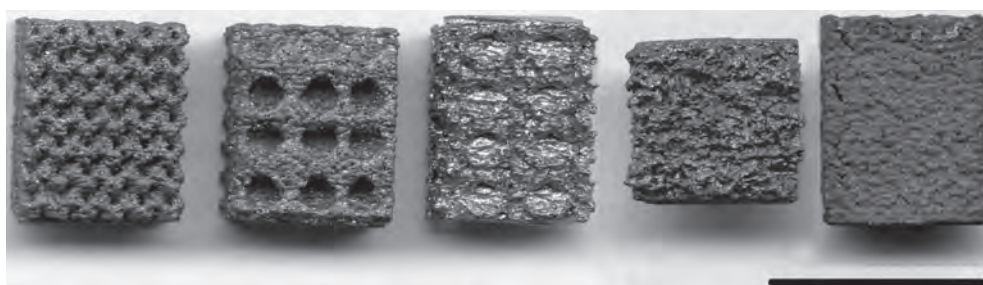


Figure 2. 3-dimensional E-beam structures. From left to right: gyroid, cubic enlarged and star E-beam structure, the Ti sponge and rough HA surface. Bar = 10 mm

Surface characterization

MicroCT analysis (SCANCO Medical, Switzerland, resolution 50µm) was performed to define the pore size, porosity, pore connectivity and surface area of each specimen.

Surface roughness values of the specimens were determined using a Universal Surface Tester (UST) (Innowep, Wurzburg, Germany).

Experimental design

Surgery was performed on ten female, skeletal mature goats (*Capra Hircus Sana*), weighing 49-67 kg (mean 55 kg). The specimens were implanted in the trabecular bone of the distal femur. Each goat received 2 specimens; one in the medial and one in the lateral condyl of the right leg. The different implants were equally divided among the goats and implantation areas (n=5 for each group).

The goats were anaesthetized with propofol ((4 mg/kg B. Brown, Melsungen, Germany), intubated and anesthesia was maintained using isoflurane. The goats were placed in a lateral position and the implantation procedure was performed under strict sterile conditions. The knee was approached lateral, visualizing the origin of the lateral collateral ligament. Approximately 1.5 cm from the origin a hole (Ø 4.0 mm) was drilled reaching into the medial condyle. Saline was used

during the drilling to prevent heat induced necrosis. Sharp osteotomes with increasing size (4x4mm to 4x8mm) were used to shape the hole to the size of the specimen. The implantation area was inspected to guarantee the specimen would be completely surrounded by trabecular bone. Just above the origin of the lateral collateral ligament a second implantation area was created (in the lateral condyl). The specimens were inserted press-fit into the holes and the fascia and skin were closed separately with resorbable sutures.

The goats received ampicillin (7.5 mg/kg Intervet, Boxmeer, The Netherlands) for 4 days after surgery. Fluorochromes were administered by subcutaneous injection at 2 (Calcein green, 25 mg/kg), 4 (Xylenol Orange, 30 mg/kg) and 6 weeks (Tetracyclin, 25 mg/kg) after surgery during two consecutive days in order to generate ingrowth data of different time points for each animal. Goats were sacrificed 6 weeks post-operative by an overdose of barbiturate pentobarbital (Euthesate, Ceva Santa Animale, Libourne, France). This study was approved by the animal ethics committee of the Radboud University Nijmegen.

Histological analysis

The thickness of the coating on the cubic enlarged HA surface and rough HA surface was measured on 10 slices.

Statistical analysis

Statistical analysis was performed with a one way ANOVA and a LSD post hoc test using SPSS (16.0, SPSS Inc., Chicago, USA). A p-value less than 0.05 was considered significant.

Results

Surface characterization

The pore size of the E-beam produced surfaces ranged from 0.40 to 1.35 mm. All E-beam produced surfaces had a relatively high porosity (44 to 73%). The titanium sponge control had a pore size of 0.23 mm and a porosity of 34%. All surfaces had a good pore connectivity index and a large surface area. (**Table 2**) The surface morphology before implantation showed the characteristic appearances of E-beam surfaces without additional treatment (A, B), with additional treatment (acid-etched and HA coated surfaces (C, D and E, F respectively) and the titanium plasma sprayed control (G). (**Figure 3,4**)

The roughness measurements showed that the roughness decreased after the etching treatment and increased after application of a hydroxyapatite coating. (**Table 3**)

Histomorphometric analysis (Figure 5)

One Ti sponge specimen was implanted too close to the intercondylar notch and was not surrounded by trabecular bone. Therefore this specimen was excluded for further analysis. Histological analysis of the specimens showed no sign of infection or metal debris.

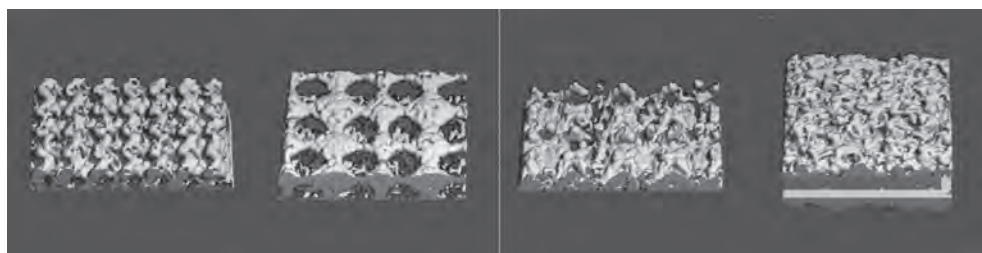


Figure 3. Micro-CT images. From left to right: gyroid, cubic enlarged, star and Ti sponge surface

Table 2. Surface characteristics. The pore size (mm), porosity (%), pore connectivity (1/mm³) and surface area (mm²) of the tested surfaces.

Surface	Pore size (mm)	Porosity (%)	Pore connectivity (1/mm ³)	Surface area (mm ²)
Gyroid	0.40	44	2.71	328
Cubic enlarged	1.35	73	1.73	239
Gyroid etched	0.47	61	4.52	306
Star etched	0.67	70	0.82	169
Cubic enlarged HA	1.23	61	0.65	297
Ti sponge	0.23	34	6.35	423

The cubic enlarged surface structure and the cubic enlarged HA surface showed best bone ingrowth depth. Bone ingrowth depth of the cubic enlarged structure was significantly greater compared to the gyroid (at 4 and 6 weeks, $p=0.01$ and $p=0.002$ respectively) and the Ti sponge surface (at 2, 4 and 6 weeks, $p=0.03$, $p=0.003$ and $p=0.002$ respectively). (**Figure 6**)

With respect to percentage direct bone implant contact, the cubic enlarged HA, rough HA and cubic enlarged surface scored best. The percentage direct bone implant contact was significantly better for the cubic enlarged structure than for the gyroid structure ($p=0.03$). Coating with HA significantly increased the bone implant contact of the cubic enlarged structure ($p=0.01$). This cubic enlarged HA surface was significantly better compared to the Ti sponge control ($p<0.001$). The rough HA surface showed significantly higher bone implant contact than the gyroid structure ($p<0.001$) and the Ti sponge surface ($p=0.001$). No significant effect of chemical etching on bone implant contact was seen, although both etched surface structures showed a low amount of bone implant contact. (**Figure 7**)

The thickness of the HA coating after 6 weeks implantation was $61.6 \mu\text{m} (\pm 10.7)$ for the cubic enlarged HA surface and $64.3 \mu\text{m} (\pm 10.5)$ for the rough HA surface.

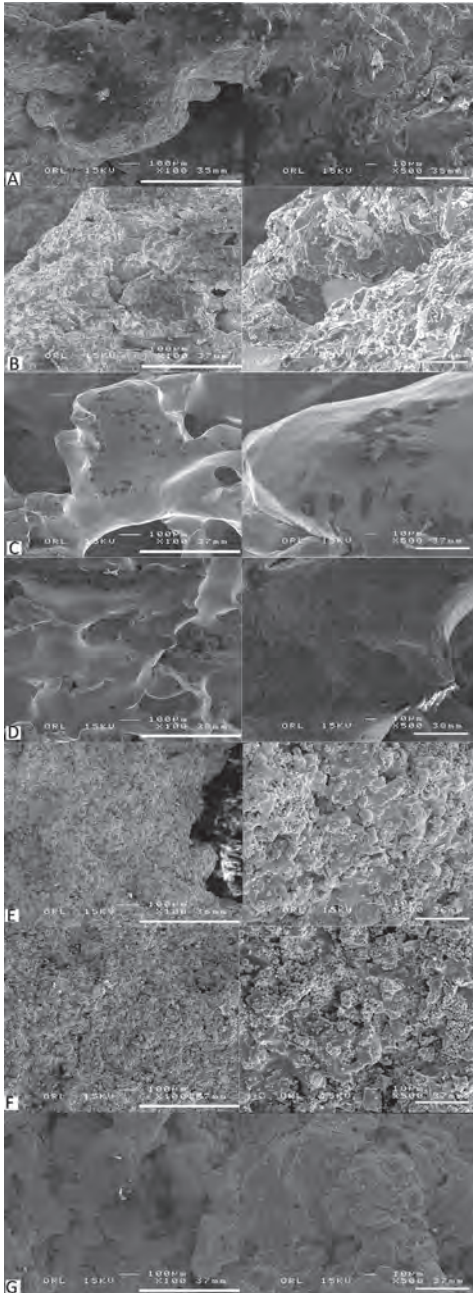


Figure 4. Surface characterization. SEM images of the gyroid (A), cubic enlarged (B), gyroid etched (C), star etched (D), cubic enlarged HA (E), rough HA (F) and Ti Sponge (G) implant surfaces. Left column: bar = 500 µm, right column: bar = 50 µm

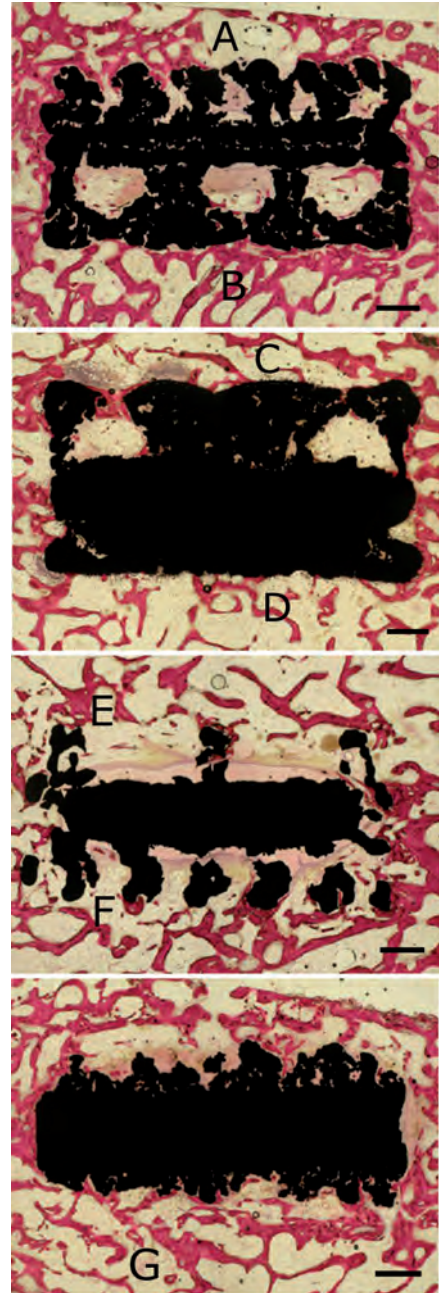


Figure 5. Histomorphology. Microscopic images of histology slides of gyroid (A), cubic enlarged (B), cubic enlarged HA (C), rough HA (D), star etched (E), gyroid etched (F) and Ti Sponge (G) implant surfaces. Bar = 1 mm.

Table 3. Surface roughness. The surface roughness (Ra) (μm) of the tested surfaces.

Surface	Roughness (Ra) (μm)
Gyroid	3.92
Cubic enlarged	4.43
Gyroid etched	3.34
Star etched	5.62
Cubic enlarged HA	4.52
Rough HA	4.39

Figure 6. Bone ingrowth depth. Graph showing bone ingrowth depth for the different implant surfaces at 2,4 and 6 weeks after surgery. Significance is indicated by*.

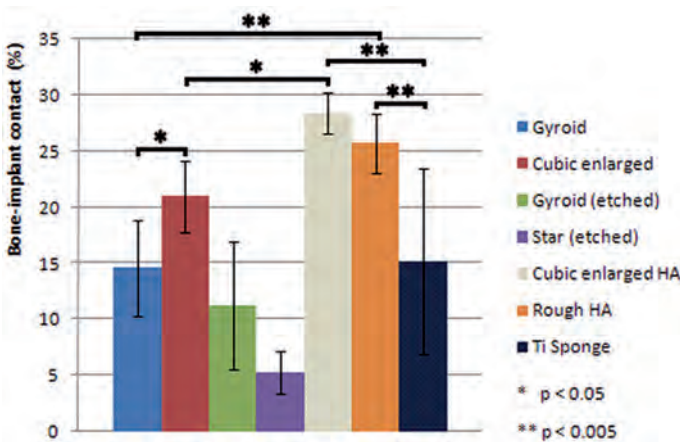
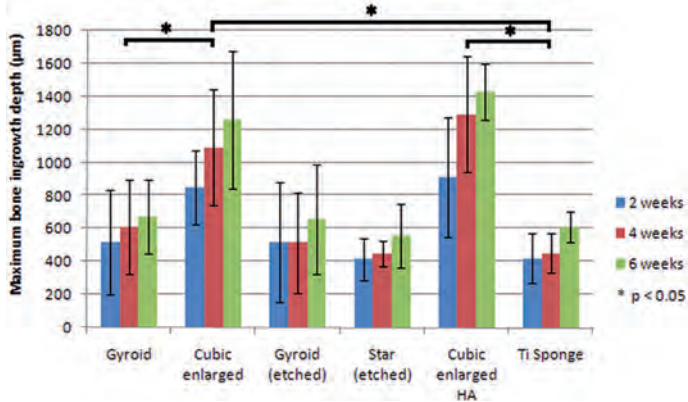


Figure 7. Bone implant contact. Graph showing the percentage of bone implant contact for the different implant surfaces. *p < 0.05, ** p < 0.005.

Discussion

In the current study, the bone ingrowth potential of E-beam produced surface structures were compared to a Ti plasma spray coating with similar porosity. Furthermore the effect of additional treatment, hydroxyapatite and chemical etching, was investigated. This experiment was limited to surface characterization and histological analysis. No tests for mechanical strength of the bone implant interface were performed. Although many implant

surfaces were evaluated with a limited amount of goats, the choice of the surfaces implicated some restrictions. In some cases it was not clear whether the effect on bone ingrowth was caused by the E-beam structure or by the additional treatment. The surface characterization by microCT analysis is limited by the resolution, which means that pores under 50 μm cannot be detected. This will affect the measurements on the Ti sponge surface the most, due to the design of the surface (with the smallest pores). The absence of weight bearing in the model is a limitation of this study as well.

The cubic enlarged surface showed a significant better bone ingrowth compared to the gyroid structure and Ti sponge surface. No additional treatment was used for all these surfaces. Therefore one could say that differences in bone ingrowth potential between these surfaces are due to either the E-beam technology itself or the surface characteristics. Comparable results of the E-beam gyroid structure and Ti sponge (with similar pore size and porosity), made clear that the E-beam technology itself does not benefit or harm the bone ingrowth potential. The superior bone ingrowth of the cubic enlarged structure compared to the gyroid structure is therefore likely to be caused by its surface topography. This structure has a large pore size (1.35 mm) and a high porosity (73%). So there is a clear beneficial effect of large pore size and high porosity on the bone ingrowth potential, which is supported by the literature.[6;18] Recently, various authors have showed that besides porosity, pore interconnectivity is a critical factor for bone ingrowth.[7;19] However, Otsuki et al.[7] found no differences in vascularization between two groups with different interconnectivities and suggested that the number of interconnections is a more important factor compared to the size of the interconnections. Nevertheless, no clear influence of the amount of interconnections, as determined by microCT analysis, on the amount of bone ingrowth could be concluded from this study.

Concerning the effect of additional treatments, HA significantly increased the bone ingrowth potential of a porous E-beam structure. This enhancement in bone ingrowth was visible in the early postoperative period, suggesting that HA accelerates bone ingrowth as well. The acceleration of bone ingrowth achieved by the HA coating could be beneficial with regard to post-operative partial weight-bearing and rehabilitation.[20] The fact that hydroxyapatite enhances and accelerates bone ingrowth when applied on implant surfaces is well known. [12-14;21] However, in this study, both these positive effects are achieved with a plasma spray technique on a porous surface.

No beneficial effect of the etching procedure on bone ingrowth could be found. This is in contrast to other studies.[11;15] This difference could be explained by the fact that in our study the acid etching was performed on a 3D surface structure. Furthermore, as explained earlier, the success of acid etching is influenced by acid mixture, etching time and temperature.[11] However, although the acid etching procedure did not enhance bone ingrowth, the procedure did not harm the bone ingrowth as well.

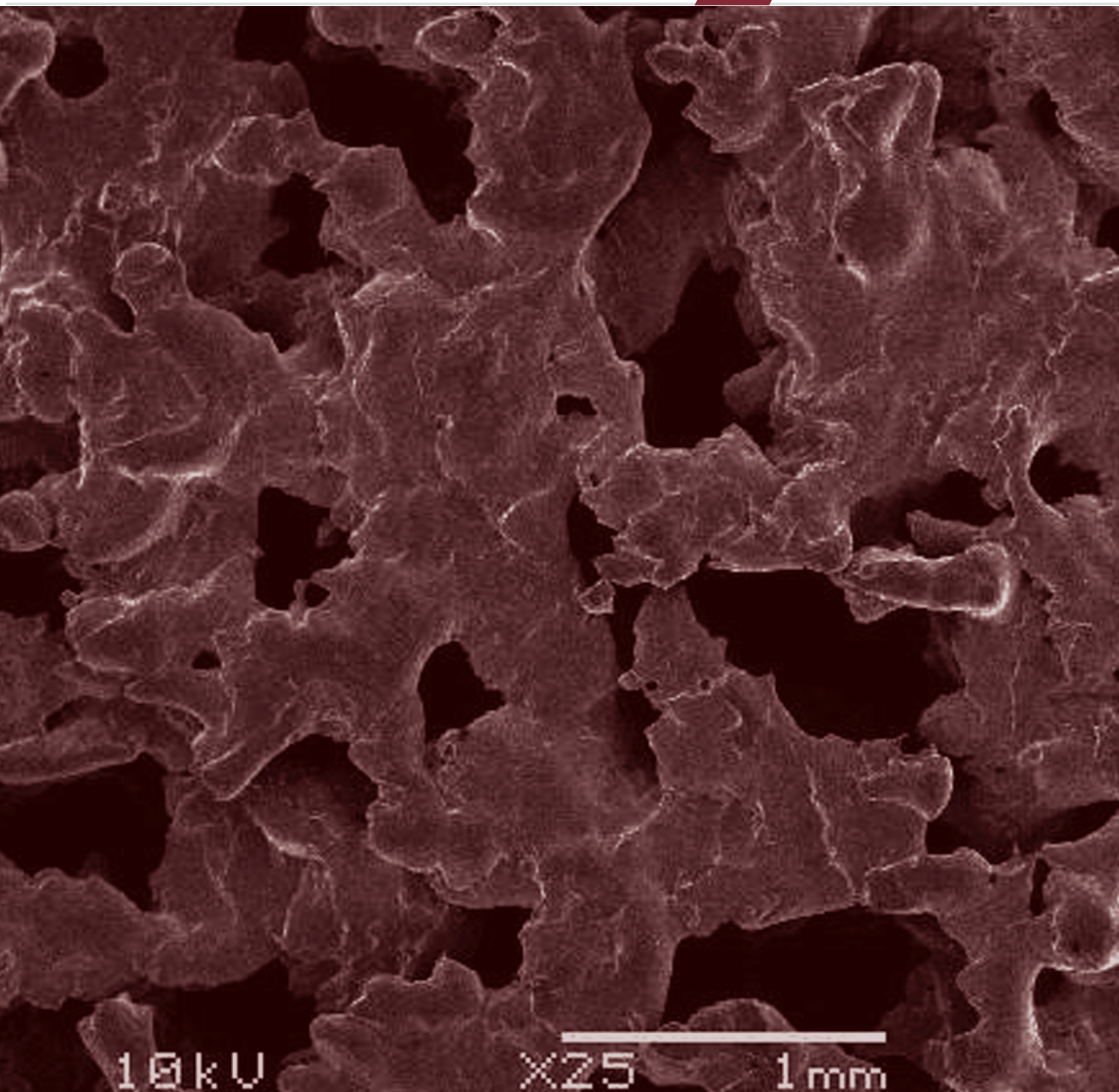
Conclusion

In conclusion, the E-beam technique provides the ability to promote enhanced bone ingrowth compared to a porous, conventionally made control specimen. Additional treatment of the 3-dimensional E-beam implant surface structures with a hydroxyapatite coating (applied by plasma spray technique), further improves the bone ingrowth potential of these structures. Acid-etching of the E-beam structures did not influence bone ingrowth.

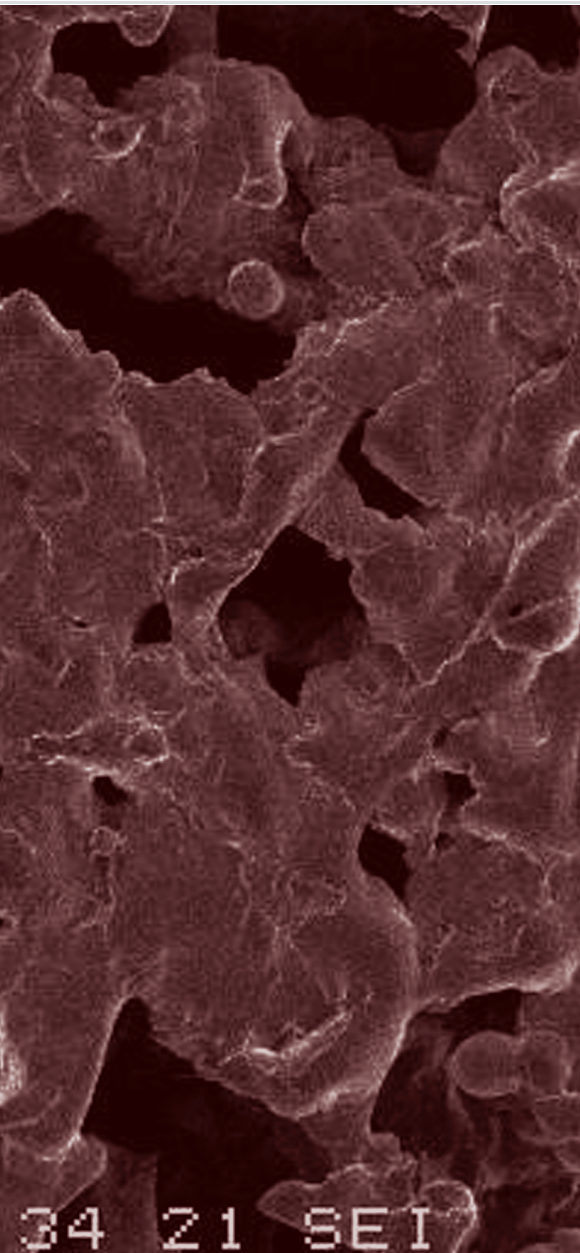
References

1. Eskelinen A, Remes V, Helenius I, Pulkkinen P, Nevalainen J, Paavolainen P: Uncemented total hip arthroplasty for primary osteoarthritis in young patients: a mid-to long-term follow-up study from the Finnish Arthroplasty Register. *Acta Orthop* 77(1):57, 2006
2. Karrholm J, Garellick G, Herberts P. Annual Report 2006. Swedish National Hip Arthroplasty Register. 2007.
3. McAuley JP, Szuszczewicz ES, Young A, Engh CA, Sr.: Total hip arthroplasty in patients 50 years and younger. *Clin Orthop Relat Res*(418):119, 2004
4. Basarir K, Erdemli B, Can A, Erdemli E, Zeyrek T: Osseointegration in arthroplasty: can simvastatin promote bone response to implants? *Int Orthop* 33(3):855, 2009
5. Karageorgiou V, Kaplan D: Porosity of 3D biomaterial scaffolds and osteogenesis. *Biomaterials* 26(27):5474, 2005
6. Bobyn JD, Stackpool GJ, Hacking SA, Tanzer M, Krygier JJ: Characteristics of bone ingrowth and interface mechanics of a new porous tantalum biomaterial. *J Bone Joint Surg Br* 81(5):907, 1999
7. Otsuki B, Takemoto M, Fujibayashi S, Neo M, Kokubo T, Nakamura T: Pore throat size and connectivity determine bone and tissue ingrowth into porous implants: three-dimensional micro-CT based structural analyses of porous bioactive titanium implants. *Biomaterials* 27(35):5892, 2006
8. Majkowski RS, Bannister GC, Miles AW: The effect of bleeding on the cement-bone interface. An experimental study. *Clin Orthop Relat Res*(299):293, 1994
9. Heini P, Rottmair A, Körner C, Singer R: Cellular Titanium by Selective Electron Beam Melting. *Advanced Engineering Materials* 9(5):360, 2007
10. Heini P, Müller L, Körner C, Singer RF, Müller FA: Cellular Ti-6Al-4V structures with interconnected macro porosity for bone implants fabricated by selective electron beam melting. *Acta Biomater* 4(5):1536, 2008
11. Daugaard H, Elmengaard B, Bechtold JE, Soballe K: Bone growth enhancement in vivo on press-fit titanium alloy implants with acid etched microtexture. *J Biomed Mater Res A* 87(2):434, 2008
12. Barrere F, van der Valk CM, Meijer G, Dalmeijer RA, de GK, Layrolle P: Osteointegration of biomimetic apatite coating applied onto dense and porous metal implants in femurs of goats. *J Biomed Mater Res B Appl Biomater* 67(1):655, 2003
13. Tsukeoka T, Suzuki M, Ohtsuki C, Tsuneizumi Y, Miyagi J, Sugino A, Inoue T, Michihiro R, Moriya H: Enhanced fixation of implants by bone ingrowth to titanium fiber mesh: effect of incorporation of hydroxyapatite powder. *J Biomed Mater Res B Appl Biomater* 75(1):168, 2005
14. Sun L, Berndt CC, Gross KA, Kucuk A: Material fundamentals and clinical performance of plasma-sprayed hydroxyapatite coatings: a review. *J Biomed Mater Res* 58(5):570, 2001
15. Hacking SA, Harvey EJ, Tanzer M, Krygier JJ, Bobyn JD: Acid-etched microtexture for enhancement of bone growth into porous-coated implants. *J Bone Joint Surg Br* 85(8):1182, 2003
16. Silva TS, Machado DC, Viezzer C, Silva Junior AN, Oliveira MG: Effect of titanium surface roughness on human bone marrow cell proliferation and differentiation: an experimental study. *Acta Cir Bras* 24(3):200, 2009
17. Stöver M, Renke-Gluszko M, Schratzenstaller T, Will J, Klink N, Behnisch B, Kastrati A, Wessely R, Hausleiter J, Schömg A, Wintermantel E: Microstructuring of stainless steel implants by electrochemical etching. *J Mater Sci* 41:5569, 2006
18. Lopez-Heredia MA, Goyenvalle E, Aguado E, Pilet P, Leroux C, Dorget M, Weiss P, Layrolle P: Bone growth in rapid prototyped porous titanium implants. *J Biomed Mater Res A* 85(3):664, 2008
19. Jones AC, Arns CH, Hutmacher DW, Milthorpe BK, Sheppard AP, Knackstedt MA: The correlation of pore morphology, interconnectivity and physical properties of 3D ceramic scaffolds with bone ingrowth. *Biomaterials* 30(7):1440, 2009
20. Habibovic P, Barrère F, van Blitterswijk CA, de GK, Layrolle P: Biomimetic hydroxyapatite coating on metal implants. *J Am Ceram Soc* 85(3):517, 2002
21. Davis JR: Coatings. p. 179. In Davis & Associates (ed): *Handbook of Materials for Medical Devices*. ASM International; Ohio, 2005

Chapter 7



Bone ingrowth potential of electron beam and selective laser melting produced trabecular-like implant surfaces with and without a biomimetic coating



Abstract

The bone ingrowth potential of trabecular-like implant surfaces produced by either selective laser melting (SLM) or electron beam melting (EBM), with or without a biomimetic calciumphosphate coating, was examined in goats. For histological analysis and histomorphometry of bone ingrowth depth and bone implant contact specimens were implanted in the femoral condyle of goats. For mechanical push out tests to analyse mechanical implant fixation specimens were implanted in the iliac crest. The follow up periods were 4 (7 goats) and 15 weeks (7 goats).

Both the SLM and EBM produced trabecular-like structures showed a variable bone ingrowth after 4 weeks. After 15 weeks good bone ingrowth was found in both implant types. Irrespective to the follow up period, and the presence of a coating, no histological differences in tissue reaction around SLM and EBM produced specimens was found. Histological no coating was detected at 4 and 15 weeks follow up. At both follow up periods the mechanical push out strength at the bone implant interface was significantly lower for the coated SLM specimens compared to the uncoated SLM specimens. The expected better ingrowth characteristics and mechanical fixation strength induced by the coating were not found. The lower mechanical strength of the coated specimens produced by SLM is a remarkable result, which might be influenced by the gross morphology of the specimens or the coating characteristics, indicating that further research is necessary.

Introduction

The long term success of cementless prostheses depends on primary stability and thereafter fixation by bone ingrowth in the early postoperative period.[1] Implant surfaces, as scaffolds for osteogenesis, should mimic bone morphology and structure in order to optimize integration into the surrounding tissue.[2] Human trabecular bone has a porosity of 50-90% [3] with pore sizes in the order of 1 mm in diameter.[4] The importance of mimicking human trabecular properties for implant surfaces is confirmed by research that showed that a substantial increase in fixation strength can be obtained by increasing the porosity of implants to 75-80%.[5]

Using rapid prototyping techniques, implants and porous trabecular bone like surfaces can be produced in one manufacturing step. With these techniques the implants are built up out of metal powder in a layer-by-layer fashion based on CAD data. This enables the development of a large variety of complex 3-dimensional structures. Rapid prototyping is therefore perfectly suited to produce a trabecular-like implant surface.[6] Electron beam melting (EBM) and selective laser melting (SLM) are rapid prototyping techniques in which the metal powder is melted by an electron beam and laser beam respectively.[6] SLM is a more accurate technique than EBM, which means more delicate structures can be build.

Previous work of our group showed good attachment, proliferation and differentiation of mesenchymal stem cells on E-beam produced surfaces.[7] The bone ingrowth potential of EBM produced surfaces was comparable to, and after 15 weeks better than, the bone ingrowth of a titanium plasma spray coating.[8] Warnke et al. showed that SLM specimens were biocompatible, with good vitality and spreading of human osteoblast on the specimens.[9] New bone formation on the surface of SLM specimens was demonstrated when implanted in the femoral condyles of rabbits.[10] To the best of our knowledge, a direct comparison of bone ingrowth potential between electron beam and laser melting has never been published.

Calciumphosphate (CaP) coatings have been successfully applied on orthopedic and dental implants. The advantages of these coatings are enhancement of bone formation and accelerated bonding between implant and bone. With biomimetic coating techniques it is possible to apply a CaP coating on porous and irregular surfaces.[11] Addition of a CaP coating to 3-dimensional EBM produced surfaces has been shown to significantly increase bone ingrowth.[8]

The goal of this study was to investigate and compare the bone ingrowth potential of trabecular like implant surfaces produced by either EBM or SLM, with and without the addition of a biomimetic hydroxyapatite coating.

Materials and methods

Specimens:

Surfaces structures were produced by SLM or EBM (Figures 1 A, B and 2 A, B for SLM and EBM, respectively). The pore size was 250-800 μm for the SLM build specimens and 350-1400 μm for the EBM build specimens, whereas the porosity was 63% and 49%, respectively. The thickness

of the trabecular layer was 1800 μ m for the EBM and 1500 μ m for the SLM. The specimens used for histological analysis were composed of two separate specimens produced by SLM and EBM which were held together by small titanium pins. For each production technique (SLM and EBM) surfaces were coated with a calciumphosphate coating or were left uncoated. (n=7)

Electron beam melting:

EBM is a rapid prototyping process, in which the implants are build up out of Ti6Al4V powder. The powder size used in the E-beam process ranged from 45 to 100 μ m. The EBM specimens were created using a 3D CAD model which was segmented into layers of 0.1 mm in order to generate layer information. Subsequently, a homogeneous powder layer was applied on the process platform in a vacuum chamber at constant high temperature ($\pm 700^{\circ}\text{C}$). The electron beam scanned the powder layer line by line and melted the loose powder particles at programmed locations forming a compact layer in the desired shape. The process platform was then lowered by one layer thickness (0.1mm) and a new powder layer (of 0.1 mm thickness) was applied after which the process is repeated.[12-14] EBM specimens were grossly cleaned by residual beads by shotpeening after manufacturing with the same powder used in the process. The overall accuracy of the EBM technology in terms of computer model reconstruction is specific geometry dependent (e.g. $\pm 150 \mu$ m).

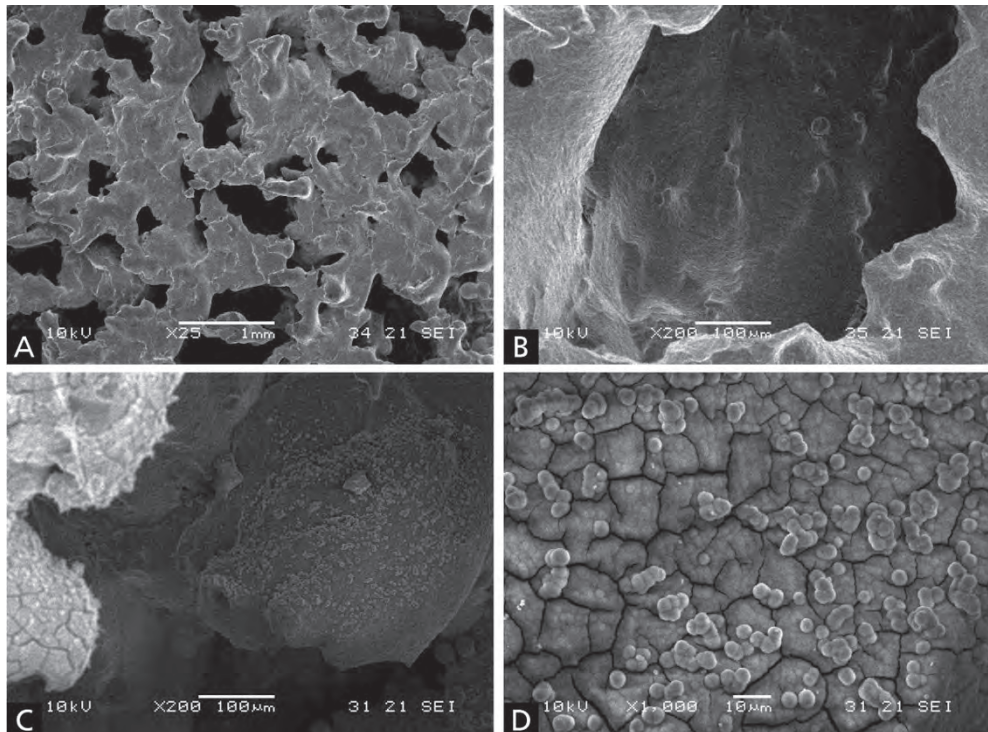


Figure 1. SEM micrographs of SLM produced specimens. A, B uncoated specimens, C and D coated specimens. Notice the globular surface at high magnification (D).

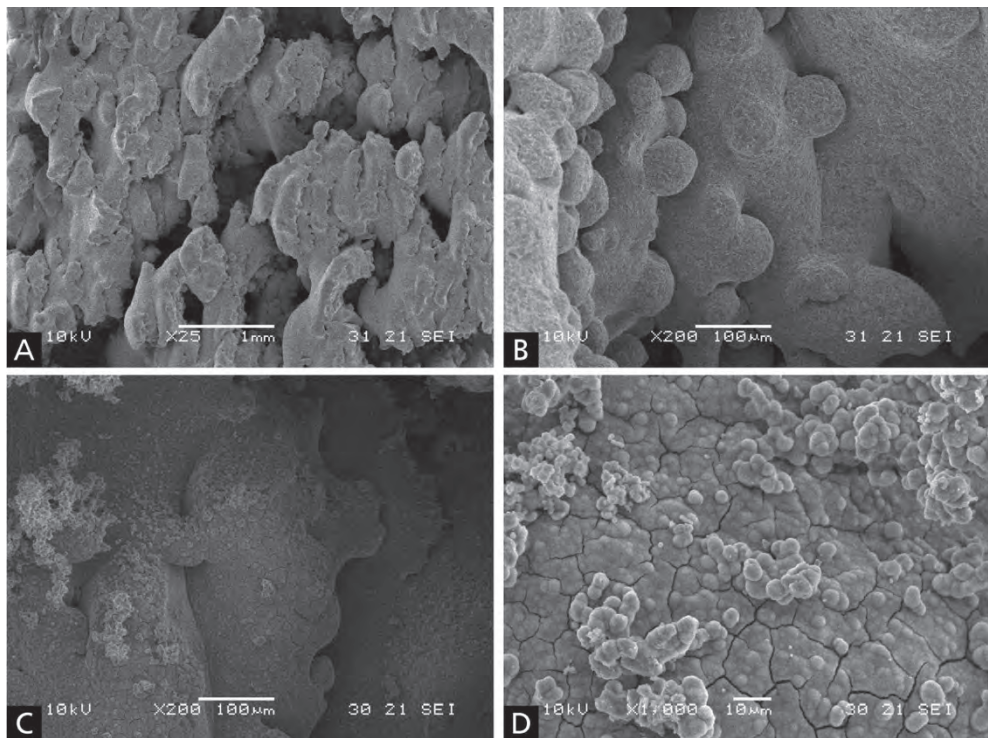


Figure 2. SEM micrographs of EBM produced specimens. A, B uncoated specimens, C and D coated specimens. Notice the globular surface at high magnification (D).

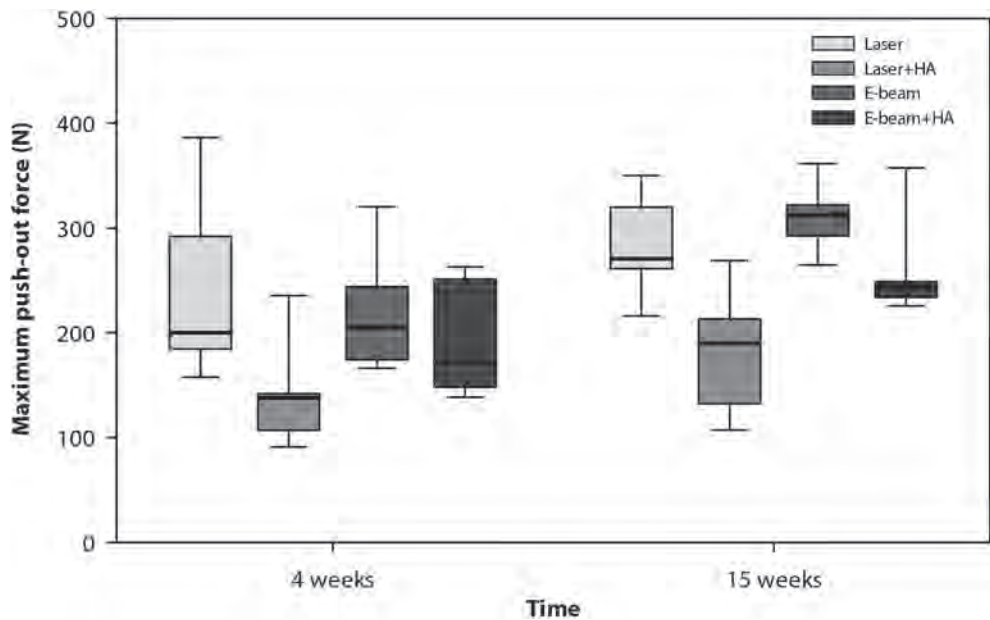


Figure 3. Push-out mechanical data of SLM and EBM specimens after 4 and 15 weeks.

Selective laser melting:

SLM is a rapid prototyping process, using a laser beam as energy source for the consolidation of Ti6Al4V powder. As all rapid prototyping techniques, SLM uses CAD data and layer-by-layer generation of the specimens. The powder size used in the SLM process ranged from 20 to 50 μm . In contrast to the EBM process, in selective laser melting no preheating of the powder is used whereas a thermal post treatment on the produced specimens is essential to allow the material to be in compliance with applicable norms. [15;16] SLM specimens were grossly cleaned by residual beads by corundum sandblasting after manufacturing. The accuracy of the selective laser melting technique is geometry dependent but substantially lower than EBM (e.g. $\pm 50\text{ }\mu\text{m}$).

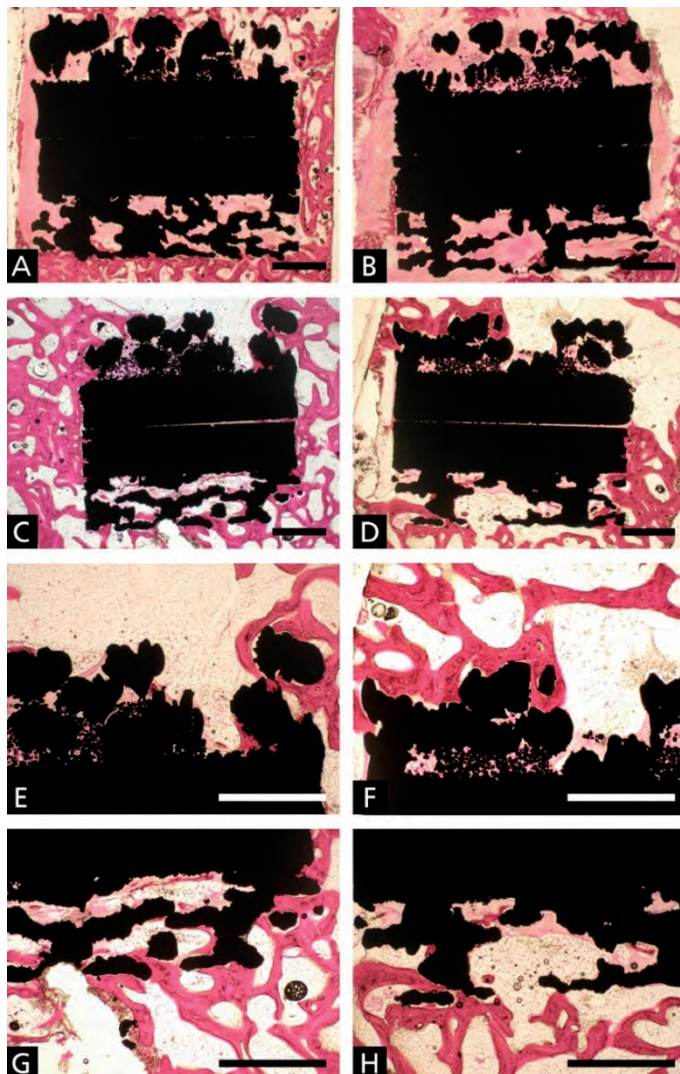


Figure 4 A-H. Histology of samples implanted in femoral condyles. A, C with biomimetic coating, B and D non-coated specimens. In all figures the EBM coating is at the top and the laser at the bottom. A and B 4 weeks follow up, C and D 15 weeks follow up. E, G and F, H magnifications of C and D, respectively. Bar in A-D is 1 mm, bar in E-F is 1.5 mm.

Calciumphosphate coating:

The calcium phosphate coating was applied by immersing specimens in a calcifying solution for a few hours (pH 7.2, 37° C). The coating (5-10 µm) consists of two layers, a homogeneous layer directly on the metal and a surface layer of globular aggregates (Figures 1 C, D and 2 C, D). [17] The resulting coating appeared to be hydroxyapatite nano-crystalline.

Experimental design:

Specimens were made in two different sizes and shapes. Cylindrical specimens of Ø 4mm and height 10 mm with one surface were used for mechanical push out testing and specimens of 5x6.5x10 mm were used for histological analysis (n=7 for each time point). Surgery was performed on 14 female, skeletal mature goats (*Capra Hircus Sana*), weighing 42-72 kg (mean 60 kg). The goats were divided in two groups, one group (7 goats) was sacrificed 4 weeks after surgery and the second group (7 goats) 15 weeks after surgery. 4 specimens (one of each surface, intended for mechanical testing) were implanted bilaterally in the iliac crest of each goat. Furthermore, each goat received 2 specimens, one with and one without coating (intended for histological analysis) in the distal femur; one in the medial and one in the lateral condyle of one knee joint.

The goats were anaesthetized with propofol (4 mg/kg B.Brown, Melsungen, Germany), intubated and anesthesia was maintained using isoflurane. The goats were placed in a prone position and the implantation procedure was performed under strict sterile conditions. For the implantation of the push out specimens, a transverse skin incision was made over the iliac crest. The incision was continued subcutaneously to the periosteum. The periosteum was opened, after which the iliac crest was fully exposed. Two implant areas were created in the iliac crest using a sharp drill (Ø 4.0mm). The specimens were inserted press-fit into the holes and the periosteum and skin were closed separately with resorbable sutures. This procedure was repeated on the contralateral side.

For implantation of the histology specimens the knee was approached lateral, visualizing the origin of the lateral collateral ligament. Approximately 1.5 cm from the origin a hole (Ø 5.0 mm) was drilled reaching into the medial condyle. A sharp osteotome was used to shape the hole to the size (6.2 x 6.4mm) of the specimen. Just above the origin of the lateral collateral ligament a second implantation area was created in the same way (in the lateral condyle). The specimens were inserted press-fit into the holes and the fascia and skin were closed separately with resorbable sutures. In both locations, iliac crest and distal femur, saline was used during the drilling to prevent heat induced necrosis and the implantation areas were inspected to guarantee that the specimens were completely surrounded by trabecular bone. The goats received ampicillin (7.5 mg/kg Intervet, Boxmeer, The Netherlands) during 4 days after surgery.

Goats were sacrificed 4 or 15 weeks post-operative by an overdose of pentobarbital (Euthesate, Ceva Santa Animale, Libourne, France). After sacrificing of the animals, the distal femurs and iliac crests were retrieved. This study was approved by the animal ethics committee of the Radboud University Nijmegen.

Mechanical testing:

The specimens from the iliac crest with surrounding bone were stored in the freezer until the test was performed. Based on X-ray images (Faxitron), the surrounding bone was sawed into a cube with the implant surrounded by bone, the top and bottom of the specimen free of tissues and the implant exactly perpendicular to the surfaces of top and bottom. Subsequently this cube was placed in a jig, which supported only the surrounding bone and not the implanted specimen. The clearance between specimen and support by the jig was 0.7 mm.[18] The load (MTS, load cell 1kN) was placed on top of the specimen and pushed the specimen out the surrounding bone with a fixed speed (1 mm/min) and continuous load versus displacement data were recorded. The maximum force was identified in order to define the mechanical strength of the bone-implant interface.

Histological analysis:

Each femoral specimen with surrounding bone tissue was fixated in phosphate-buffered 4% formaldehyde solution for 4 days and embedded in PMMA. Serial slices of ca. 40 μm , perpendicular to the length of the specimen, were cut using a sawing microtome (SP 1600, Leitz, Wetzlar, Germany). Quantitative analyses of bone ingrowth depth and bone-implant contact were performed on 5 hematoxylin/eosin (HE) stained slices which were homogeneously distributed over the length of the implant. Each slice was analyzed using computer assisted image analysis (AnalySIS 3.2 Soft Imaging System, Münster, Germany). For the measurement of bone ingrowth depth at 4 and 15 weeks a line was drawn from the deepest bone ingrowth to the outline of the specimen. The direct bone-implant contact (BIC) was determined by the linear extent of direct bone apposition divided by the total surface perimeter of the implant.

Statistical analysis:

All mechanical and histological datasets were evaluated non-parametrically, as normal distribution could not be assumed for all parameters. Within time point comparisons of mechanical strength of the bone-implant interface, ingrowth depth and bone-implant contact were performed with a Wilcoxon Signed Rank test. Differences between medians were considered statistically significant for p-values <0.05 . Statistical analysis was performed using SPSS (16.0, SPSS Inc., Chicago, USA).

Results

Mechanical testing

7 samples intended for push-out testing were excluded, 6 due to faulty placement of the samples, and 1 due to errors during preparation for push out test. Authors (PB, GH) involved in exclusion of the samples were blinded. Of the 7 exclusions, 1 belonged to the uncoated SLM (4 weeks group), 2 to the SLM-HA (1 sample of the 4 weeks group and 1 sample of the 15 weeks

group), 1 to the uncoated EBM (4 weeks group), and 3 to the EBM-HA group (2 samples of the 4 weeks group and 1 sample of the 15 weeks group). At both 4 and 15 weeks no differences in mechanical strength of the bone implant interface between the specimens produced by EBM or SLM were found. For the EBM produced specimens no significant differences in push out force were found between specimens with and without a HA coating. However, the uncoated SLM specimen had a significantly higher mechanical strength compared to the HA coated SLM specimens, at both 4 ($p=0.03$) and 15 weeks ($p=0.03$) of implantation. (**Figure 3**)

Histological analysis

Five surfaces intended for histology and histomorphometric analysis were excluded due to faulty placement of the samples. Authors (PB, GH) involved in exclusion process were blinded. Of the 5 excluded surfaces, 1 belonged to the uncoated SLM (15 weeks group), 3 belonged to the SLM-HA (1 surface of the 4 weeks group and 2 surfaces of the 15 weeks group), and 1 to the EBM-HA (15 weeks).

At 4 weeks after implantation a variable bone reaction was found around the specimens (**Figure 4 A,B**). One surface (coated SLM) was completely covered by a rather thick reactive tissue membrane. This membrane was ca 1-2 mm in thickness and of fibrous nature. New woven bone was formed in the membrane but no direct bone implant contact or only very limited bone ingrowth onto the specimen was found. The other specimens showed direct contact with bone. The bone ingrowth depth was variable between different specimens but quite constant for the two surfaces of one implant (**Figure 4 A, B**). No effect of the coating, such as osteoconduction along the surface or isolated bony spots on the surface of the implants that were not directly connected with host bone were seen. Also no differences in ingrowth depth and bone-implant contact were found between the two groups. The “trabeculae” of all other EBM and SLM surfaces were intimately connected to the host bone (**Figure 4 C-H**). Particularly the outer layer of metal “trabeculae” was almost completely surrounded by new host bone. No qualitative differences in the bone morphology were seen between the coated and uncoated surfaces.

Histomorphometry indicated that the uncoated EBM specimens showed significantly higher bone-implant contact compared to the uncoated SLM produced specimens at 15 weeks follow-up ($p = 0.03$). The addition of a biomimetic coating did not result in a significant change in ingrowth depth and bone-implant contact as compared to the uncoated samples (**Figures 5 and 6**).

Discussion

In this study the bone ingrowth potential of a trabecular like implant surface produced by either electron beam melting or selective laser melting was investigated. The original design of the trabecular implant surface was similar for both production techniques. However, the SLM and EBM specimens that resulted after production were different in gross morphology

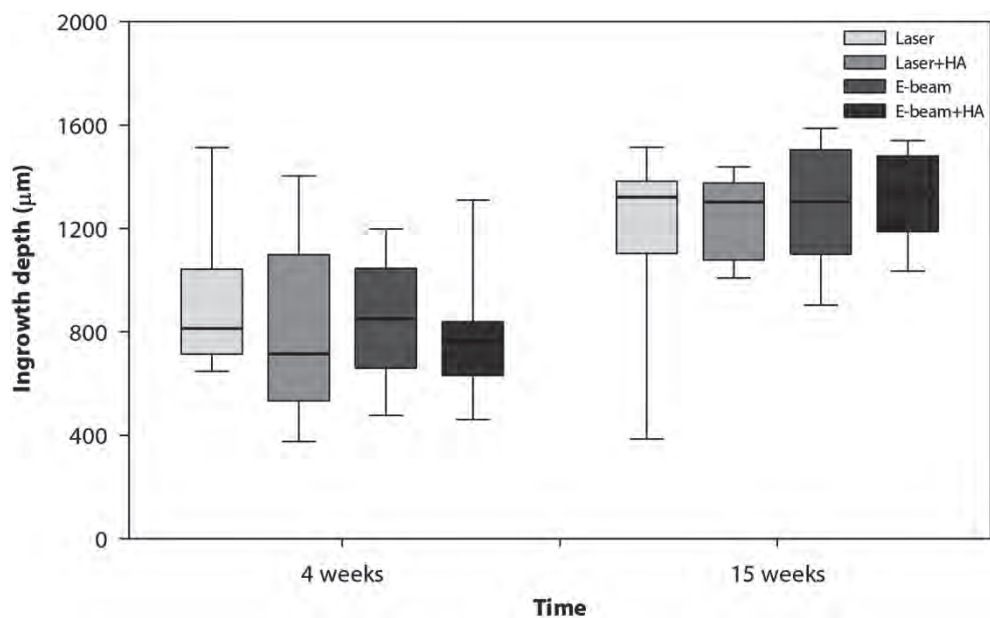


Figure 5. Ingrowth depth after 4 and 15 weeks.

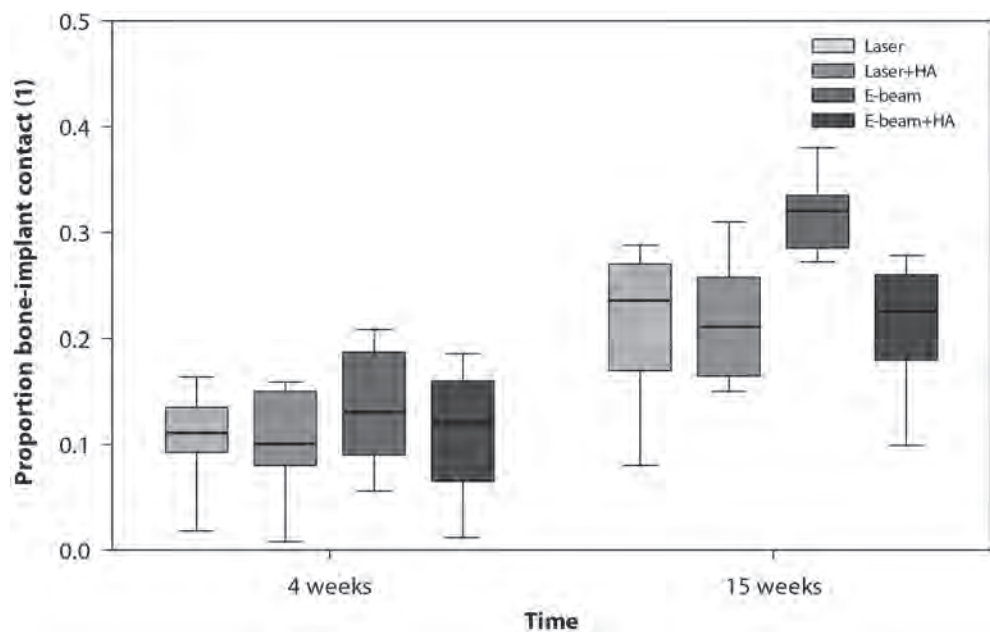


Figure 6. Proportion of bone implant contact after 4 and 15 weeks

and surface texture. In the EBM specimens the individual titanium granules could be clearly seen whereas this was not the case in the SLM specimens. The macroscopic surface of the SLM specimens was flatter as compared to EBM produced surfaces. Also the gross morphology and the porosity of the specimens clearly differed. Both the surface post treatments protocols and the difference in accuracy between the production technologies might have been responsible for these differences. This is a major limitation of this study.

A second limitation is the different models used for mechanical push out analysis and the model for histological evaluation. This does not allow the direct comparison between push out data and the qualitative and morphometric evaluation of the ingrowth potential. The push out model have been previously published. The femoral model has been previously used in our group, however, not to place square samples. The trauma reaction associated with placing the samples might have played a role in the variation in results observed in the 4 week specimens. Moreover the ingrowth measurements in these square samples makes a direct comparison with similarly produced structures with different geometries or implanted at different locations in the body difficult.

Several trabecular like implant surfaces have been developed during the last decade and are currently commercially available. One of them, based on tantalum metal, has been widely used as implant surface, mainly in revision surgery with or without bone defects.[19] Implants with such a 'trabecular metal' surface show good mid-term survival in primary arthroplasties [20] and good short-term survival in revision arthroplasties [21]. A comparison between the results of previously published animal experiments with this commercially available, successful 'trabecular metal' and the current study cannot be made due to differences in measurement methods and animal models used.

The direct comparison between SLM and EBM in this experiment showed no differences except for the higher bone-implant contact of EBM specimens at 15 weeks of implantation. A difference was not found in the push-out test, which reflects the actual strength at the bone implant interface. We do not know what caused the discrepancy between the higher bone implant contact and the similar push out strength. Of course a direct comparison is not possible since the push out strength and bone implant contact were analysed in different models with potentially a different bone ingrowth pattern to the implant. However, based on all histological and push-out test results, it can be concluded that there are no large differences in bone ingrowth potential between SLM and EBM produced implant surfaces with the same design.

The second goal of the study was to evaluate the effect of the addition of a biomimetic coating to the SLM and EBM produced trabecular surface structures. At 4 and 15 weeks of implantation the push out force was significantly lower for the SLM-HA specimens compared to the uncoated SLM specimens. Although this effect on the push out strength of the biomimetic coating was not significant in the EBM specimens, there was also a non-significant trend towards a lower mechanical push out force in the 15 week follow up EBM-HA specimens. This is a remarkable result, which is in contrast with previous work of our group with biomimetic coatings on EBM

specimens. However, a coating with different characteristics had been used in that study [8]. In literature the results of biomimetic coatings are in general positive on the interface strengths of bone with the implant[22;23], but not all coatings induce a better fixation.[24] Yang et al. performed removal torque tests in rabbit femurs of a biomimetic phosphate coating on a titanium implant and compared these results to electrochemically deposited HA and uncoated implants. The biomimetic coating did not increase the torque values compared to the uncoated implants, whereas the electrochemically deposited HA did increase torque values.[24]

Possible explanations for the lower push out strength of the biomimetic coated specimens in this experiment can be multifactorial, involving the thickness of the coating, the fixation strength of the coating to the metal, the chemical nature of the coating and the dissolution speed. The coating used in this experiment was rather thin (5-10 μm) and if the dissolution speed was fast the positive postoperative effect of the coating could have been lost before bone progenitors were in the direct vicinity of the implant. In this respect it should also be mentioned that the model used in this experiment to analyse the histological response towards the implants was rather invasive. A round drill hole was manually shaped with sharp osteotome into a square hole, which might have induced a rather large trauma reaction in the bone. A resorptive phase associated with such reaction might have obscured a potential positive effect of a coating with a rapid dissolution speed, which might explain the lack of histological detectable effect of the coating. Furthermore it is known that a coating can chip off during the press-fit implantation of the specimen. However, the coating inside the pores will nevertheless not be affected by the implantation. Even when chipped off the coating could have had a beneficial effect on bone ingrowth. Furthermore the bonding between the porous implant and the coating can be a point of concern, as seen by Yang et al, who found that the biomimetic coating failed at the implant coating interface whereas the electrochemically deposited HA failed at the bone during the torque test [24].

Since the numerous listed variables that could play a role in the lower push out force of the SLM produced specimens compared to the EBM specimens, further research is needed before a final assessment of the effect of coatings on bone ingrowth can be made.

In conclusion

SLM and EBM produced specimens showed variable bone ingrowth after 4 weeks but showed good bone ingrowth characteristics after 15 weeks. Non-coated SLM specimens have a superior push out strength compared to the coated specimens. Further investigations are needed how to further improve the biological and mechanical responses of the EBM and SLM produced specimens.

References

1. Basarir K, Erdemli B, Can A, Erdemli E, Zeyrek T: Osseointegration in arthroplasty: can simvastatin promote bone response to implants? *Int Orthop* 33(3):855, 2009
2. Karageorgiou V, Kaplan D: Porosity of 3D biomaterial scaffolds and osteogenesis. *Biomaterials* 26(27):5474, 2005
3. Kaplan FS, Lee WC, Keaveny TM: Forms and functions of bone. p. 127. In Simon SP (ed): *Orthopedic basic science*. American Academy of Orthopedic Surgeons; Columbus, OH, 1994
4. Keaveny TM, Morgan EF, Niebur GL, Yeh OC: Biomechanics of trabecular bone. *Annu Rev Biomed Eng* 3:307, 2001
5. Bobyn JD, Stackpool GJ, Hacking SA, Tanzer M, Krygier JJ: Characteristics of bone ingrowth and interface mechanics of a new porous tantalum biomaterial. *J Bone Joint Surg Br* 81(5):907, 1999
6. Murr LE, Quinones SA, Gaytan SM, Lopez MI, Rodela A, Martinez EY, Hernandez DH, Martinez E, Medina F, Wicker RB: Microstructure and mechanical behavior of Ti-6Al-4V produced by rapid-layer manufacturing, for biomedical applications. *J Mech Behav Biomed Mater* 2(1):20, 2009
7. Biemond JE, Hannink G, Verdonschot N, Buma P: The effect of E-beam engineered surface structures on attachment, proliferation and differentiation of human mesenchymal stem cells. *Bio-medical materials and engineering* 2011
8. Biemond JE, Eufrazio TS, Hannink G, Verdonschot N, Buma P: Assessment of bone ingrowth potential of biomimetic hydroxyapatite and brushite coated porous E-beam structures. *J Mater Sci Mater Med* 22(4):917, 2011
9. Warnke PH, Douglas T, Wollny P, Sherry E, Steiner M, Galonska S, Becker ST, Springer IN, Wiltfang J, Sivananthan S: Rapid prototyping: porous titanium alloy scaffolds produced by selective laser melting for bone tissue engineering. *Tissue Eng Part C Methods* 15(2):115, 2009
10. Pattanayak DK, Fukuda A, Matsushita T, Takemoto M, Fujibayashi S, Sasaki K, Nishida N, Nakamura T, Kokubo T: Bioactive Ti metal analogous to human cancellous bone: Fabrication by selective laser melting and chemical treatments. *Acta Biomater* 7(3):1398, 2011
11. Habibovic P, Barrère F, van Blitterswijk CA, de Groot K, Layrolle P: Biomimetic hydroxyapatite coating on metal implants. *J Am Ceram Soc* 85(3):517, 2002
12. Heintl P, Rottmair A, Körner C, Singer R: Cellular Titanium by Selective Electron Beam Melting. *Advanced Engineering Materials* 9(5):360, 2007
13. Heintl P, Müller L, Körner C, Singer RF, Müller FA: Cellular Ti-6Al-4V structures with interconnected macro porosity for bone implants fabricated by selective electron beam melting. *Acta Biomater* 4(5):1536, 2008
14. Facchini L, Magalini E, Robotti P, Molinari A: Microstructure and mechanical properties of Ti-6Al-4V produced by electron beam melting of pre-alloyed powders. *Rapid Prototyping Journal* 15(3):171, 2009
15. Facchini L, Magalini E, Robotti P, Molinari A, Hoges S, Wissenbach K: Ductility of a Ti-6Al-4V alloy produced by selective laser melting of prealloyed powders. *Rapid Prototyping Journal* 16(6):450, 2010
16. Mullen L, Stamp RC, Fox P, Jones E, Ngo C, Sutcliffe CJ: Selective laser melting: a unit cell approach for the manufacture of porous, titanium, bone in-growth constructs, suitable for orthopedic applications. II. Randomized structures. *J Biomed Mater Res B Appl Biomater* 92(1):178, 2010
17. Redepenning J, Schlessinger T, Burnham S, Lippiello L, Miyano J: Characterization of electrolytically prepared brushite and hydroxyapatite coatings on orthopedic alloys. *J Biomed Mater Res* 30(3):287, 1996
18. Dhert WJ, Verheyen CC, Braak LH, de Wijn JR, Klein CP, de Groot K, Rozing PM: A finite element analysis of the push-out test: influence of test conditions. *J Biomed Mater Res* 26(1):119, 1992
19. Levine BR, Sporer S, Poggie RA, Della Valle CJ, Jacobs JJ: Experimental and clinical performance of porous tantalum in orthopedic surgery. *Biomaterials* 27(27):4671, 2006
20. Sembrano JN, Cheng EY: Acetabular cage survival and analysis of factors related to failure. *Clin Orthop Relat Res* 466(7):1657, 2008
21. Unger AS, Lewis RJ, Gruen T: Evaluation of a porous tantalum uncemented acetabular cup in revision total hip arthroplasty: clinical and radiological results of 60 hips. *J Arthroplasty* 20(8):1002, 2005
22. Barrère F, van der Valk CM, Meijer G, Dalmeijer RA, de Groot K, Layrolle P: Osteointegration of biomimetic

-
- apatite coating applied onto dense and porous metal implants in femurs of goats. *J Biomed Mater Res B Appl Biomater* 67(1):655, 2003
23. Tsukeoka T, Suzuki M, Ohtsuki C, Tsuneizumi Y, Miyagi J, Sugino A, Inoue T, Michihiro R, Moriya H: Enhanced fixation of implants by bone ingrowth to titanium fiber mesh: effect of incorporation of hydroxyapatite powder. *J Biomed Mater Res B Appl Biomater* 75(1):168, 2005
 24. Yang GL, He FM, Hu JA, Wang XX, Zhao SF: Biomechanical comparison of biomimetically and electrochemically deposited hydroxyapatite-coated porous titanium implants. *J Oral Maxillofac Surg* 68(2):420, 2010

Chapter 8



Summary, closing remarks and future perspectives



Chapter 1

Although the overall results of total hip replacement are good, 5 to 10 percent of the cementless implants still fail within 10 years of implantation, mainly due to aseptic loosening. The frequency of failure is likely to increase due to implantation in younger and more active patients. Revision surgery after failure of an implant creates a large burden for both the patient and society, indicating an urgent need for improvement of cementless implants in order to avoid aseptic loosening.

The long term success of cementless implants is dependent on bone ingrowth, whereby the initial press fit fixation transfers to a secondary mechanical fixation. Bone ingrowth has been shown to be influenced by several factors, including the surface characteristics of the implants.

In chapter 1 an overview of the basic science and current state of techniques to produce porous implant surfaces is presented, and relevant items such as additional treatments are discussed.

Chapter 2

In chapter 2 the long term survival of the cementless Spotorno (CLS) femoral component was evaluated in a consecutive series of 85 patients (100 hips) under 50 years of age. The mean follow-up was 12.3 years. The survival rate of the CLS stem was 96.9% (93.6%-100%) after 13 years based on revision of the stem for any reason. The survival of the stem with revision for aseptic loosening as the end point was 97.9% (95.1%-100%) at 13 years. The mean Harris hip score at time of follow-up was 94. According to consensus in literature this is an excellent survival of the CLS stem in young patients.

Chapter 3

In order to achieve successful bone ingrowth, a series of events on cellular level should occur, consisting of cell attachment, proliferation and differentiation of stem cells or pre-osteoblasts. Surface characteristics, like roughness, pore size and porosity play a key role in these processes leading to bone ingrowth.

In chapter 3 two newly designed highly porous E-beam engineered surface structures were evaluated with respect to attachment, proliferation and differentiation of human mesenchymal stem cells (hMSCs). These results were compared to those of a solid sandblasted control. SEM analyses showed that the E-beam structures allowed cells to attach and spread. Proliferation on the new surface structures was comparable to the solid control. Furthermore, differentiation of the hMSCs into cells with a bone phenotype on the 3D structures was comparable to the control specimen. When culturing the hMSCs for 10 days, one of the structures showed a significantly higher differentiation rate compared to the control specimen, indicating that the newly designed surfaces supported a bone differentiation of stem cells.

Chapter 4

Directly after press-fit implantation the prosthesis will be stabilized by friction at the bone implant interface. Sufficient frictional stability will reduce micromotion at the bone implant interface and enable bone ingrowth into the surface of the implant, resulting in a long lasting mechanical interlock of the implant and optimal secondary mechanical stability.

In chapter 4 two new 3-dimensional E-beam surface structures were examined with respect to frictional properties and in vivo bone ingrowth potential. A commercially available titanium plasma spray coating and a plain, sandblasted E-beam surface were used as controls. The structures and the controls were pushed alongside human cortical bone in order to define the friction coefficient. Furthermore the E-beam structures and controls were implanted into the femoral condyles of 6 goats. Six weeks after surgery the goats were sacrificed and the percentage direct bone-implant contact was measured using histomorphometry.

The frictional and bone ingrowth properties of the new E-beam produced surface structures were similar to the plasma sprayed control. However, due to the high porosity and large pore size, the maximal bone ingrowth had not been reached for the E-beam structures during the relatively short-term period (6 weeks), although it is not clear if extra bone ingrowth would have increase the interface strength.

Chapter 5

Calciumphosphate (CaP) coatings have been successfully applied on orthopedic and dental implants. The advantages of these coatings are enhancement of bone formation and accelerated bonding between implant and bone. With the biomimetic coating technique it is possible to apply a CaP coating on porous and irregular surfaces.

In chapter 5 the bone ingrowth potential of two biomimetic CaP coatings (hydroxyapatite and brushite) applied on a porous E-beam structure was examined and compared to a similar uncoated porous structure and a conventional titanium plasma spray coating. Specimens were implanted in the iliac crest of goats for a period of 3 (4 goats) or 15 weeks (8 goats). Mechanical implant fixation strength generated by bone ingrowth was analyzed by a push out test. Furthermore, histological analysis was performed to assess bone ingrowth potential.

The uncoated and hydroxyapatite-coated E-beam structure had significantly higher mechanical strength at the interface compared to the Ti plasma spray coating at 15 weeks of implantation. Bone ingrowth was significantly larger for the hydroxyapatite- and brushite-coated structures compared to the uncoated structure at 5, 10 and 15 weeks after implantation.

In conclusion, the porous E-beam surface structure showed higher bone ingrowth potential compared to a conventional implant surface after 15 weeks of implantation. Addition of a calcium phosphate coating to the E-beam structure enhanced bone ingrowth significantly. Furthermore, the calcium phosphate coating appears to work as an accelerator of bone ingrowth.

Chapter 6

In chapter 6 the bone ingrowth potential of new E-beam structures was examined and compared to a porous plasma spray control. Furthermore the effect of additional treatment by application of a hydroxyapatite coating and acid etching was evaluated. Specimens were implanted in the distal femur of goats for 6 weeks. The structure with a large pore size and high porosity showed the best bone ingrowth. The E-beam produced surface showed significantly more bone ingrowth compared to the control surface. Additional treatment of the E-beam surface structures with a hydroxyapatite coating further improved the bone ingrowth potential of these structures significantly. Acid-etching of the E-beam structures did not influence bone ingrowth.

Chapter 7

In chapter 7 the bone ingrowth potential of a trabecular-like implant surface produced by either selective laser melting or electron beam melting with and without a biomimetic coating was investigated. A goat model was used, in which specimens were implanted in the iliac crest and distal femur for mechanical push out testing and histological analysis respectively. The goats were sacrificed after 4 and 15 weeks.

Both the laser and E-beam produced trabecular-like structure showed good bone ingrowth, with no clear difference between the two production methods. The mechanical strength at the bone implant interface of the laser produced specimens was significantly lower for the coated specimens compared to the uncoated specimens. Histological analysis showed no significant difference between the specimens with and without the coating. The lower mechanical strength of the coated laser-produced specimens is however a remarkable result, indicating further research is necessary.

Closing remarks and future perspectives

Due to an ageing population the estimated number of total hip replacements will rise substantially to approximately 25.000 in 2020 in the Netherlands [1] and approximately 65.000 total hip arthroplasties in the United Kingdom in 2026.[2] The growing number of total hip replacements in younger and more active patients will increase this number even further. The combination of joint arthroplasty in young patients and an increased life expectancy in general demands enhanced survival of prostheses.

The hip prostheses that are on the market nowadays show good survival according to the current standards.[3] However, concerning the aforementioned, these standards might have to be extended in the future. A higher survival at 10 years and a prolonged follow up may be required although the last will be difficult due to the constant innovation and design of new implants by the medical device industry. There is a need for advanced implant surfaces with enhanced bone ingrowth properties to meet the extended standards.

Numerous implant surfaces (mostly coatings) have been developed in an attempt to achieve this enhanced bone ingrowth, some with good results, others with no effect on the fixation by bone ingrowth.[4] Drawbacks of the use of a coating are the risk of loose particles, the enlargement of the surface area and subsequently the prolonged time needed for bone ingrowth.

Theoretically, a true mechanical interlock between bone and the 3-dimensional porous surface of an implant should provide fixation for life. This is the idea behind the development of the new porous implant surfaces examined in this thesis.

The bone ingrowth potential of the new porous implant surfaces, produced by rapid prototyping techniques with and without additional calciumphosphate coatings were compared to more conventionally produced implant surfaces. The new surfaces showed a comparable bone ingrowth potential at a short follow-up period as compared to a well-performing conventional surface. After a relatively long period the new surfaces showed even better bone ingrowth.

However, it is not clear whether the observed increase in bone ingrowth in animal models will lead to prolonged survival of prostheses implanted in patients. The survival may be limited by other factors, such as wear. The downside of full bone ingrowth is the difficulty to remove the implant when necessary.

The possibilities with implant surfaces produced by rapid prototyping techniques are endless; in this thesis variations in technique, surface geometry, the use of acid etching and addition of calciumphosphate coating have been investigated. Although the design of new surfaces by rapid prototyping is an opportunity, the number of potential structures is large and direct comparison is complicated, which implies that it is hard to define which implant structure is the best. A pre-screening by in vitro mechanical testing or by finite element modelling could potentially select optimal structures that can be further tested in animals. Further possibilities to improve the biology of surfaces produced by rapid prototyping techniques are the incorporation of growth factors such as bone morphogenetic proteins, or other modifying drugs into the coating. Also the application of specific designed 3-dimensional implant surfaces for different parts of the prostheses could induce an optimal local tissue behaviour. An example if thus would be a coating on the proximal part of a hip prosthesis that would avoid stress shielding.

Furthermore, with rapid prototyping it is possible to design a prosthesis based on patient data, a so called personalized prosthesis. This is probably the application with the highest potential. In future, it might be possible to develop and produce a customized, personalized prosthesis which offers enhanced bone ingrowth especially in the more demanding areas of this specific patient, for example in patients with osteoporosis. It is known that the initial fixation may be compromised in osteoporotic bone.[5;6] With a surface geometry or coating in the area of, for example Gruen zone 7, a cementless implant can be successful in patients with osteoporosis. [7] Patients with substantial bone defects, in revision or tumour surgery, are a second group that can benefit from such a personalized prosthesis.

To achieve the aforementioned clinical use, further research is necessary. First of all, the field of personalized implant design has to be developed to a higher level. Currently a customized femoral stem, which can correct leg length, anteversion and deformation of the femur as seen in, for example Perthes disease is on the market. Although this customized femoral stem shows promising results, long term survival is not available yet. Patient selection for the customized stem is also challenging.[8] With this personalized femoral component only the shape of the implant is customized, not the implant surface. It would be interesting to customize the implant on both CT data and bone mineral density measurements, in order to facilitate enhanced bone ingrowth in areas with bone defects and osteoporosis. Furthermore the ideal, patient independent areas to apply 3-dimensional implant surfaces on the prosthesis are not yet known. Finite element modelling and eventually animal experiments are necessary to define the ideal areas for fixation, optimizing the balance between bone ingrowth, stress shielding, revisability, etc.

Secondly, micromotions were not taken into account in this thesis. The relative motion between the prosthesis and bone evoked by weight bearing might influence bone ingrowth in a negative way[9] Although the effect is patient specific, each surface has a different vulnerability for micromotion and therefore the bone ingrowth potential of the new surface structures should be tested under controlled micromotion. Unfortunately, all current animal models to investigate the effect of micromotion on bone ingrowth of an implant surface have their limitations, such as external parts, the inability to control force and displacement and the inability to monitor the displacement. So, in fact a new micromotion model has to be developed.

Finally, a new implant surface, probably fitted in a personalized joint arthroplasty design should be tested thoroughly in animal experiments and after that in patients. Hopefully, in this way, rapid prototyping finds its place to improve the outcome of joint arthroplasty.

References

1. Ostendorf M, Johnell O, Malchau H, Dhert WJ, Schrijvers AJ, Verbout AJ: The epidemiology of total hip replacement in The Netherlands and Sweden: present status and future needs. *Acta Orthop Scand* 73(3):282, 2002
2. Birrell F, Johnell O, Silman A: Projecting the need for hip replacement over the next three decades: influence of changing demography and threshold for surgery. *Ann Rheum Dis* 58(9):569, 1999
3. NHS National Institute for Clinical Excellence (NICE). Guidance on the selection of prostheses for primary total hip replacement. 2000.
4. Yang GL, He FM, Hu JA, Wang XX, Zhao SF: Biomechanical comparison of biomimetically and electrochemically deposited hydroxyapatite-coated porous titanium implants. *J Oral Maxillofac Surg* 68(2):420, 2010
5. Alm JJ, Makinen TJ, Lankinen P, Moritz N, Vahlberg T, Aro HT: Female patients with low systemic BMD are prone to bone loss in Gruen zone 7 after cementless total hip arthroplasty. *Acta Orthop* 80(5):531, 2009
6. Dorr LD, Faugere MC, Mackel AM, Gruen TA, Bognar B, Malluche HH: Structural and cellular assessment of bone quality of proximal femur. *Bone* 14(3):231, 1993
7. Meding JB, Galley MR, Ritter MA: High survival of uncemented proximally porous-coated titanium alloy femoral stems in osteoporotic bone. *Clin Orthop Relat Res* 468(2):441, 2010
8. Benum P, Aamodt A: Uncemented custom femoral components in hip arthroplasty. A prospective clinical study of 191 hips followed for at least 7 years. *Acta Orthop* 81(4):427, 2010
9. Kienapfel H, Sprey C, Wilke A, Griss P: Implant fixation by bone ingrowth. *J Arthroplasty* 14(3):355, 1999

Chapter 9



Samenvatting, afsluitende opmerkingen en toekomstig onderzoek



Hoofdstuk 1

De resultaten van de operatie waarbij een versleten heup wordt vervangen door een kunstheup, ook wel totale heup arthroplastiek genoemd, zijn goed. Toch faalt nog steeds 5 tot 10 procent van de ongecementeerde implantaten binnen 10 jaar na implantatie, voornamelijk door aseptische loslating. Het is aannemelijk dat het percentage implantaten dat faalt gaat stijgen omdat steeds meer jonge en actieve patiënten worden geopereerd. Revisie van de gefaalde component(en) is een grote belasting voor de individuele patiënt en de samenleving. Er zijn dus betere ongecementeerde implanten nodig, die een lagere kans hebben op aseptische loslating. Het succes van ongecementeerde prothesen op de lange termijn is afhankelijk van de verbinding die de prothese met het bot aangaat. Een initiële 'press fit' mechanische fixatie gaat op termijn over in een permanente secundaire fixatie waarbij de botingroei de mechanische stabiliteit levert. De botingroei wordt beïnvloed door verschillende factoren waaronder de karakteristieken van het poreuze oppervlak van de prothese.

In hoofdstuk 1 werd een overzicht gegeven van de wetenschappelijke achtergrond en huidige staat van technieken om poreuze implantaat oppervlakken te maken en werden relevante zaken zoals additionele coatings besproken.

Hoofdstuk 2

In hoofdstuk 2 werd de lange termijn overleving van de ongecementeerde Spotorno (CLS) femorale component (Zimmer Inc., Warsaw, USA) onderzocht in een opeenvolgende serie van 85 patiënten (100 heupen) jonger dan 50 jaar. De mediane follow up was 12,3 jaar.

De overleving van de CLS femorale component was 96,9% (93,6% tot 100%) na 13 jaar, gebaseerd op revisie voor alle redenen. De overleving van de steel met revisie voor aseptische loslating als eindpunt was 97,9% (95,1% tot 100%) na 13 jaar. De mediane Harris Hip Score was 94 ten tijde van de follow up. Dit is een uitstekende lange termijn overleving van de CLS steel bij patiënten jonger dan 50 jaar.

Hoofdstuk 3

Succesvolle botingroei begint op cel-niveau; Stamcellen of pre-osteoblasten moeten hechten op het implantaat en vervolgens prolifereren, differentiëren en botmatrix gaan maken. De oppervlak karakteristieken van het implantaat, zoals de ruwheid, grootte van de poriën en mate van porositeit, spelen een belangrijke rol in deze cellulaire processen.

In hoofdstuk 3 is de hechting, proliferatie en differentiatie van humane stamcellen op twee nieuwe poreuze E-beam oppervlak structuren en een niet-poreuze gezandstraalde controle getest. SEM analyse wees uit dat de stamcellen zich hechten aan en zich uitstrekken op de E-beam structuren. De proliferatie en differentiatie op de nieuwe 3-dimensionale structuren was vergelijkbaar met die op het controle oppervlak. De differentiatie van de stamcellen op

één van de E-beam structuren was zelfs significant beter in vergelijking met de gezandstraalde controle wanneer de cellen gekweekt werden gedurende 10 dagen. Dit toont aan dat de nieuwe E-beam oppervlak structuren differentiatie van stamcellen naar bot kunnen stimuleren.

Hoofdstuk 4

Tijdens het implanteren van een ongecementeerde prothese wordt een perfecte aansluiting tussen prothese en bot nagestreefd (press-fit implantatie). De prothese wordt vanaf het moment van deze press-fit implantatie gestabiliseerd door wrijving op het bot-implantaat oppervlak. Voldoende wrijving is een voorwaarde voor botingroei in de prothese, welke zorgt voor een langdurige mechanische vergrendeling tussen de prothese en het omliggende bot en dus een optimale secundaire stabiliteit.

In hoofdstuk 4 werden twee nieuwe E-beam structuren onderzocht met betrekking tot hun wrijvings- en botingroei kwaliteiten. Een commercieel verkrijgbare titanium plasma spray coating en een gezandstraalde E-beam oppervlak werden gebruikt als controle. De wrijvingscoëfficiënt werd bepaald door de E-beam structuren en de controles langs menselijk corticaal bot te schuiven. Tevens werden de implantaten van alle 4 de groepen gedurende 6 weken in het distale femur van 6 geiten geplaatst. Na het offeren van de geiten werd de hoeveelheid botingroei bepaald in histologische coupes door middel van histomorphometrie. De wrijving- en botingroei kwaliteiten van de nieuwe E-beam oppervlak structuren zijn gelijk aan die van de plasma spray controle. Door de hoge porositeit en grote poriën was de maximale botingroei waarschijnlijk nog niet bereikt in de relatief korte periode (6 weken) van dit onderzoek. Het is niet zeker of een eventuele toename van botingroei ook nog tot een sterkere bot-implantaat interface leidt.

Hoofdstuk 5

Calciumfosfaat (CaP) coatings worden al succesvol toegepast op tandheelkundige en orthopedische implantaten. Deze coatings bevorderen de botvorming en versnellen de hechting tussen implantaat en bot. Met de biomimetische coating techniek is het mogelijk om een CaP coating aan te brengen op poreuze en onregelmatige prothese oppervlakken.

In hoofdstuk 5 werd de botingroei capaciteit onderzocht van twee biomimetische CaP coatings (hydroxyapatite en brushite) welke zijn aangebracht op een poreuze E-beam structuur. De ongecoate versie van deze structuur en een implantaat met een conventionele titanium plasma spray coating werden gebruikt als controles. De specimens werden geïmplanteerd in de bekkenkam van geiten. Na 3 (4 geiten) of 15 weken (8 geiten) werd de mechanische fixatie sterkte van het implantaat aan het bot bepaald door middel van een 'push out' test. Een histomorphometrische analyse werd verricht om de botingroei capaciteit te bepalen.

De ongecoate structuur en structuur met hydroxyapatite coating hadden na 15 weken beiden een significant hogere mechanische fixatie sterkte van het implantaat aan het bot in vergelijking

met de titanium plasma spray coating. De botingroei was na 5, 10 en 15 weken significant groter voor de implantaten met een hydroxyapatite of brushite coating in vergelijking met de ongecoate implantaten.

Concluderend heeft de poreuze E-beam oppervlakstructuur na 15 weken een hogere botingroei capaciteit in vergelijking met een conventioneel prothese oppervlak. Het aanbrengen van een calciumfosfaat coating op de E-beam structuur bevordert de botingroei significant en lijkt de botingroei te versnellen.

Hoofdstuk 6

In hoofdstuk 6 werd de botingroei capaciteit van nieuwe E-beam structuren onderzocht en vergeleken met een poreuze plasma spray coating. Ook werd het effect van nabehandeling van de prothese oppervlakken door middel van toevoegen van een hydroxyapatite coating en etsen onderzocht. Implantaten werden in het distale femur van geiten geplaatst voor een periode van 6 weken. De E-beam structuur met grote porieën en een hoge porositeit liet de beste botingroei zien. De E-beam structuur had significant betere botingroei in vergelijking met het controle implantaat. Nabehandeling van de E-beam structuren met een hydroxyapatite coating verhoogde de botingroei verder. Het etsen van de E-beam structuren had geen invloed op de botingroei.

Hoofdstuk 7

In hoofdstuk 7 werd het vermogen tot botingroei van een oppervlak structuur in de vorm van trabekels onderzocht. De structuur was geproduceerd met zowel selective laser melting als electron beam melting en met en zonder biomimetische coating. Er werd gebruik gemaakt van een geitenmodel, waarbij de implantaten in de bekkenkam en het distale femur werden geplaatst voor respectievelijk een push out test en histologie. De geiten werden geofferd na 4 en 15 weken.

Zowel de laser als E-beam oppervlakstructuur in de vorm van trabekels toonde goede botingroei, zonder duidelijk verschil tussen de twee productie technieken. De mechanische sterkte op de bot-implantaatinterface van de laser geproduceerde implantaten was significant lager voor de gecoate implantaten in vergelijking met de ongecoate implantaten. Histologische analyse toonde geen verschil tussen de gecoate en ongecoate implantaten. De lagere mechanische sterkte van de laser geproduceerde, gecoate implantaten is een opmerkelijk resultaat, wat verder onderzocht moet worden.

Afsluitende opmerkingen en toekomstig onderzoek

Volgens schattingen zal door de vergrijzing van de bevolking het aantal totale heup prothesen substantieel stijgen tot ongeveer 25.000 in 2020 in Nederland[1] en ongeveer 65.000 in het

Verenigd Koninkrijk in 2026.[2] Deze aantallen zullen zelfs verder toenemen door het groeiende aantal heupprothesen dat wordt geplaatst bij jonge en actieve patiënten. De combinatie van heupartroplastiek / totale heupvervanging in jonge patiënten en de toegenomen levensverwachting van deze patiënten vraagt langere overleving van prothesen.

De heupprothesen die nu op de markt zijn, hebben volgens de huidige richtlijnen een goede overleving.[3] Echter, gezien het bovenstaande, moeten de eisen in deze richtlijnen mogelijk naar boven moeten worden bijgesteld in de toekomst. Een betere overleving na 10 jaar en een langere follow-up is wenselijk, alhoewel dit laatste lastig zal zijn door constante innovatie en de ontwikkeling van nieuwe implantaten door de medische industrie. Nieuwe geavanceerde prothese oppervlakken met verbeterde botingroei-eigenschappen zijn nodig om te voldoen aan de bijgestelde richtlijn(en).

Vele prothese oppervlakken (vooral coatings) zijn ontwikkeld in een poging om deze verbeterde botingroei te verwezenlijken, sommige met goede resultaten, andere zonder effect op de fixatie door botingroei.[4] Nadelen van het gebruik van een coating zijn de kans op losse partikels, de vergroting van de oppervlakte en dientengevolge de verlengde tijd die nodig is voor botingroei.

In theorie zou een echte verankering tussen bot en een 3-dimensionaal poreus prothese oppervlak een levenslange fixatie geven. Deze gedachte vormt het idee achter de nieuwe oppervlak structuren die onderzocht zijn in dit proefschrift.

De botingroei in nieuwe poreuze prothese oppervlakken, die gemaakt zijn met een 'rapid prototyping'-techniek met en zonder toevoeging van een calcium-fosfaat coating zijn vergeleken met conventionele prothese oppervlakken. De botingroei van de nieuwe oppervlakken is vergelijkbaar met de botingroei in het goed presterende conventionele oppervlak. Na een langere periode was de botingroei in de nieuwe oppervlakken zelfs beter.

Toch is het niet duidelijk of een betere botingroei in diermodellen ook een langere overleving van de prothese bij patiënten betekent. De overleving kan worden beperkt door andere factoren, zoals slijtage. Een nadeel van volledige botingroei is dat het moeilijk is om de prothese te verwijderen wanneer dit nodig zou zijn.

De mogelijkheden met prothese oppervlakken die geproduceerd zijn met 'rapid prototyping'-technieken zijn eindeloos. In dit proefschrift worden variaties in techniek, geometrie, gebruik van zuren om het oppervlak te etsen en toevoegen van een calcium-fosfaat coating onderzocht. Hoewel het produceren van nieuwe oppervlakken door 'rapid prototyping' kansen biedt, is het aantal mogelijke structuren zeer groot wat directe vergelijking moeilijk maakt en het bepalen welke structuur het beste is haast onmogelijk. Een voorselectie door in vitro mechanische experimenten of eindige elementen analyse kan mogelijk de meest optimale structuren opleveren, die vervolgens getest kunnen worden in dierproeven. Andere mogelijkheden om de biologie van 'rapid prototyping' implantaatoppervlakken te verbeteren zijn het inbedden van groeifactoren zoals bot morfogenetische eiwitten in de coating. Ook het gebruik van 3-dimensionale oppervlakken op verschillende delen van de prothese kan leiden tot een optimale weefselreactie rond het implantaat. Een voorbeeld hiervan is een coating op

het proximale deel van de femurcomponent van een heup prothese zodat stress-shielding kan worden voorkomen.

Verder is het met 'rapid prototyping' mogelijk om een prothese te ontwerpen aan de hand van patiënt informatie om zo een patiënt-specifieke prothese te maken. Deze patiënt-specifieke prothese is waarschijnlijk de meest veelbelovende toepassing van de 'rapid prototyping' techniek in de gewrichtvervangende operaties. In de toekomst is het wellicht mogelijk om een patiënt-specifieke prothese te ontwikkelen en te produceren welke vergrote botingroei induceert in de meer preciaire plaatsen bij deze patiënt, bijvoorbeeld bij patiënten met osteoporose. Het is bekend dat de initiële fixatie verminderd kan zijn in osteoporotisch bot. [5;6] Met een oppervlak geometrie of coating in het gebied van bijvoorbeeld Gruen zone 7, kan een ongecementeerde prothese succesvol zijn in patiënten met osteoporose.[7] Patiënten met substantiële botdefecten, bij revisie- of tumorchirurgie, zijn een tweede groep die baat kunnen hebben bij zo'n patiënt-specifieke prothese.

Om het bovengenoemde klinische gebruik van patiënt-specifieke prothesen te kunnen bereiken, is verder onderzoek noodzakelijk. Ten eerste moet het concept van de patiënt-specifieke prothese verder ontwikkeld worden. Er is inmiddels een patiënt-specifieke femorale steel op de markt, die kan corrigeren voor beenlengte, anteversie en deformatie van het femur, zoals ontstaat bij bijvoorbeeld de ziekte van Perthes. Hoewel deze patiënt-specifieke prothese veelbelovende resultaten laat zien, zijn er nog geen lange termijn resultaten beschikbaar. De selectie van patiënten voor deze prothese vormt een uitdaging.[8] Bij deze patiënt-specifieke femorale component, kan alleen de vorm van de prothese worden aangepast aan de patiënt, niet het implantaat oppervlak. Het zou interessant zijn om het implantaat aan te passen op basis van zowel CT gegevens als botdichtheidsmetingen, om zo vergrote botingroei in gebieden met osteoporose en botdefecten te faciliteren. De meest ideale, patiënt-onafhankelijke gebieden om 3-dimensionele implantaatoppervlakken aan te brengen, zijn nog niet bekend. Eindige elementen studies en uiteindelijk dierproeven zijn noodzakelijk om de ideale gebieden voor fixatie te bepalen, waarbij botingroei, stress-shielding, de mogelijkheid tot reviseren, enz. in balans zijn.

Ten tweede zijn microbewegingen niet meegenomen in dit proefschrift. De relatieve beweging tussen de prothese en het bot welke wordt veroorzaakt door het belasten van de prothese heeft mogelijk een negatief effect op de botingroei.[9] Alhoewel dit effect patiëntspecifiek is, heeft elk protheseoppervlak een eigen kwetsbaarheid voor microbewegingen en moet de botingroei van nieuwe prothese oppervlakken getest worden onder blootstelling aan gecontroleerde microbewegingen. Helaas hebben alle diermodellen die tot nu toe gebruikt worden om het effect van microbewegingen te testen beperkingen, zoals de onmogelijkheid om kracht en verplaatsing te controleren en de verplaatsing te monitoren. Er is daarom behoefte aan een nieuw model om het effect van microbewegingen te meten.

Tot slot zal een nieuwe implantaatoppervlak, mogelijk toegepast in een patiënt-specifieke gewrichtsprothese uitgebreid getest moeten worden in dierexperimenten en daarna in patiënten. Hopelijk zal op deze manier het gebruik van 'rapid prototyping'-technieken een plek vinden om de resultaten van gewrichtsvervangende te verbeteren.

Referenties

1. Ostendorf M, Johnell O, Malchau H, Dhert WJ, Schrijvers AJ, Verbout AJ: The epidemiology of total hip replacement in The Netherlands and Sweden: present status and future needs. *Acta Orthop Scand* 73(3):282, 2002
2. Birrell F, Johnell O, Silman A: Projecting the need for hip replacement over the next three decades: influence of changing demography and threshold for surgery. *Ann Rheum Dis* 58(9):569, 1999
3. NHS National Institute for Clinical Excellence (NICE). Guidance on the selection of prostheses for primary total hip replacement. 2000.
4. Yang GL, He FM, Hu JA, Wang XX, Zhao SF: Biomechanical comparison of biomimetically and electrochemically deposited hydroxyapatite-coated porous titanium implants. *J Oral Maxillofac Surg* 68(2):420, 2010
5. Alm JJ, Makinen TJ, Lankinen P, Moritz N, Vahlberg T, Aro HT: Female patients with low systemic BMD are prone to bone loss in Gruen zone 7 after cementless total hip arthroplasty. *Acta Orthop* 80(5):531, 2009
6. Dorr LD, Faugere MC, Mackel AM, Gruen TA, Bognar B, Malluche HH: Structural and cellular assessment of bone quality of proximal femur. *Bone* 14(3):231, 1993
7. Meding JB, Galley MR, Ritter MA: High survival of uncemented proximally porous-coated titanium alloy femoral stems in osteoporotic bone. *Clin Orthop Relat Res* 468(2):441, 2010
8. Benum P, Aamodt A: Uncemented custom femoral components in hip arthroplasty. A prospective clinical study of 191 hips followed for at least 7 years. *Acta Orthop* 81(4):427, 2010
9. Kienapfel H, Sprey C, Wilke A, Griss P: Implant fixation by bone ingrowth. *J Arthroplasty* 14(3):355, 1999

List of abbreviations

3D	3-dimensional
AL	Aseptic loosening
ALP	Alkaline phosphatase
AVN	Avascular Necrosis
BIC	Bone implant contact
BMD	Bone mineral density
CAD	Computer aided design
CaP	Calciumphosphate
CLS	Cementless Spotorno
CT	Computed tomography
DNA	Deoxyribonucleic acid
Ebeam	Electron beam melting
EBM	Electron beam melting
HA	Hydroxyapatite
HE	Hematoxylin/Eosin
HHS	Harris hip score
hMSCs	human mesenchymal stem cells
MTS	Material testing systems
NICE	National Institute for Health and Clinical Excellence
NSAID	Non-steroidal anti-inflammatory drug
OA	Osteoarthritis
(P)MMA	(Poly)methylmethacrylaat
PT	Posttraumatic
SD	Standard deviation
SEM	Scanning electron microscopy
SLM	Selective laser melting
THR	Total hip replacement

Dankwoord

Het is klaar! Wat begonnen is met een idee voor betere protheses in Italië, heeft geleid tot het opereren van in totaal 42 geiten, en daarmee tot 6 artikelen. 5 jaar geleden ben ik begonnen met het onderzoek, waarvan ik er ruim 2 jaar full time aan heb gewerkt. Ik heb tijdens deze periode veel geleerd, maar ik weet nu ook dat ik altijd meer dokter dan doctor zal zijn.. Een promotieonderzoek doe je niet alleen, veel mensen hebben een bijdrage geleverd:

Pieter, bedankt voor alles. Jij hebt veel vertrouwen in me gehad, alhoewel ik als jonge arts eigenlijk geen onderzoekservaring had. Ik kon altijd bij je binnenlopen, voor een korte vraag of een groot probleem. Mijn enthousiasme over snelle tijdsschema's, enz wist je soms te temperen, maar bij een tegenslag was jij de eerste die weer een (praktische) uitweg zag. Hierbij verloor je de lijn en het grotere geheel nooit uit het oog, wat je een erg goede begeleider maakt. Je bent niet alleen als promotor erg betrokken geweest. Je hebt je ook ingespannen om mij de opleiding in te loodsen. Verder ben je een zeer prettig mens, en waardeer ik je eigenschap om te genieten van elke dag met mooi weer (en dan het liefste thuis..)

Nico, jij hebt de eerste contacten met Eurocoating gelegd en bent altijd betrokken geweest bij mijn onderzoek. Jouw biomechanische blik gaf een frisse kijk op het onderzoek. Samen met Pieter creëer je een geweldige sfeer op het lab. Bedankt!

Gerjon, vanaf het eerste moment dat jij bij mijn onderzoek betrokken bent, heb je me ontzettend veel geholpen. Jouw kennis van statistiek en computerprogramma's was onmisbaar, evenals je heldere kijk op het onderzoek. Bovendien ben je erg gezellig in de pauzes en in de kroeg, wat ik ook zeer kan waarderen. Sinds de start van mijn opleiding, kon ik ook bij je terecht voor het regelen van reference manager, SPSS analyses enz. Volgens mij heb je daarvoor nog aardig wat drankjes van me tegoed, ik wil mijn schuld graag inlossen op het feestje!

Prof. Jansen, Prof. Ritskes en Prof. Bulstra, bedankt voor het beoordelen van mijn manuscript.

Pierfrancesco, Emanuele, Giacomo, Francesco and Eleonora from Eurocoating, thanks for the great collaboration during the last 4 years. Without your pioneering work on implant surfaces and the funding this thesis would not exist. I do appreciate your patience and faith in the work we performed together. I really enjoyed the visits to Italy and will not forget the Italian lunches and dinners.. Grazie mille!

René, bedankt voor alle keren dat je me geassisteerd hebt tijdens de operaties. Jouw actieve assistentie maakte het veel makkelijker om de verantwoordelijkheid voor de operaties te dragen. En fijn dat ik niet op een bankje moest staan!



Dean, tijdens mijn coschappen heb je me enthousiast gemaakt voor het meewerken aan jouw onderzoek. Een rijdende trein beloofde je me. En dat was ook zo, vrij gemakkelijk hebben we de follow up studie afgerond, wat twee artikelen heeft opgeleverd. Bedankt voor de samenwerking en het feit dat je mij een artikel gunde.

Annemarijn, Suzanne, Mauro en Dimitri, bedankt voor het werk dat jullie tijdens je stage voor mij gedaan hebben!

Willem, al na een paar maanden begreep ik dat ik moest promoveren voordat jij met pensioen zou gaan. Als ik weer eens een (vaag) plan had voor een apparaat/osteotoom/boortje enz, had je dat altijd binnen enkele uren voor me uitgedacht, getekend en gemaakt. Voor haast elk probleem heb jij een praktische oplossing, bovendien heb ik veel plezier gehad van jouw grote netwerk op de universiteit. Ik heb het (net) gered om klaar te zijn voor je pensioen, dank je wel voor alle hulp.

Léon, je hebt voor mij oneindig veel coupes geplastificeerd, gezaagd, gekleurd en gemeten. Het gemak waarmee jij de specimens die ik geïmplanteed had, zonder beschadiging weer uit het bot zaagde toont je klasse. Bedankt!

Alex, Wilma, Maikel, Conrad en alle andere medewerkers van het CDL. Bedankt voor jullie begeleiding in het oerwoud van de administratie van de dierproeven, de assistentie bij de operaties en de goede zorgen voor mijn geitjes. Ik heb het heel gezellig gevonden om bij jullie te opereren en de 'patiënten' te bezoeken op de boerderij.

Ineke, je bent een geweldige secretaresse. Bedankt voor alles wat je voor me geregeld hebt!

Collega's van het ORL: Anne, Astrid, Dennis, Eric, Erwin, Esther, Hendi, Huub, Jorrit, Loes, Maud, Miranda, Pieter, bedankt voor alle gezelligheid!

Er zijn veel mensen die niets met dit proefschrift te maken hebben, maar wel belangrijk voor me zijn en daarmee toch hun bijdrage leverden: Boukje, Eefje, Saskia, Marcella, Nienke, Marieke, Mireille, Karen, Toon, Els, Joey, Taya, Stevie, Esther en mijn (ex)collega's in Apeldoorn en Nijmegen.

Daan en Maria, toen ik aan dit onderzoek begon had ik niet bedacht dat het me echte vrienden zou opleveren. Dat zijn jullie wel geworden. Ik heb met jullie een kamer op het lab gedeeld en daarmee ook lief en (onderzoeks-)leed. Samen hebben we ook gezellige avondjes doorgebracht en zijn we op stap geweest naar binnen- en buitenland.

Daan, zoals je al noemde in je proefschrift vroeg je me op mijn eerste werkdag wat mijn favoriete chemische element was. Deze eerste indruk heb je meer dan goed weten te maken. Ik kon alles aan jou vertellen en heb veel met je gelachen.

Maria, the trip with Daan to Milan and Poland was unforgettable. I enjoyed the many dinners and drinks that we had together. Without you I would never have experienced pierogi with vodka and would never have learned my first polish words "Ladny kombinezon". Dziękuję za wszystko!

Noëmi, al sinds het begin van onze studie zijn we goede vrienden. Gelukkig ben je vorig jaar ook naar Utrecht verhuisd, zodat we elkaar nog steeds vaak zien. Fijn dat je er altijd voor me bent en op deze belangrijke dag naast me staat!

Hoe bijzonder is het als 3 kinderen uit 1 gezin promoveren.. Christiaan en Benjamin, jullie zijn geweldige broers! Misschien komt het wel door jullie dat ik me zo thuis voel in een mannenvak.

Pap en mam, jullie waren soms nog enthousiaster dan ikzelf als er een artikel was geaccepteerd. Jullie steunen mij onvoorwaardelijk en zijn er altijd voor me. Bedankt!

Jesse, hoe fantastisch ik mijn werk ook vind, thuiskomen bij jou is altijd nog leuker. Je bent alles voor me!

Curriculum vitae

Liesbeth Biemond was born in Rotterdam, the Netherlands, on the 29th of March 1983. In 2001 she graduated (gymnasium) at the Norbertus College in Roosendaal. She studied medicine at the Radboud University Nijmegen, the Netherlands and obtained her medical degree in 2007. In the fourth year of her study a research internship at the Robert Jones and Agnes Hunt Orthopaedic Hospital in Oswestry, UK was done. In that period the interest in Orthopaedics started.

From November 2007 until 2010 Liesbeth worked as a clinical researcher in the Orthopaedic Research Laboratory at the Radboud University Medical Centre, under supervision of Prof. dr. P. Buma and Prof. dr. ir. N. Verdonchot, resulting in this thesis. The research period was paused for half a year to work as a resident at the department of orthopaedic surgery in the Radboud University Medical Centre.

From 2011 until June 2012 a 1.5 year surgical residency took place at the Gelre Ziekenhuizen in Apeldoorn (dr. W. Bouma and dr. P. van Duijvendijk). In July 2012 Liesbeth started the orthopaedic residency in the Sint Maartenskliniek Nijmegen (dr. A. Wymenga), Radboud University Nijmegen Medical Centre (dr. M. de Waal Malefijt) and Rijnstate Hospital Arnhem (dr W. Rijnberg).

Liesbeth lives in Utrecht with Jesse Martens.



